

**MINERALIZED TISSUE ENGINEERING, STEM CELL THERAPIES AND  
PROTEOMICS APPROACHES**

by

**Pang-ning Teng**

B.S. Biomedical Engineering, Washington University at St. Louis, 2001

M.S. Bioengineering, University of Pittsburgh, 2003

Submitted to the Graduate Faculty of  
Swanson School of Engineering in partial fulfillment  
of the requirements for the degree of  
Doctor of Philosophy

University of Pittsburgh

2009

UNIVERSITY OF PITTSBURGH  
SWANSON SCHOOL OF ENGINEERING

This dissertation was presented

by

Pang-ning Teng

It was defended on

March 26, 2009

and approved by

Harvey S. Borovetz, Professor, Department of Bioengineering

Bruno Péault, Professor, Department of Bioengineering

Billy W. Day, Professor, Department of Pharmaceutical Sciences

Tianyi Wang, Assistant Professor, Department of Infectious Diseases and Microbiology

Dissertation Director: Charles Sfeir, Associate Professor, Department of Bioengineering

Copyright © by Pang-ning Teng

2009

# **MINERALIZED TISSUE ENGINEERING, STEM CELL THERAPIES AND PROTEOMICS APPROACHES**

Pang-ning Teng, Ph.D.

University of Pittsburgh, 2009

Cellular therapy holds tremendous potential in regeneration of mineralized tissues such as bones and teeth. I have characterized and identified pericytes as a unique population of dental pulp stem cells (DPSCs) that can be sorted by CD146+CD34-CD45-CD56-, expanded in culture, and differentiated into osteogenic, chondrogenic, and adipogenic lineages. A well-characterized stem cell source and an appropriate microenvironment containing growth factors and/or extracellular matrix (ECM) proteins to stimulate differentiation and mineralization are required for successful cellular therapies. To understand cell-ECM protein interaction, I studied the signaling role of phosphophoryn (PP), an ECM protein found in dentin and bone. PP signals through integrins, mitogen activated protein kinase (MAPK), and Smad pathways. There is also signaling crosstalk between the MAPK and Smad pathways. To better understand the complex signaling pathways involved in stem cell differentiation during dentin or bone formation, I have utilized quantitative proteomic strategies to study stem cell differentiation triggered by PP and BMP-2. Proteins upregulated and downregulated during differentiation were identified by mass spectrometry. With the ultimate goal of better enabling the regeneration of diseased or damaged mineralized tissue, my findings in this study have enhanced our understanding in stem cell differentiation to the osteoblastic/odontoblastic lineages and lay foundations for the development of future craniofacial regeneration.

## TABLE OF CONTENTS

<b>NOMENCLATURE.....</b>	<b>XIII</b>
<b>ACKNOWLEDGEMENTS .....</b>	<b>XVI</b>
<b>1.0 INTRODUCTION.....</b>	<b>1</b>
<b>1.1 TISSUE ENGINEERING FOR CRANIOFACIAL REGENERATION .....</b>	<b>1</b>
<b>1.2 STEM CELL SOURCE FOR CELLULAR THERAPY .....</b>	<b>2</b>
<b>1.2.1 Cellular Therapies .....</b>	<b>2</b>
<b>1.2.2 Pericytes as a Unique Stem Cell Population .....</b>	<b>3</b>
<b>1.2.3 Stem Cell Populations in Dental Pulp.....</b>	<b>5</b>
<b>1.3 EXTRACELLULAR MATRIX PROTEINS DIRECTS STEM CELL DIFFERENTIATION .....</b>	<b>7</b>
<b>1.3.1 ECM Proteins Involved in Bone and Dentin Formation.....</b>	<b>7</b>
<b>1.3.1.1 PP .....</b>	<b>8</b>
<b>1.3.1.2 BMP-2 .....</b>	<b>10</b>
<b>1.4 MECHANISMS UNDERLYING STEM CELL DIFFERENTIATION.....</b>	<b>11</b>
<b>1.4.1 Proteomic Approaches to Understanding Stem Cell Differentiation and Signaling Pathways .....</b>	<b>14</b>
<b>1.4.1.1 Quantitative Proteomics.....</b>	<b>15</b>
<b>1.4.1.2 Phosphoproteomics.....</b>	<b>16</b>

1.5	<b>HYPOTHESES .....</b>	<b>17</b>
1.6	<b>SPECIFIC AIMS &amp; RATIONALE.....</b>	<b>17</b>
1.6.1	<b>Specific Aim 1: Characterization, identification, and isolation of dental pulp stem cells (pericytes).....</b>	<b>17</b>
1.6.2	<b>Specific Aim 2: Identification of cell surface receptors and signaling crosstalk in PP signaling in hMSCs.....</b>	<b>18</b>
1.6.3	<b>Specific Aim 3: Proteomic profiling of mouse embryonic fibroblasts (C3H10T1/2) during differentiation into osteoblasts and odontoblasts.....</b>	<b>18</b>
1.6.4	<b>Rationale of Different Cell Types Selected for Each Aim.....</b>	<b>18</b>
2.0	<b>MULTILINEAGE POTENTIAL OF PRICYTES SORTED FROM HUMAN DENTAL PULP .....</b>	<b>20</b>
2.1	<b>SUMMARY .....</b>	<b>20</b>
2.2	<b>INTRODUCTION .....</b>	<b>21</b>
2.3	<b>MATERIALS AND METHODS .....</b>	<b>22</b>
2.3.1	<b>Antibodies.....</b>	<b>22</b>
2.3.2	<b>Tooth Procurement and Cell Isolation .....</b>	<b>23</b>
2.3.3	<b>Immunohistochemistry .....</b>	<b>23</b>
2.3.4	<b>FACS and Cell Culture.....</b>	<b>24</b>
2.3.5	<b>Colony Forming Units-fibroblast (CFU-f) Assay .....</b>	<b>24</b>
2.3.6	<b>Immunocytochemistry.....</b>	<b>25</b>
2.3.7	<b>Osteogenic Differentiation .....</b>	<b>25</b>
2.3.8	<b>Chondrogenic Differentiation.....</b>	<b>26</b>
2.3.9	<b>Adipogenic Differentiation.....</b>	<b>27</b>

2.4	<b>RESULTS</b> .....	28
2.4.1	<b>Identification of Perivascular Cells on Dental Pulp Sections</b> .....	28
2.4.2	<b>FACS of Human Dental Pulp Perivascular Cells</b> .....	30
2.4.3	<b>Clonogenic Capacity and Phenotype of Cultured Dental Pulp Pericytes</b> . 30	
2.4.4	<b><i>In vitro</i> Multilineage Differentiation of Cultured Dental Pulp Pericytes</b> . 33	
2.5	<b>DISCUSSION</b> .....	35
2.6	<b>ACKNOWLEDGMENTS</b> .....	37
3.0	<b>PHOSPHOPHORYN SIGNALING MECHANISM IN HMSCS, INVOLVEMENT OF INTEGRINS AND CROSSTALK AMONG MAPK AND SMAD PATHWAYS</b> .....	38
3.1	<b>SUMMARY</b> .....	38
3.2	<b>INTRODUCTION</b> .....	39
3.3	<b>MATERIALS AND METHODS</b> .....	41
3.3.1	<b>Antibodies</b> .....	41
3.3.2	<b>Generation of rPP</b> .....	41
3.3.3	<b>Cell Culture</b> .....	42
3.3.4	<b>Blocking of Integrins</b> .....	42
3.3.5	<b>siRNA</b> .....	43
3.3.6	<b>Western Blot Analysis</b> .....	43
3.4	<b>RESULTS</b> .....	44
3.4.1	<b>PP Signals through Integrins <math>\alpha v\beta 3</math> and <math>\alpha 2\beta 1</math></b> .....	44
3.4.2	<b>MAPK and Smad Crosstalk</b> .....	49
3.4.2.1	<b>ERK Inhibits the Activation of Smad1</b> .....	50

3.4.2.2	p38 Enhances the Activation of ERK and Smad1 .....	51
3.5	DISCUSSION.....	52
3.6	ACKNOWLEDGEMENT .....	54
4.0	PROTEOMIC PROFILING OF PP AND BMP-2 DIRECTED STEM CELL DIFFERENTIATION.....	55
4.1	SUMMARY .....	55
4.2	INTRODUCTION .....	55
4.3	MATERIALS AND METHODS.....	57
4.3.1	SILAC and Cell Treatment .....	57
4.3.2	Cell Lysis .....	58
4.3.3	Desalting .....	58
4.3.4	Fractionation by 1D-PAGE and In-Gel Digestion.....	59
4.3.5	Phosphoenrichment with Titanium Dioxide (TiO <sub>2</sub> ) .....	59
4.3.6	Mass spectrometry and Data Analysis.....	60
4.3.7	Ingenuity Pathway Analysis .....	62
4.3.8	Western Blot Analyses.....	63
4.3.9	Immunohistochemistry .....	64
4.4	RESULTS.....	65
4.4.1	Heavy Lysine and Arginine Labeling in C3H10T1/2 Cells.....	66
4.4.2	Protein Fractionation by 1D-PAGE.....	67
4.4.3	Global Protein Profiling of PP and BMP-2 Treated C3H10T1/2 Cells ....	69
4.4.4	Phosphoprotein Profiling of PP and BMP-2 Treated C3H1-T1/2 Cells...	73
4.4.5	Protein Validation.....	75

4.5	<b>DISCUSSION</b> .....	78
4.6	<b>ACKNOWLEDGEMENTS</b> .....	81
5.0	<b>CONCLUSIONS AND FUTURE DIRECTIONS</b> .....	82
5.1	<b>DENTAL PULP PERICYTES</b> .....	83
5.1.1	<b>Differentiation Potential of the Dental Pulp Pericytes</b> .....	83
5.1.2	<b>Different Cell Populations in the Dental Tissues</b> .....	83
5.2	<b>PP SIGNALING MECHANISM</b> .....	84
5.2.1	<b>Receptors for PP</b> .....	84
5.2.2	<b>Effect of PP on Different Cell Types</b> .....	85
5.2.3	<b>PP Signaling Mechanisms</b> .....	85
5.3	<b>GLOBAL PROTEOMICS APPROACHES</b> .....	86
5.3.1	<b>SILAC</b> .....	86
5.3.2	<b>iTRAQ</b> .....	86
5.3.3	<b>Phosphoenrichment</b> .....	87
5.3.4	<b>Absolute Quantification</b> .....	87
5.4	<b>SCAFFOLD FOR MINERALIZED TISSUE ENGINEERING</b> .....	88
	<b>APPENDIX A</b> .....	89
	<b>APPENDIX B</b> .....	96
	<b>APPENDIX C</b> .....	98
	<b>BIBLIOGRAPHY</b> .....	100

## LIST OF TABLES

Table 1-1. List of abbreviations .....	xiii
Table 2-1. Markers used for IHC .....	28
Table 4-1. Proteins selected for validation experiments .....	76
Table 5-1. Proteins with unique peptides upregulated by PP treatment .....	89
Table 5-2. Proteins with unique peptides downregulated by PP treatment .....	90
Table 5-3. Proteins with unique peptides upregulated by BMP-2 treatment .....	90
Table 5-4. Proteins with unique peptides downregulated by BMP-2 treatment .....	91
Table 5-5. Proteins with common peptides upregulated by PP treatment .....	92
Table 5-6. Proteins with common peptides downregulated by PP treatment .....	93
Table 5-7. Proteins with common peptides upregulated by BMP-2 treatment .....	94
Table 5-8. Proteins with common peptides downregulated by BMP-2 treatment .....	95
Table 5-9. Experiment groups with cells grew on different coated surfaces .....	98

## LIST OF FIGURES

Figure 1-1. Genomic organization of the mouse DMP-3 gene. Exons 2,3 and 4 code for DSP and exon 5 codes for PP.....	10
Figure 1-2. Mechanisms of stem cell differentiation triggered by ECM proteins remain a black box.....	11
Figure 1-3. Working model of PP and BMP signaling pathways.....	13
Figure 2-1. Immunodetection of pericytes in human dental pulp. A, B - CD146 in red) $\alpha$ -SMA (green) C, D - CD146 (green), CD34 (red). Pericytes (P). Endothelial cells (EC). E - CD146 (red), vWF (green). F - CD146 (green), CD56 (red). G - CD146 (green) NG2 (red) H - CD146 (green) CD45 (red). Nuclei were stained blue with DAPI. A, B, D: bar = 50 $\mu$ m. ....	29
Figure 2-2. FACS, morphology, CFU-f analysis, and immunocytochemistry of cultured dental pulp pericytes. A, B – exclusion of CD56+ and CD45+ cells. C - Selection of CD146+CD34- population. D - Pericytes morphology. E - CFU-f analysis. F – CD146 (red), G – NG-2 (red), H – $\alpha$ SMA (green), I – PDGFR- $\beta$ (red), J – CD44 (red), K – CD90 (red), L - CD166 (red), M – Runx2 (green), N – Osteocalcin (green). Nuclei were stained blue with DAPI. D: Bar = 100 $\mu$ m. F-N: 20x magnification.....	32
Figure 2-3. Multilineage differentiation of cultured dental pulp pericytes. A, B - alkaline phosphatase and von Kossa stainings of pericytes cultured in control or osteogenic media. C, E – Alcian blue and D – Safranin O stainings of pellet section of cells cultured in chondrogenic media. F – Oil red O staining of cells cultured in adipogenic media. A-D: bar = 100 $\mu$ m, E-F: bar = 50 $\mu$ m. ....	34
Figure 3-1. Blocking of $\alpha$ v $\beta$ 3 in hMSCs prior to treating the PP.....	45

Figure 3-2. Blocking of $\alpha 2\beta 1$ in hMSC prior to treating the PP.....	46
Figure 3-3. Blocking of $\alpha v\beta 3$ in hMSC prior to treating the PP. Normalized p-ERK. ....	46
Figure 3-4. Blocking of $\alpha v\beta 3$ in hMSC prior to treating the PP (* $p < 0.05$ ). Normalized p-JNK. ....	47
Figure 3-5. Blocking of $\alpha v\beta 3$ in hMSC prior to treating the PP (* $p < 0.05$ ). Normalized p-p38. .	47
Figure 3-6. Blocking of $\alpha 2\beta 1$ in hMSC prior to treating the PP. Normalized p-ERK. ....	48
Figure 3-7. Blocking of $\alpha 2\beta 1$ in hMSC prior to treating the PP. Normalized p-JNK. ....	48
Figure 3-8. Blocking of $\alpha 2\beta 1$ in hMSC prior to treating the PP. Normalized p-p38. ....	49
Figure 3-9. ERK and Smad1 activity after ERK knockdown by siRNA.....	51
Figure 3-10. ERK and Smad1 activity after p-38 knockdown by siRNA .....	52
Figure 4-1. SILAC-based experimental workflow .....	66
Figure 4-2. Peptide isotope pair showing a difference of $m/z$ 5 amu for the heavy arginine-containing peptide with a relative abundance of 1:1 between control and treated. ....	67
Figure 4-3. Protein fractionation by 1D-PAGE .....	68
Figure 4-4. Normal distribution of binned protein counts vs. Log2 Ratio for PP/control group..	70
Figure 4-5. Normal distribution of binned protein counts vs. Log2 Ratio for BMP-2/control group .....	70
Figure 4-6. Distribution of protein functions in PP/control group.....	72
Figure 4-7. Distribution of protein functions in BMP-2/control group .....	72
Figure 4-8. Top network of PP/control ( $TiO_2$ enriched, unique peptides).....	74
Figure 4-9. Western blot validation of proteins identified from mass spectrometry .....	77
Figure 4-10. Androgen receptors staining in cells treated with BMP-2, PP, or untreated control	78
Figure 5-1. FACS analysis of periodontal ligament cells. ....	97
Figure 5-2. Alkaline phosphatase and von Kossa staining of SAOS-2 cells seeded on tissue culture plastic, PLA, and different % of KK89 at week two. ....	99

## NOMENCLATURE

**Table 1-1.** List of abbreviations

$\alpha$ -SMA	$\alpha$ -smooth muscle actin
AmB	Amonium bicarbonate
ACN	Acetonitrile
BMP-2	Bone morphogenetic protein-2
BMP-2/4	Bone morphogenetic protein-2 and 4
BMP-7 (OP-1)	Bone morphogenetic protein-7
BSP	Bone sialoprotein
C3H10T1/2	Mouse embryonic fibroblasts
CFU-f	Colony forming unit-fibroblasts
CID	Collision induced dissociation
DAPI	4',6-diamidino-2-phenylindole
DHB	Dihydroxybenzoic acid
DIGE	Difference in-gel electrophoresis
DMP-1	Dentin matrix protein-1
DMP-3	Dentin matrix protein-3
DPSC	Dental pulp stem cell
DSP	Dentin sialoprotein
DSPP	Dentin sialophosphoprotein
ECM	Extracellular matrix
EGF	Epidermal growth factor
EGM-2	Endothelial cell growth medium
Eif2A	Eukaryotic initiation factor 2A
Erk	Extracellular signal regulated kinase
FACS	Fluorescence activated cell sorting
FA	Formic acid
FAK	Focal adhesion kinase
FBS	Fetal bovine serum

F-PP	Full length phosphophoryn
HA	Hydroxyapatite
hMSC	Human mesenchymal stem cell
HRP	Horseradish peroxidase
ICAT	Isotope coded affinity tags
IHC	Immunohistochemistry
IMAC	Immobilized metal affinity chromatography
IRB	Institutional review board
iTRAQ	Isobaric tag for relative and absolute quantitation
JNK	c-Jun N-terminal kinase
LC-MS	Liquid chromatography - mass spectrometry
LIT	Linear ion trap
MAPK	Mitogen activated kinase
MC3T3-E1	Mouse osteoblasts
MEPE	Matrix extracellular phosphoglycoprotein
MS	Mass spectrometry
MSC	Mesenchymal stem cell, bone marrow stromal cells
NIH3T3	Mouse fibroblasts
OCN	Osteocalcin
ON	Osteonectin
OPN	Osteopontin
Osx	Ostrix
PAGE	Polyacrylamide gel electrophoresis
PbAE	Poly(ethylene oxide)-modified poly( $\beta$ -amino ester)
PBS	Phosphate buffered saline
PCR	Polymerase chain reaction
PDGF	Platelet derived growth factor
Perk	Eukaryotic translation initiation factor 2 alpha kinase 3
p-ERK	Phosphorylated ERK
PFA	Paraformaldehyde
p-FAK	Phosphorylated FAK
PI3K	Phosphatidylinositol 3-kinase
p-JNK	Phosphorylated JNK
PLA	Poly(L-lactic acid)
PP	Phosphophoryn
p-P38	Phosphorylated P38
PTH	Parathyroid hormone
PTHrp	Parathyroid hormone related peptide
rhBMP-2	Recombinant human BMP-2

RIPA	Radio immunoprecipitation assay buffer
RPLC	Reverse phase liquid chromatography
rPP	Recombinant PP (truncated version of full length PP)
RT	Room temperature
Runx-2 (Cbfa1)	Runt-related transcription factor 2/core binding protein A-1
SCAP	Stem cells from the apical papilla
SDS	Sodium dodecyl sulfate
SHED	Stem cells from human exfoliated deciduous teeth
SIBLINGs	Small integrin binding ligand N-linked glycoproteins
SILAC	Stable isotope labeling of amino acids
siRNA	Small interfering RNA
Smad	Homologs of drosophila protein, mothers against decapentaplegic (MAD) and C.elegans protein SMA (S)
TBST	Tris buffered saline with Tween
TCEP	Tris(2-carboxyethyl)phosphine
TFA	Trifluoroacetic acid
TGF- $\beta$	Transforming growth factor- $\beta$
TiO <sub>2</sub>	Titanium dioxide
vWF	von Willebrand factor
YWHAE (14-3-3 $\epsilon$ )	Tyrosine 3-moxygenase/tryptophan 5-monoxygenase activating protein, epsilon polypeptide

## ACKNOWLEDGEMENTS

First, I would like to acknowledge my advisors, Drs. Charles Sfeir and Bruno Péault, who were wonderful mentors and teachers during my research efforts. Not only did they provide me the opportunity to pursue my graduate study, they have shown me the ropes so to speak towards effective and productive science, research and integrity. I whole-heartedly thank them for their guidance during my exploration in my interest in stem cells and tissue engineering. I would also like to give special thanks to Drs. Harvey Borovetz, Billy Day, and Tianyi Wang for being on my thesis committee and giving me invaluable advice over the years.

Much of what I was able to accomplish would not have been possible without the support and interaction from my peers. For that I would like to thank my colleagues Tea Soon Park, Bin Sun, Mihaela Crisan, Alison Logar, Solomon Yap, Hong Wu, Jin Hua Li, Linda Zhang, Paul Ko, Pui-yan Lee, Dana Olton, Donghyun Lee, Yuan Yuan Duan, Guliz Guncu, Lynzy Maruca, Fatima Syed-Picard, Mai Sun, Janice Kim for sharing their expertise and for providing an enjoyable working environment. To the students I interacted with and trained during my research, Pieter Heemstra, Neil Robertson, Benjamin Barbetta, Ann Chernayak, Amishha Guyral, Michael Breskiewicz, and Neeta Kannan, thank you for your enthusiasm in the research and assistance in the lab. I especially would like to acknowledge our collaborators, Drs. Prashant Kumta, Elia Beniash, Steve Little, and Thomas Conrads for providing exceptional technical

assistance and sharing their knowledge during the course of research together. And for all of their administrative and general assistance, I thank Lynette Spataro, Joan Williamson, Rosanne Perry, Michele Leahy, and Diane Turner.

I am particularly grateful to my family for all their love and support. My parents Jin-ru Wang and Yao-kun Teng, and my brother Pang-yu Teng, have provided me the strength and courage to persist and accomplish my dreams during the course of my graduate study. I owe much to my dear friends Sean Jefferson, Carol Liu, Tea Soon Park, Ludovic Zimmerlin, Karanee Leelavanichkul, Leonard Liaw, Shelly Tong, Eden Tung, and Terry Lin. They have been my family away from home and provided me with camaraderie, company and encouragement. Finally, I thank my love Brian Hood for his endless love, care, and encouragement. You have been tremendously helpful and understanding. I could not have done this without all your help. Thank you.

## **1.0 INTRODUCTION**

### **1.1 TISSUE ENGINEERING FOR CRANIOFACIAL REGENERATION**

Craniofacial reconstruction is necessary to replace or repair damaged or lost tissue in the oral-facial region. Tissue lost in the oral-facial region can arise for many different situations including injury or diseases such as head and neck trauma, cancer, genetic diseases, tooth injury, or alveolar bone loss due to periodontal disease. The current technology for treating craniofacial defects is to implant an allograft bone substitute seeded with bone marrow aspirate from the ilia crest. The grafted defect could be stabilized by titanium screws or bars if the need arises. Another approach is to harvest segments of bone from the patient's ulna or tibia to replace the damaged craniofacial tissues; however, this introduces a second injury site that may elicit complications and infection.

Current research in this field is focused on developing tissue engineering strategies to regenerate craniofacial defects. To this end, a wide variety of tissues are needed including bone, muscle, fat, cartilage, dentin, periodontal ligament, cementum, and dental pulp. Our specific interest is in mineralized tissue engineering which is the regeneration of hard tissues such as bone and dentin.

## **1.2 STEM CELL SOURCE FOR CELLULAR THERAPY**

The source of stem cells is an important consideration for cellular therapy. Different types of stem cells possess different abilities to differentiate and are suitable for repairing various tissues. Stem cells can be categorized into embryonic stem cells, fetal stem cells and adult stem cells. The definition of a stem/progenitor cell is that it can self-renew as well as differentiate into at least one cell type. For cellular therapy, rejection poses a potential issue; therefore autologous stem cells are preferred. Embryonic and fetal stem cells may elicit a body rejection and also raise ethical concerns. Cells harvested from tissues that are discarded such as human umbilical vein endothelial cells, umbilical cord blood, foreskin, and dental pulp are convenient cell sources for cellular therapies. In specific, adult stem cells such as those derived from the bone marrow and dental pulp have been shown to be able to differentiate into the bone/dentin lineages and thus will be used in our study.[1,2]

### **1.2.1 Cellular Therapies**

One approach to repair mineralized tissues is to utilize cellular therapies. Stem cell based mineralized tissue engineering requires a well-characterized population of stem cells that can be easily sorted, expanded, and induced by growth factors or extracellular matrix proteins (ECM) for the desired differentiation. Human bone marrow stromal cells, or mesenchymal stem cells (MSC), have been widely studied for differentiation toward osteogenic, chondrogenic, and adipogenic lineages.[1] However, mesenchymal stem cells from the craniofacial region have been shown to behave differently than those from iliac crest.[2, 3] The differences between the MSCs in the craniofacial region and those in the iliac crest might be due to their origin. Most

skeletal tissues are derived from the mesoderm except those in the craniofacial region. Neural crest cells form much of the mesenchyme of the head and neck, and are derived from the ectoderm found at the edges of the neural plate. These cells are also termed neuroectoderm or ectomesenchyme.[4] The pulp of adult third molars contains stem cells derived from the ectomesenchyme. Because of their unique neural crest origin, dental pulp stem cells may serve as a favorable alternative to bone marrow stromal cells for craniofacial tissue regeneration. Dental pulp stem cells from the adult third molars, isolated using fluorescent activated cell sorting (FACS), can be induced to differentiate by appropriate growth factors and incorporated into biocompatible scaffolds which can be useful for bioengineering of craniofacial mineralized tissues. In addition, they can provide a model to better understand the biological phenomena involved in cell differentiation towards the osteoblastic/odontogenic lineages and bone regeneration. Finally, these dental pulp stem cells can also be used to study epithelial-mesenchymal interactions instrumental to the formation of future bioengineered teeth.

### **1.2.2 Pericytes as a Unique Stem Cell Population**

Pericytes, also known as Rouget or mural cells, are microvascular cells surrounding the endothelial cells that emerged from the mesodermal origin.[5] Pericytes reside around the walls of microvessels (precapillaries, capillaries, and postcapillary venules) and are neither endothelial cells nor smooth muscle cells.[6, 7] Pericytes are distributed throughout the vasculature in the body with diverse characteristics, function, and location.[8] For example, pericytes in liver, also known as Ito cells, serve as a mediator between sinusoids and hepatocytes to facilitate metabolic interactions.[9] In general, pericytes interact with endothelial cells to regulate endothelial cell proliferation and differentiation.[10] Pericytes are also involved in angiogenesis, maintaining

blood flow, as well as providing mechanical strength to the microvessels.[7, 10, 11] It has been suggested that pericytes may play a role in the growth, maintenance and repair of the skeleton.[12] Pericytes may also be associated with diseases involving ectopic calcification.[13]

Studies have shown pericytes to be a mesenchymal stem cell (MSC)-like population with the capacity to differentiate into multiple mesenchymal lineages: smooth muscle cells, osteoblasts, chondrocytes, and adipocytes.[5, 10, 14-16] Bone marrow stromal cells, or MSCs, are in fact perivascular cells that are viewed as a special subset of pericytes.[17] Pericytes have been isolated from retina, brain, epididymal fat pad, skin, lung, placenta, aorta, and dental pulp from various species (human, bovine, rat, monkey).[8, 10, 18, 19] Studies have shown pericytes to behave osteoblast-like *in vitro* even without addition of  $\beta$ -glycerophosphate.[20, 21] Human placental pericytes express bone associated proteins, matrix Gla protein and osteopontin (OPN).[19, 20] Pericytes from bovine retinal microvessels express alkaline phosphatase, runx2, OPN, osteonectin (ON), osteocalcin (OCN), and bone sialoprotein (BSP) at different stages of differentiation.[10, 15] Osteocalcin concentration is higher in the bone cell when compared to pericytes.[22] Bovine retina pericytes have also been shown to have osteogenic potential *in vivo* using diffusion chambers.[23]

However, pericytes used in the studies mentioned above were not sorted, but identified to be pericytes by the source of isolation, morphology, and characteristics such as forming nodules post confluence. There is no specific marker for pericytes, but there are markers expressed by pericytes as well as other cell populations such as 3G5, NG2, CD146, Stro-1,  $\alpha$ -SMA, Desmin, and ON.[7, 8, 11, 18, 24] Studying pericytes is therefore extremely challenging and there is a significant need for a combination of specific markers to sort pericytes exclusively. Dr. Péault's group has characterized and isolated pericytes from human white adipose tissue, fetal and adult

muscle, fetal pancreas, and fetal lung using the combination of markers CD146+CD34-CD45-CD56- and showed multilineage potential of sorted pericytes.[25] In collaboration with Dr. Péault we will test this combination of markers for pericytes to isolate human dental pulp tissue.

### 1.2.3 Stem Cell Populations in Dental Pulp

Dental pulp is a highly vascularized tissue and has been proposed to be a stem cell niche.[3, 26] Pulp cells, like osteoblasts/odontoblasts, express bone/dentin markers such as bone sialoprotein (BSP), alkaline phosphatase, type I collagen, OCN, ON, parathyroid hormone/parathyroid hormone related peptide (PTH/PTHrp) receptor, and dentin sialophosphoprotein (DSPP).[26, 27] However, the identity of stem cell populations in the dental pulp remain unclear.

Shi et al. have recently identified mesenchymal stem cells in adult human dental pulp and human primary teeth: dental pulp stem cells (DPSC) and stem cells from human exfoliated deciduous teeth (SHED). DPSC and SHED were reported to have stem cell like qualities such as self-renewal ability and multi-lineage differentiation.[26] Shi et al. observed clonogenic populations of DPSCs that were not sorted, but isolated by its ability to adhere to plastic, similar to bone marrow stromal cells. DPSCs also share similar gene expression profile with bone marrow stromal cells.[28] Non-sorted DPSCs form mineralized nodules *in vitro* and generate dentin-pulp-like tissue *in vivo*. [29, 30] SHEDs were isolated (but not sorted), expanded, and showed 9% Stro-1 positive by FACS. Sections of deciduous incisor pulp were positive for CD146 and Stro-1 for cells in perivascular areas. SHEDs are clonogenic and able to differentiate into neural cells, adipocytes, and odontoblasts *in-vitro* as well as osteogenic and odontogenic *in vivo*. [31]

The studies mentioned above suggested the stem cells are perivascular cells in the dental pulp by a descriptive manner using immunohistochemistry (IHC) but they were not sorted routinely with FACS. There has been little effort in characterization and differentiation of sorted dental pulp cells. In only one study, Shi and Gronthos' group sorted DPSCs by Stro-1, a mesenchymal stem cell marker, and then characterized them by IHC to be positive for the perivascular markers CD146 and 3G5, but negative for the endothelial and hematopoietic markers VWF, CD34, and CD45. They also sorted DPSCs by CD146 and observed ectopic dentin formation in immunocompromised mice.[32] Non-sorted pulp cells isolated by Alliot-Licht's group formed mineralized nodule and expressed alpha-SMA (a marker for pericytes and smooth muscle cells).[33] Tacles et al. showed pulp stem cells in the perivascular area proliferate in response to dentin injury.[34] Together, these results led us to our hypothesis that pericytes in the dental pulp are in fact a stem cell population, but we needed to develop a strategy to isolate the pericytes since Stro-1 and CD146 are also expressed by other cell types. In this study, we will characterize the pericytes by immunohistochemistry and determine an optimal combination of specific markers to specifically sort dental pulp pericytes by FACS. From our immunohistochemistry results, we have characterized pericytes from the dental pulp to be positive for CD146 but negative for CD34, CD45, and CD56 similar to pericytes found in other tissues. Using these results, we developed a protocol to isolate the pericytes by FACS by first excluding CD45+ and CD56+ cells, then selecting for the CD146+CD34- population. This provides us with a well-characterized stem cell population with high purity from human dental pulp that can be routinely sorted for expansion and differentiation.

However, other stem cells populations could exist in the dental pulp. For example, Laino et al. showed Stro-1+ckit+CD34+CD45- sorted population to be stem cells from the dental

pulp.[35] Further studies comparing various stem cell populations in the dental pulp different are warranted.

### **1.3 EXTRACELLULAR MATRIX PROTEINS DIRECTS STEM CELL DIFFERENTIATION**

Stem cell maintenance and differentiation is directed by signals in the stem cell niche or microenvironment. These signals include mechanical stimuli, chemical stimuli, ECM-cell stimuli and cell-cell interaction. The ECM provides structure as well as contains growth factors that instruct cells to proliferate, migrate or differentiate.

#### **1.3.1 ECM Proteins Involved in Bone and Dentin Formation**

Many of the processes involved in bone and dentin formation are very similar. Osteoblast and odontoblasts secrete a specialized extracellular matrix that will mineralize. The ECM is believed to provide the appropriate signals to maintain the osteoblastic and odontoblastic phenotype. The ECM contains collagen and non-collagenous proteins, such as Small Integrin-Binding Ligand N-Linked Glycoproteins (SIBLINGs). SIBLINGs are found in bone and dentin during mineralization and play an important role in directing biomineralization and by signaling stem cell differentiation. SIBLINGs include OP, BSP, dentin matrix protein-1 (DMP-1), DSPP (also called dentin matrix protein-3 or DMP-3), and matrix extracellular phosphoglycoprotein (MEPE).[36] Post-translational modifications of SIBLINGs such as phosphorylation, glycosylation, and proteolytic processing can affect its structure and function, as a result

directing osteogenesis and dentinogenesis.[37] Our interest is to determine the effect of phosphophoryn (PP) on cell signaling and stem cell differentiation in comparison to bone morphogenetic protein-2 (BMP-2).

### **1.3.1.1 PP**

The DSPP gene codes for two proteins: dentin sialoprotein (DSP) and phosphophoryn (PP). PP is primarily found in dentin, but also found in bone at much lower levels. Due to its unique and exclusive secretion in mineralized tissues, we hypothesized that phosphophoryn would be needed for dentin formation, thus making it of significant interest to study if it has a role in stem cell differentiation to osteoblasts or odontoblasts. The isolation of the DMP-3 or DSPP mouse genomic clone in our laboratory as well as others demonstrated that DSP and PP are cleavage products of a single transcript coded by DMP-3.[38][39] The same organization of the gene was also described in the rat species.[40, 41] The intron/exon structure we obtained was characterized and the gene contains 5 exons and 4 introns and ~1.5 kb and 6 kb 3' flanking regions. A diagram of the  $\lambda$  clone is shown in Figure 1.1. Exons 2, 3 and 4 code for DSP and exon 5 codes for PP, comprised primarily of a repetitive motif: (DSS)<sub>n</sub>. The (DSS)<sub>n</sub> motif confirms the partial degradation studies of phosphophoryns performed earlier.[42] DSPP is localized to chromosome 4, linking mutations in the gene to dentinogenesis imperfecta type II.[43, 44] Although initially thought to be tooth-specific, Dspp message is also localized in mouse calvaria and rat tibia, although at much lower levels.[37]

PP is the most abundant NCP in dentin ECM, comprising approximately 50% of the ECM protein sector.[44] Like other proteins in the bone/dentin microenvironment, PP is highly phosphorylated and anionic in character.[45] PP is exceedingly rich in aspartic acid (D) and serine (S) residues, and approximately 85-90% of the serine residues are phosphorylated.[46, 47]

The majority of the protein sequence consists of (DSS)<sub>n</sub> repeats as shown in Figure 1-1.[39, 48] Odontoblasts secrete PP along the mineralization front.[49-51] PP has been implicated as a regulator of mineral crystal formation.[44, 45, 52, 53] Typical of other non-collagenous proteins, the physiochemical properties of PP dictate high affinity for Ca<sup>2+</sup> which implicates a role in nucleation or modulation of HA crystal formation.[54-56] An RGD domain is present at the N-terminal end of PP[52, 54], suggesting an auxiliary function in ECM-cell communication and initiation of intracellular signaling pathways.

PP also has a signaling role similar to that of growth factors to regulate cell differentiation. Our group has shown that PP can act as a signaling molecule and upregulate osteogenic genes in human mesenchymal stem cells (hMSCs), mouse fibroblasts (NIH3T3), and mouse osteoblasts (MC3T3-E1). PP regulates hMSC differentiation through the integrin/mitogen activated protein kinase (MAPK) signaling pathway.[57] We have also shown that PP activates the Smad pathway, which is important in osteogenesis and dentinogenesis.[58] Runx2, Osterix, alkaline phosphatase, and osteocalcin were upregulated in hMSCs treated with PP.[57] PP has also been reported to act as a co-factor that can enhance BMP-2 in bone formation in a rat model.[59] Therefore, we feel that PP is a promising candidate for inducing osteogenic and odontogenic differentiation of stem cells.



hydroxyapatite.[68-70] Understanding the effect of BMP-2 on stem cell differentiation can provide valuable information in bone development and tissue engineering.

#### 1.4 MECHANISMS UNDERLYING STEM CELL DIFFERENTIATION

Stem cell differentiation is a complex process where the microenvironment plays an important role. This microenvironment contains growth factors and ECM proteins that play a major role in cell differentiation and signaling through the activation of signal transduction pathways. After the binding of growth factors to specific cell surface receptors, a cascade of signaling events leads to the recruitment of transcription factors to the cell nucleus, which then initiates specific gene expressions. However, how stem cells become osteoblasts/odontoblasts remains unclear. (Figure 1-2) One of the goals of our research is to investigate intracellular signaling pathways to better understand the differentiation process of stem cells.

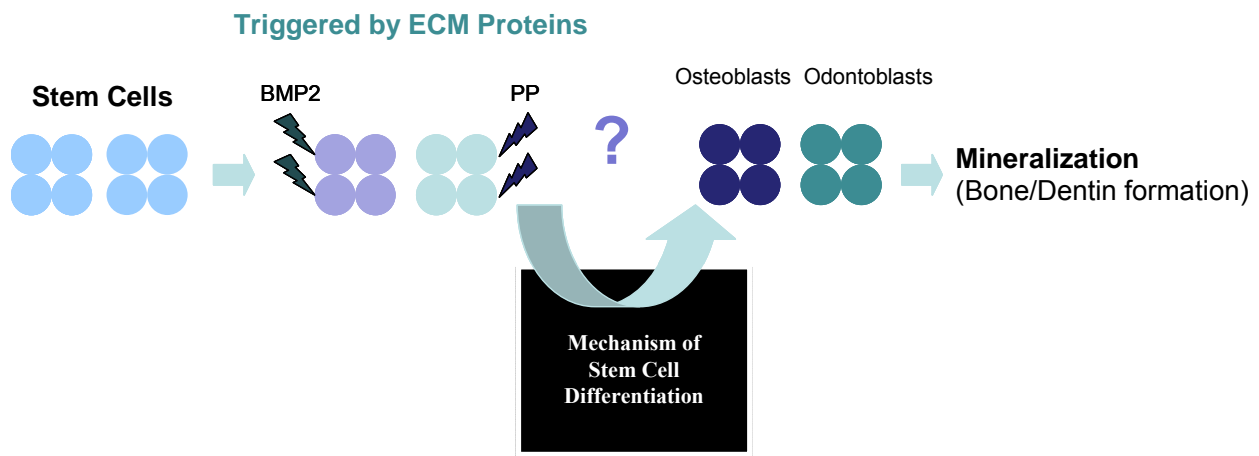


**Figure 1-2.** Mechanisms of stem cell differentiation triggered by ECM proteins remain a black box.

Our recent data show that PP interacts with  $\alpha_v\beta_3$  integrin and signals through the mitogen-activated protein kinase (MAPK) and Smad pathways. PP appears to play an important role during cell differentiation towards the osteoblastic lineage. Our goal is to understand the role of PP during cell differentiation. Since BMP-2 is a well known factor in the differentiation of cells into osteoblasts, we will utilize BMP-2 as a positive control and compare its signaling effects to the signaling role played by PP. In addition, PP and BMP-2 both activate the Smad pathway which leads us to speculate on how PP activates Smad1. Figure 1-3 illustrates how PP signals through  $\alpha_v\beta_3$  integrin, via the MAPK pathway by activating Jnk, Erk, and P38, but its activation of the Smad pathway does not appear to arise from interaction with the BMP receptor. However, we do not know whether PP binds to only integrin  $\alpha_v\beta_3$  or if it also interacts with other cell surface receptors. We will investigate other integrins, such as  $\alpha_2\beta_1$ , which have been shown to be expressed in hMSCs and are involved in osteoblastic differentiation.

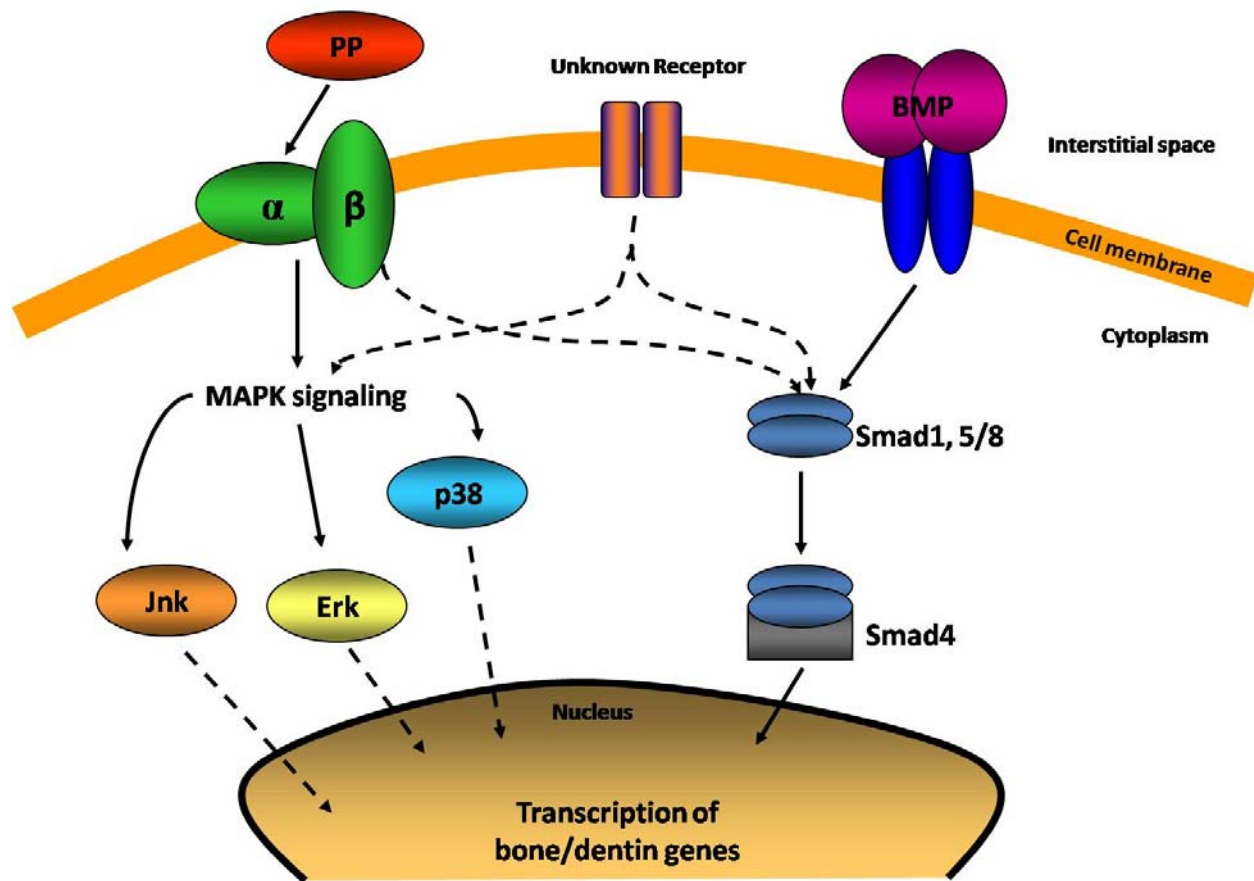


Figure 1-3. Working model of PP and BMP signaling pathways

We are interested in comparing PP signaling to BMP-2 signaling pathways because PP activates Smads similarly to BMP-2. BMP-2 binds to two types of serine/threonine kinase receptors, type I and type II receptors. After BMP binds to its receptor, signals get propagated by phosphorylation of the receptor and through its downstream molecules, Smad1, 5, and 8. These Smad molecules form a complex which then interacts with Smad4 which translocates to the nucleus and interacts with transcription factors such as Runx2 to regulate target gene expression. Although BMP-2 has been extensively studied, the mechanism that it induces towards osteoblast differentiation is still not fully understood. BMP-2 also stimulates tyrosine phosphorylation and

phosphatidylinositol 3-kinase (PI3K)/Akt pathways which are involved in osteoblast differentiation. It is well known that there is cross-talk between Smads and PI3K/Akt. PI3K, a lipid kinase, is often activated by tyrosine phosphorylation induced by binding of specific growth factors. PI3K functions as a control point in the signaling cascade.[71] Crosstalk also exists between the MAPK and Smad pathways under BMP-2 signaling.[72-74] Erk activation has been shown to inhibit Smad[75] while inhibition of P38 was shown to decrease Smad signaling.[76] Since we know that PP signals through the MAPK and Smad pathways similarly to BMP-2, we have investigated phosphorylated proteins present during differentiation to identify key players involved in this process after cells have been treated with recombinant PP (rPP) and recombinant human BMP-2 (rhBMP-2).

#### **1.4.1 Proteomic Approaches to Understanding Stem Cell Differentiation and Signaling Pathways**

Signal transduction underlying stem cell differentiation is extremely complex. While one approach to study these complex phenomena is to assess one signaling pathway, one molecule at a time, this is a lengthy and time consuming process. Novel proteomic strategies utilizing mass spectrometry (MS) can provide a systematic and efficient way to provide insight in signaling molecules or key players involved in stem cell differentiation. The proteome of mesenchymal stem cells has been studied using MS-based methods to understand changes in signaling molecules during differentiation.[77] Global proteomic analyses of osteoblast differentiation from hMSCs has been studied using 2D-polyacrylamide gel electrophoresis (PAGE)-MS.[78] Aside from the identification of signaling proteins involved in differentiation, utilizing quantitative methodologies in combination with mass spectrometry will provide the ability to

determine proteins that are up- or downregulated in response to treating stem cells with specific stimuli.

#### **1.4.1.1 Quantitative Proteomics**

A variety of MS-based quantification techniques exist to determine relative protein abundance changes in samples include metabolic labeling such as stable isotope labeling of cells in culture (SILAC), chemical labeling such as isobaric tag for relative and absolute quantitation (iTRAQ) or isotope coded affinity tags (ICAT), and difference in-gel electrophoresis (DIGE).[79, 80] Studies utilizing these techniques can differentially compare proteomes on a global scale from which specific information regarding signaling networks and pathways may be revealed in order to determine divergent signaling mechanisms from different treatment conditions. In a recent study using the iTRAQ technology, embryonic stem cell differentiation during noggin induced neural and BMP-4 induced epidermal ectoderm was investigated.[81] A recent SILAC study discovered how epidermal growth factor (EGF) could stimulate mesenchymal stem cell differentiation into osteoblasts but not platelet derived growth factor (PDGF). Although more than 90% of the signaling proteins were used by both ligands, it was found that the PI3K pathway was activated by PDGF but not EGF resulting in a much different effect on the cells.[82] Quantitative proteomics has also been used to profile the differential expression of membrane proteins of a hMSC cell line during osteoblast differentiation.[83] We used a SILAC-based global proteomics approach to further investigate the signaling pathways involved in stem cell differentiation into the osteogenic and odontogenic lineages stimulated by BMP-2 and PP respectively.

### 1.4.1.2 Phosphoproteomics

Protein phosphorylation is one of the most relevant and ubiquitous posttranslational modifications and it plays significant roles in cellular processes. Signals received from outside of the cells travels through a cascade of phosphorylation events of multiple proteins into the nucleus. An evaluation of the phosphoproteome presents an opportunity to identify and quantify these signaling proteins to better understand the cascade of events and processes leading to cellular transformation. Phosphorylation occurs mostly on amino acids serine, threonine and tyrosine[84] with an approximate ratio of the phosphorylation of those residues in the order of 1800:200:1.[85] Globally, phosphorylated proteins in the cell exist at diminishingly low abundances of 1-2%.[86] In order to address this analytical hurdle, several methods have been developed for enriching phosphopeptides from these complex mixtures including immunoprecipitation using phosphospecific antibody such as anti-phosphotyrosine, immobilized metal affinity chromatography (IMAC) with  $\text{Fe}^{3+}$ ,  $\text{Ga}^{3+}$ , or  $\text{Al}^{3+}$ , and titanium dioxide ( $\text{TiO}_2$ ).[87] Each of these techniques have been shown to have different phosphoenrichment efficiencies[88, 89] and therefore each technique must be specifically suited to the experimental design in question. With the recent successes that have been demonstrated using the  $\text{TiO}_2$ -based methodologies, we have utilized that workflow to evaluate the signaling events involved in differentiation following treatment with PP or BMP-2 .[90, 91]

## 1.5 HYPOTHESES

Hypothesis 1: Pericytes are a stem cell population residing in the dental pulp.

Hypothesis 2: PP plays a signaling role in stem cell differentiation toward the osteoblastic/odontoblastic lineage.

Hypothesis 3: SILAC-based MS will efficiently quantify proteins identified from C3H10T1/2 cells treated with PP and BMP-2.

In order to support these hypotheses, the following specific aims have been developed

## 1.6 SPECIFIC AIMS & RATIONALE

### 1.6.1 Specific Aim 1: Characterization, identification, and isolation of dental pulp stem cells (pericytes)

I will characterize and identify pericytes from human dental pulp by IHC using different combinations of marker antibodies, flow cytometry techniques that relies on a combination of surface markers CD146+CD34-CD45-CD56-. In addition, I will characterize that the sorted pericytes are clonogenic and have multilineage differentiation potential.

### **1.6.2 Specific Aim 2: Identification of cell surface receptors and signaling crosstalk in PP signaling in hMSCs.**

I will identify integrin receptor involvement in PP signaling and assess the crosstalk between the MAPK and Smad1 pathways.

### **1.6.3 Specific Aim 3: Proteomic profiling of mouse embryonic fibroblasts (C3H10T1/2) during differentiation into osteoblasts and odontoblasts.**

I will use SILAC to quantify the proteins identified from C3H10T1/2 cells treated with PP and BMP-2.

### **1.6.4 Rationale of Different Cell Types Selected for Each Aim**

The rationale of using different cell types in each of the specific aims is as the following. In specific aim 1, dental pulp pericytes were studied due to the interest in isolating a novel stem cell population. Although it would be interesting to test their response to PP, the cell numbers obtained were insufficient for those required for specific aim 2. In addition, studies of PP signaling were based on previous work in our lab which was done in hMSCs. Therefore, we chose to use hMSCs for the second aim of this thesis. For specific aim 3, our original thoughts were to use dental pulp pericytes or hMSCs for studying the effect of PP and BMP-2 on odontogenic/osteogenic differentiation. However, in order to achieve successful labeling of heavy amino acids in cell culture, cells were required to be cultured for at least five doubling times. Also, a large quantity of cells is required for mass spectrometry of the phosphoproteome.

In this case, dental pulp pericytes would not be suitable due to the limited number of cells obtained from FACS. hMSCs are also not suitable because cells might differentiate or stop proliferation after multiple passages during heavy amino acid labeling. Therefore, mouse embryonic fibroblasts C3H10T1/2 cells, which have multilineage differentiation potential and can be expanded extensively in culture, were selected for the SILAC experiments.

## **2.0 MULTILINEAGE POTENTIAL OF PERICYTES SORTED FROM HUMAN DENTAL PULP**

### **2.1 SUMMARY**

We document the existence of a perivascular stem cell population in the human dental pulp. Pericytes in human dental pulp were characterized by immunohistochemistry as expressing CD146,  $\alpha$ -smooth muscle actin ( $\alpha$ -SMA), NG2, but negative for CD34, von Willebrand factor (vWF), CD45 and CD56 expression. This phenotypic description provided the basis for the purification by flow cytometry of perivascular CD146<sup>+</sup>CD34<sup>-</sup>CD45<sup>-</sup>CD56<sup>-</sup> cells from the dental pulp. Long-term cultured dental pulp perivascular cells are clonogenic colony forming units-fibroblast, express the mesenchymal stem cell markers CD44, CD166 and CD90, and give rise to osteoblasts, chondrocytes and adipocytes *in vitro*. These results suggest that mesenchymal stem cells previously isolated from the dental pulp have a perivascular origin. Pericytes sorted to homogeneity from extracted dental pulp, then multiplied in culture may represent a convenient source of therapeutic progenitor cells.

## 2.2 INTRODUCTION

The development of effective therapies for craniofacial regeneration is a clinically important long-term goal in the tissue engineering field. Craniofacial diseases and disorders ranging from periodontal disease and its associated bone loss to birth defects such as cleft lip and palate, to craniosynostosis, to injuries to the head and face, to devastating head and neck cancers require extensive surgery and would obviously benefit from innovative regenerative cell therapies. Dental pulp stem cells (DPSCs) were first described by Gronthos et al., who showed the capabilities of these cells to become osteoblastic *in vitro* and form dentin-like structures *in vivo*. [32] Characterization and isolation of the DPSCs will provide an understanding of the potential of these cells in craniofacial regeneration and dentin repair in the event of an injury. DPSCs are believed to be pericyte-like cells that migrate towards the pulpal injury site. [34, 92] Pericytes, also known as Rouget cells or mural cells, reside around the endothelium of microvessels (capillaries and postcapillary venules), hence are distributed throughout the vasculature with diverse roles in the regulation of blood flow and vessel formation. [8] For a long time, pericytes under study were not sorted, but identified in primary cultures by morphology, slow adhesion to plastic and expression of pericyte-associated (but not pericyte-specific) antigens such as 3G5, NG2, CD146, Stro-1,  $\alpha$ -SMA, desmin and osteonectin. [7, 8, 11, 18, 24, 93]

Two groups including our own have recently shown that perivascular cells can be purified from multiple human organs including placenta, pancreas, fat and muscle and showed the multilineage developmental potential of these cells, suggesting the perivascular origin of the elusive mesenchymal stem cells (MSC). [93-98] Pericytes are therefore of potential interest for regenerative medicine. While pericytes are ubiquitous in the body, harvesting these cells for autologous transplantation should be easy but from a richly vascularized organ, of no risk for the

patient and minimally invasive, hence the interest of human tissues that are shed naturally, such as fetal appendages and teeth. Teeth, which are lost in the course of normal development (primary teeth), and commonly extracted in young adults in the case of wisdom teeth, can be envisioned as a source of such autologous stem cells, especially since dental pulp is rich in blood vessels. In the present study, we have identified and purified perivascular cells present in human dental pulp. Our approach has relied first on immunohistochemistry (IHC) experiments to determine the presence of cell surface markers that could be utilized to sort dental pulp pericytes. We then confirmed that sorted dental pericytes could be expanded in culture and are multilineage mesodermal progenitors.

## **2.3 MATERIALS AND METHODS**

### **2.3.1 Antibodies**

Unconjugated antibodies used were mouse anti-human CD146, -CD34, -NG2, -CD56, -CD44, -CD90 (BD Biosciences), -CD45 (DAKO), rabbit anti-human CBFA-1/Runx-2, -osteocalcin, -PDGFR- $\beta$  (Santa Cruz Biotechnology). Conjugated antibodies included mouse anti-human CD146-Alexa488 (Chemicon), -CD146-FITC (AbSerotec), -CD45-PE-Cy5, -CD56-PE-Cy7 (BD Biosciences), - $\alpha$ -SMA-FITC (Sigma), -CD34-PE (DAKO), -CD166-biotin (Ancell), sheep anti-human vWF-FITC (US Biological), rabbit anti-human CD144-biotin (BMedSystems), donkey anti-rabbit-Alexa488, donkey anti-rabbit- Alexa594 (Molecular Probes), goat anti-mouseIgG biotin (DAKO), goat anti-mouse-IgM biotin ( $\mu$ ) (Caltag Laboratories), mouse IgG-PE, mouse

IgG-FITC (Chemicon), mouse IgG-PE-Cy7, mouse IgG-PE-Cy5 (BD Biosciences) and sheep IgG-FITC (US Biological).

### **2.3.2 Tooth Procurement and Cell Isolation**

We obtained 85 adult third molars (age 14-23 years) at the School of Dental Medicine, University of Pittsburgh, as approved by the Institutional Review Board (IRB number: 0312073). Dental pulp was digested with collagenases I, II, and IV (each at 1 mg/mL, Sigma) at 37 °C for 2 h under gentle agitation. Cell suspensions were passed through a 70 µm cell strainer (BD Falcon) to obtain single-cell suspensions.

### **2.3.3 Immunohistochemistry**

Dental pulps were frozen in Tissue Freezing Medium (Triangle Biomedical Sciences) and cryosectioned at 5-µm thickness. Tissue sections were fixed in ice cold 50% methanol and 50% ethanol for 5 min, air dried for 15 min and then incubated with 5% goat serum (Gibco) in PBS for 1 h at room temperature (RT) to prevent antibody non-specific binding. Tissue sections were incubated with primary antibody (1:100 dilution, same dilution for all primary antibodies) overnight at 4 °C. Appropriate secondary antibodies were used (1:1000 dilution) for 1 h followed by streptavidin coupled to Cy3 (1:1000 dilution, Amersham) for 30 min at RT. When two antibodies were used simultaneously, the sections were incubated for 1 h at RT with a second primary antibody that was already conjugated with either Alexa-488 or FITC. The sections were then stained with 4',6-diamidino-2-phenylindole (DAPI, 1:2000 dilution, Molecular Probes) for 5 min at RT to visualize nuclei. Coverslips were mounted with Gel/Mount mounting medium

containing anti-fading agents (Biomedica Corp.). Fluorescent images were acquired by optical and confocal microscopy using Nikon Eclipse TE2000-U and Olympus FLUOVIEW FV1000 microscopes, respectively.

#### **2.3.4 FACS and Cell Culture**

Freshly digested dental pulp cells were washed with phosphate buffered saline (PBS, Gibco) and stained with CD146-FITC, CD34-PE, CD45-PECy5 and CD56-PE-Cy7 antibodies for 30 min at 4 °C (1:100 dilution). Cells were then washed with PBS and resuspended in 1ml of Endothelial Cell Growth Medium 2 (EGM-2, Cambrex Bioscience Inc.). A FACSAria dual-laser fluorescence activated cell sorter (Becton-Dickinson) was used to isolate CD146+CD34-CD45-CD56- cells as previously described.[98]

Sorted cells were cultured at 37 °C, 5% CO<sub>2</sub> in EGM-2 on 48-well tissue culture plates coated with 2% gelatin (Calbiochem) at 10,000 cells per cm<sup>2</sup>. After cells attached to the culture plate, medium was changed to high-glucose DMEM high glucose (GIBCO) with 20% fetal bovine serum (FBS, Atlantic Biological) and 1% penicillin-streptomycin (GIBCO).

#### **2.3.5 Colony Forming Units-fibroblast (CFU-f) Assay**

Cultured dental pulp perivascular cells were seeded at a density of 100 cells/10cm<sup>2</sup> and cultured for two weeks to test their clonogenic ability. Cells were fixed with 100% methanol for 5 min, air dried for 5 min and stained with 3% Crystal violet (Sigma) for 5 min at RT. Cells were washed with distilled water and colonies (>2.5 mm or 50 cells) were counted. Percentage of CFU was calculated as the number of colonies counted divided by the number of cells plated, then

multiplied by 100. Pericytes isolated from dental pulp of three patients were analyzed. Six plates of colonies were counted and scored for each donor.

### **2.3.6 Immunocytochemistry**

Sorted dental pulp cells were seeded in 48-well tissue culture plates. Cells were fixed in 1% paraformaldehyde (PFA) in PBS or a mixture of ice-cold acetone and methanol (1:1). Cells were washed with PBS, blocked with 5% goat serum, and then incubated with primary and secondary antibodies. To detect Runx-2 expression, cells were permeabilized with 0.1% Triton X-100 (Sigma) during blocking and incubation with antibodies.

### **2.3.7 Osteogenic Differentiation**

Dental pulp perivascular cells were seeded at 25,000 cells/cm<sup>2</sup> in 6-well tissue culture plates and cultured in control medium (high-glucose DMEM with 20% FBS, 1% PS) or osteogenic medium for two weeks. Osteogenic medium is control medium supplemented with 50 µg/mL L-ascorbic acid (Fisher Biotech), 100 mM β-glycerolphosphate (Sigma), and 100 nM dexamethasone (Sigma). Medium was changed every 3 days. Cells were then fixed and subjected to alkaline phosphatase and von Kossa stainings.

Cells were washed with PBS and fixed with 4% PFA for 15 min at 4 °C. For alkaline phosphatase staining, cells were incubated with a solution containing 5 mg naphthol AS MX-PO<sub>4</sub> (Fisher Scientific) dissolved in 0.2 mL *N,N*-dimethylformamide, 25 mL Tris-HCl (0.2 M, pH 8.3, Sigma), Red Violet LB salt (30 mg, Sigma), and 25 mL distilled water for 45 min at RT. Cells were washed three times with distilled water, then incubated with 5% silver nitrate (Sigma) at

RT for 30 min and then rinsed with distilled water three times. Cells were examined and imaged by bright field microscopy. Alkaline phosphatase activity was measured quantitatively using the Alkaline Phosphatase Kit (Sigma) following manufacturer's instructions. Briefly, cell lysates were incubated with alkaline phosphatase reagents at 37 °C for 30 min. Absorbance at 405 nm was measured at times 0 and 30 min. Alkaline phosphatase activity was normalized to the total protein content measured by the BCA protein assay kit (Pierce). All measurements were done in triplicate.

### **2.3.8 Chondrogenic Differentiation**

Dental pulp perivascular cells were centrifuged for 5 min at 600 x *g* into 3-dimensional pellets (250,000 cells/pellet) and cultured for 14 days in chondrogenic medium that contains high glucose DMEM, 10 ng/mL TGF- $\beta$ 1 (Peprotech), 10  $\mu$ l/mL ITS-plus premix (BD Biosciences Clontech, final concentrations: 6.25  $\mu$ g/mL each of insulin, transferrin, and selenous acid, and 1.25 mg/mL bovine serum albumin, and 5.35  $\mu$ g/mL linoleic acid), 100 nM dexamethasone (Sigma), 50  $\mu$ g/mL ascorbic 2-phosphate (Sigma). Control medium was high-glucose DMEM containing ITS-plus premix. Medium was changed every three days. Each experiment was performed in triplicates. Cell pellets were fixed in 4% paraformaldehyde, dehydrated in ethanol/xylene series, and paraffin-embedded. Five- $\mu$ m paraffin sections were stained with 1-Alcian blue (Sigma) with nuclear fast red (Sigma) counterstain or 2-Safranin O (Sigma) with fast green (Sigma) counterstain.

### **2.3.9 Adipogenic Differentiation**

Dental pulp perivascular cells were seeded at 25,000 cells/cm<sup>2</sup> in 6-well tissue culture plates and cultured in control medium (high-glucose DMEM with 20% FBS, 1% PS) or adipogenic medium for two weeks. Adipogenic medium is control medium supplemented with 0.5 mM of 1-methyl-3-isobutylxanthine (Sigma), 1 μM dexamethasone (Sigma), 0.01 mg/mL insulin (Cell Sciences), and 0.2 mM indomethacin (Sigma). Medium was changed every three days for 21 days. Each experiment was done in triplicate. Cells were fixed and stained with oil red-O (Sigma).

## 2.4 RESULTS

### 2.4.1 Identification of Perivascular Cells on Dental Pulp Sections

IHC was performed to identify the various cells that constitute vascular areas in human dental pulp using the cell surface markers listed in Table 2-1.

**Table 2-1.** Markers used for IHC

<b>Pericytes</b>	CD146, NG2, $\alpha$ -SMA, PDGFR- $\beta$
<b>Endothelial cells</b>	CD146, CD34, vWF
<b>Hematopoietic cells</b>	CD34, CD45
<b>Myoblasts, NK cells</b>	CD56

Perivascular cells that surround endothelial cells in capillaries and microvessels are anatomically defined as Pericytes.[7, 99, 100] Frozen sections of dental pulp were stained with antibodies against pericytes, endothelial cells, neural cells, and hematopoietic cells. Pericytes are pointed with arrows. Figure 2-1 A, B, G shows that pericytes in the dental pulp coexpress CD146,  $\alpha$ -SMA and NG2. Pericytes are negative for CD34, vWF and CD45 expression (Figure 2-1 C, D, E, and H). Some cells are positive for both CD146 and CD56 expression (Figure 2-1 F). We deduced that the CD146+NG2+CD34-CD45-CD56- cell surface phenotype typifies all pericytes within human dental pulp, as it does in other tissues analyzed so far.[98]

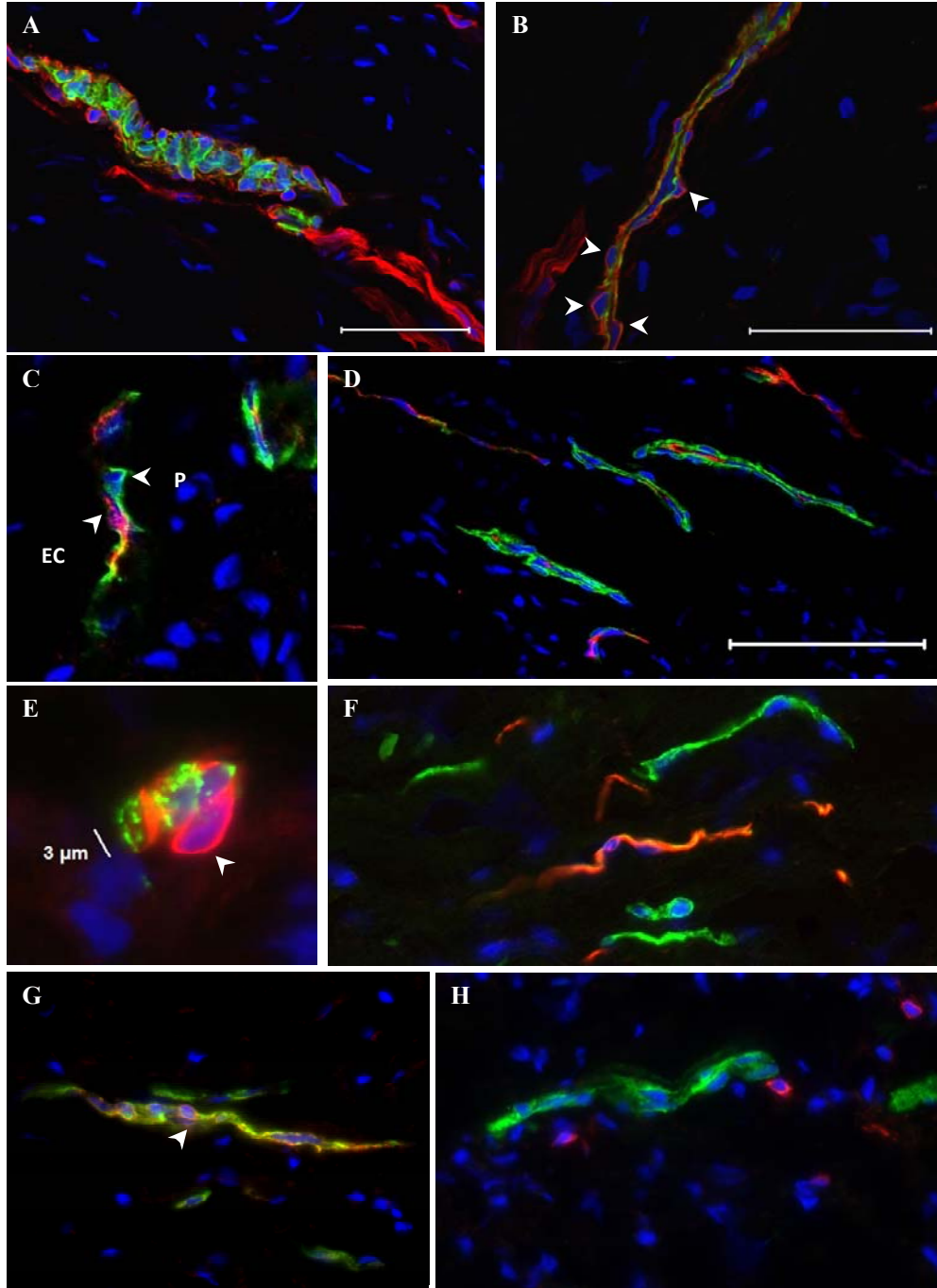


**Figure 2-1.** Immunodetection of pericytes in human dental pulp. A, B - CD146 in red)  $\alpha$ -SMA (green) C, D - CD146 (green), CD34 (red). Pericytes (P). Endothelial cells (EC). E - CD146 (red), vWF (green). F - CD146 (green), CD56 (red). G - CD146 (green) NG2 (red) H - CD146 (green) CD45 (red). Nuclei were stained blue with DAPI. A, B, D: bar = 50  $\mu$ m.

### 2.4.2 FACS of Human Dental Pulp Perivascular Cells

To isolate pericytes by flow cytometry from the enzymatically dissociated dental pulp, we first excluded CD45<sup>+</sup> hematopoietic cells and CD56<sup>+</sup> myogenic and NK cells (Figures 2-2 A, B). The dental pulp cell suspension could then be fractionated into three distinct cell populations as shown in Figure 2-2 C and outlined below:

- Endothelial cells: CD34<sup>+</sup>CD146<sup>-</sup>CD45<sup>-</sup>CD56<sup>-</sup> and CD34<sup>+</sup>CD146<sup>+</sup>CD45<sup>-</sup>CD56<sup>-</sup>
- Pericytes : CD146<sup>+</sup>CD34<sup>-</sup>CD45<sup>-</sup>CD56<sup>-</sup>
- Uncharacterized CD34<sup>-</sup>CD146<sup>-</sup>CD45<sup>-</sup>CD56<sup>-</sup> cells

CD146<sup>+</sup>CD34<sup>-</sup>CD45<sup>-</sup>CD56<sup>-</sup> pericytes were isolated. Pericytes represent  $0.62 \pm 0.41\%$ , whereas endothelial cells account for  $3.43 \pm 2.16\%$  of the total dental pulp cell population.

### 2.4.3 Clonogenic Capacity and Phenotype of Cultured Dental Pulp Pericytes

Sorted dental pulp perivascular cells were seeded in culture in EGM-2 medium on gelatin-coated plates. Cell viability was low when less than 1,000 cells were seeded after sorting. Cell viability increased when more cells were initially seeded. Cells attached to the bottom of the wells in approximately 48-72 h. One week after culture initiation, EGM-2 medium was replaced by DMEM supplemented with 20% FBS. Recently attached cells exhibited mixed elongated, spindle and polygonal shapes. After cells were passaged once, they exhibited star-like shapes with prominent nuclei and multiple cytoplasmic extensions (Figure 2-2 D, Bar = 100  $\mu\text{m}$ ).

The clonogenic capacity of cultured pericytes was determined by using the CFU-f assay. Cells were seeded at a low density of 100 cells/10cm<sup>2</sup> and colonies were observed on day 14 by crystal violet staining. *In vitro* cultured dental pulp pericytes are highly clonogenic,  $98 \pm 2\%$  of

these being CFU-f (Figure 2-2 E). Cultured pericytes at passage eight, i.e. cultured for two months, maintained expression of the pericyte markers CD146, NG2 and  $\alpha$ -SMA (Figure 2-2 F-H) and remained negative for vWF, CD144, CD45 and CD56 expression (not shown). All cultured pericytes were also positive for PDGFR- $\beta$  (Figure 2-2 I). These results show that sorted pericytes were not contaminated by other cell types and did not change their antigenic characteristics when proliferating in culture. To further characterize cultured dental pulp pericytes, we tested their expression of several mesenchymal stem cell markers. Cultured pericytes express the MSC markers CD44, CD90 and CD166 (Figure 2-2 J, K, L). Pericytes in culture express in addition both Runx-2 and osteocalcin, suggesting their inherent osteogenic capability (Figure 2-2 M, N).

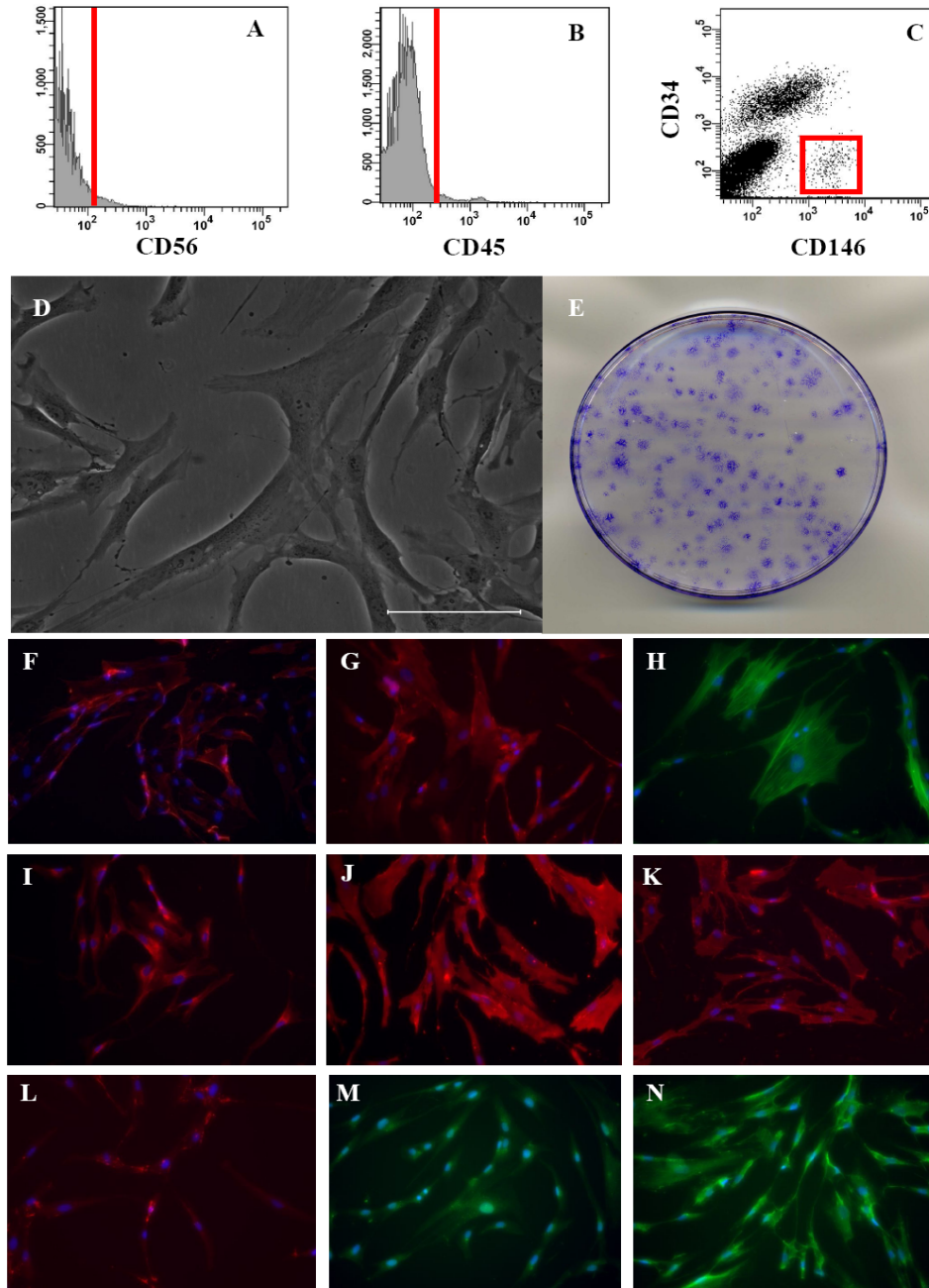


**Figure 2-2.** FACS, morphology, CFU-f analysis, and immunocytochemistry of cultured dental pulp pericytes. A, B – exclusion of CD56+ and CD45+ cells. C - Selection of CD146+CD34- population. D - Pericytes morphology. E - CFU-f analysis. F – CD146 (red), G – NG-2 (red), H –  $\alpha$  SMA (green), I – PDGFR- $\beta$  (red), J – CD44 (red), K – CD90 (red), L - CD166 (red), M – Runx2 (green), N – Osteocalcin (green). Nuclei were stained blue with DAPI. D:

Bar = 100  $\mu$ m. F-N: 20x magnification.

#### **2.4.4 *In vitro* Multilineage Differentiation of Cultured Dental Pulp Pericytes**

Cultured pericytes were successfully differentiated into osteocytes, chondrocytes and adipocytes *in vitro*. For osteogenic differentiation, pericytes were cultured in medium containing  $\beta$ -glycerol phosphate and dexamethasone. Alkaline phosphatase assay and von Kossa staining were used to characterize the progeny of pericytes grown in these conditions. Mean alkaline phosphatase activity of pericytes cultured in control and osteogenic medium after one week was  $430.24 \pm 111.02$  and  $910.77 \pm 406.15$  U/mg total protein, respectively. We therefore observed an approximate 2.1-fold increase in the experimental group when compared to the control. After two weeks of culture, pericytes cultured in osteogenic medium maintained higher alkaline phosphatase activity than control cultured cells and mineralization was revealed by von Kossa staining (Figure 2-3 A, B). To induce chondrogenic differentiation, pericytes were cultured as pellets maintained in differentiation medium containing TGF $\beta$ -1. After three weeks, pellets exhibited cartilage-like round, smooth and shiny surfaces. Proteoglycans were synthesized by differentiated chondrocytes as shown by Alcian blue and safranin O staining of pellet sections (Figure 2-3 C, D, 20x). Lacuna eye structures were observed in the cell pellets, confirming the chondrogenic differentiation of pericytes (Figure 2-3 E, 40x magnification). Alcian blue and safranin O did not stain pellets cultured in control medium, and no lacuna eye structures were observed (data not shown). For adipogenic differentiation, pericytes were cultured in medium containing 1-methyl-3-isobutylxanthin, dexamethasone, insulin and indomethacin. Pericytes began to differentiate, as shown by the appearance of lipid vesicles in the cytoplasm, at week 3 (data not shown). Pericytes cultured in adipogenic medium for 5 weeks contained accumulated lipid droplets. Oil red O brightly stained mature adipocytes (Figure 2-3 F).

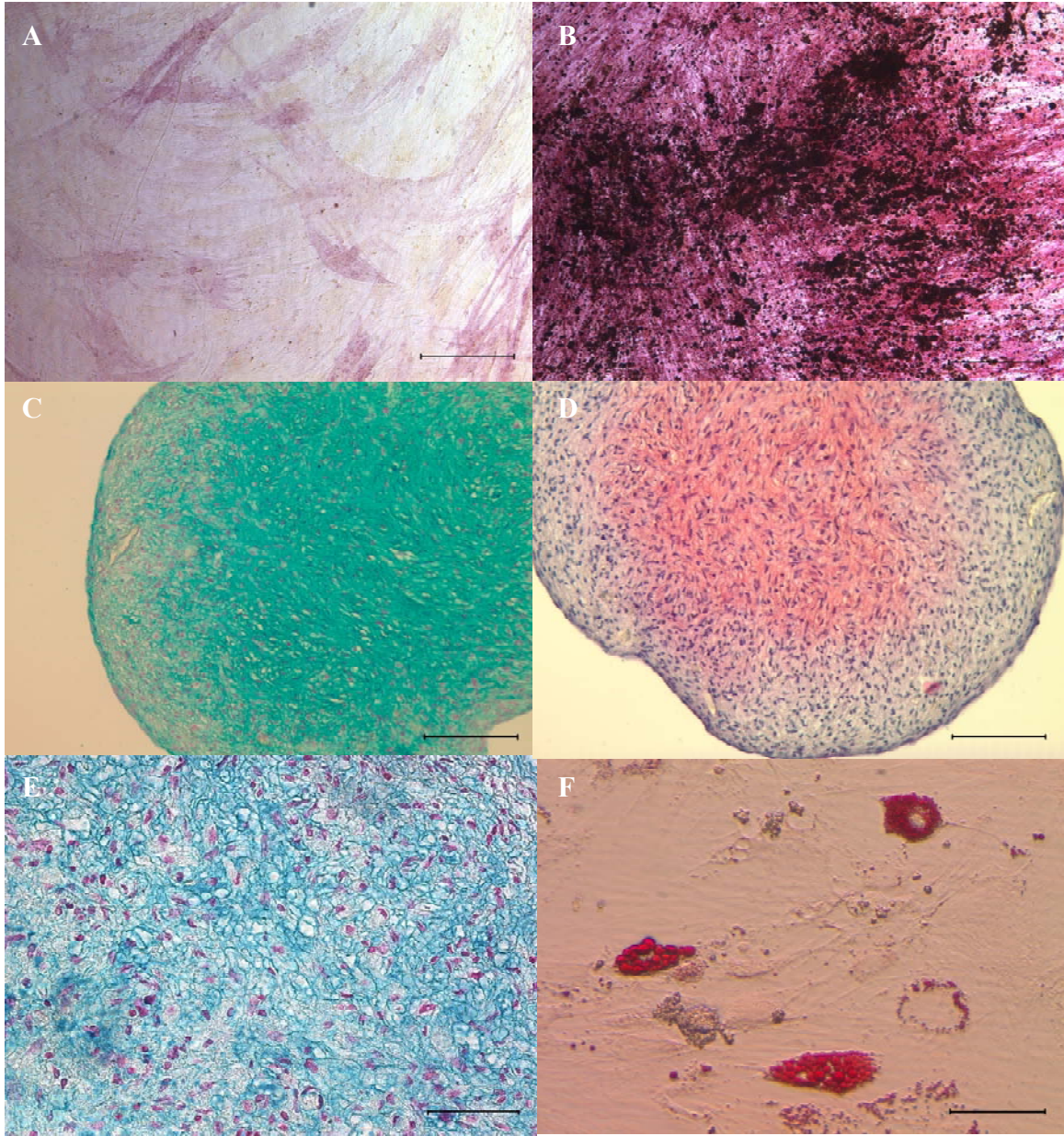


**Figure 2-3.** Multilineage differentiation of cultured dental pulp pericytes. A, B - alkaline phosphatase and von Kossa stainings of pericytes cultured in control or osteogenic media. C, E – Alcian blue and D – Safranin O stainings of pellet section of cells cultured in chondrogenic media. F – Oil red O staining of cells cultured in adipogenic media. A-D: bar = 100  $\mu\text{m}$ , E-F: bar = 50  $\mu\text{m}$ .

## 2.5 DISCUSSION

There is an enormous need to develop safe and effective methods to regenerate soft and hard tissues for craniofacial diseases such as head and neck cancers, trauma, birth defects, periodontal disease and pulp injuries. Cellular approaches provide an attractive option to develop therapies targeted for the craniofacial regeneration. Engineering cellular therapies for craniofacial regeneration requires the understanding of the cells and their regenerative potential. Current studies have focused on isolating dental pulp stem cells by utilizing different enrichment techniques, markers and various multi-lineage differentiation assessments. Many such studies used the total population of dental pulp cells and only few reported the characterization and tentative isolation of dental pulp stem cells using flow cytometry. Shi et al. were the first to characterize and compare different dental pulp candidate stem cell populations.[3] They have isolated clonogenic populations of DPSCs by their ability to adhere to plastic, similar to bone marrow stromal cells.[32] Colony-derived DPSCs formed mineralized nodules *in vitro* and generated dentin-pulp-like tissue *in vivo*. [29, 30] Using similar methods, Shi's group also isolated stem cells from human exfoliated deciduous teeth (SHEDs) and showed that these cells are clonogenic and able to differentiate into neural cells, adipocytes and odontoblasts *in vitro* as well as osteogenic and odontogenic cells *in vivo*. [31] Alliot-Licht et al. have utilized total pulp cells and have shown that a population of  $\alpha$ -SMA positive cells can form mineralized nodules *in vitro*, suggesting that the bone/dentin progenitors are perivascular cells. [33, 101] The reports mentioned above suggested that the dental pulp stem cells reside in the perivascular niche. Our group has recently demonstrated that one of the sources, if not the only one, of mesenchymal stem cells in multiple tissues is the pericyte. [98] We now extend this notion and hypothesize that pericytes are, or include, a stem cell population in the dental pulp.

We have focused on identifying and characterizing the dental pulp stem cells in the perivascular niche. Our data show that dental pulp perivascular cells express the pericyte markers CD146, SMA and NG2, but not the endothelial cell markers CD34 and vWF. These data agree with previous studies by our group and others pertaining to the isolation of pericytes from other tissues.[3, 25, 95] We have shown that CD146+CD34-CD45-CD56- sorted dental pulp pericytes are highly clonogenic and multipotent, as was also demonstrated for pericytes derived from other human tissues.[94] Cultured pericytes express CD44, CD90 and CD166, which also applies to mesenchymal stem cell populations from various tissues.[32, 102-104] This further suggests that MSCs are derived from perivascular cells.

With regard to the role of pericytes in mineralized tissues and their potential to differentiate into bone and dentin, we have shown that sorted dental pulp pericytes express Runx-2 and osteocalcin without the addition of  $\beta$ -glycerolphosphate or dexamethasone. Our data agree with previous reports showing that perivascular cells behave like osteoblasts *in vitro* even without addition of  $\beta$ -glycerolphosphate.[20, 21] In the presence of  $\beta$ -glycerolphosphate or dexamethasone, dental pulp pericytes become mineralized in a similar manner as perivascular cells from other tissues such as the retina, brain, epididymal fat pad, skin, lung, placenta and aorta.[8, 10, 18, 19, 95] Furthermore, pericytes from bovine retinal microvessels at different stages of differentiation express alkaline phosphatase, Runx-2, osteopontin, osteonectin, osteocalcin and bone sialoprotein.[10, 15] The studies above demonstrated the osteogenic potential of pericytes *in vitro*. *In vivo*, bovine retina pericytes and CD146+CD34-CD45-CD56-sorted pericytes also formed bone.[94] In addition, CD146+ dental pulp cells form ectopic dentin in immunocompromised mice.[3] Together, these results suggest the potential use of dental pulp pericytes for engineering mineralized tissues such as bone and dentin.

Our data clearly demonstrate that we have successfully isolated pericytes from human adult dental pulp as CD146+CD34-CD45-CD56- cells. This approach provides us with a well-characterized stem cell population of high purity that can be expanded and differentiated. Dental pericytes should therefore be amenable to study and develop targeted dental therapies as well as bone regeneration strategies. Specifically, dental cell therapies have recently garnered a lot of attention. Dentin, dental pulp, and cementum-periodontal complex regeneration has been shown with DPSCs, SHEDs and periodontal ligament stem cells.[105] Root-periodontal complex regeneration has been shown with cells from apical papilla and periodontal ligament.[106] Hard tissue formation with rat dental pulp cells has also been shown *in vivo*. [107] FACS isolated dental pulp pericytes provide a unique cell source to assess the *in vivo* differentiation potential of these cells into dental tissues. Due to the availability of milk teeth and extracted adult teeth, dental pulp pericytes can provide a convenient source of therapeutic cells to regenerate dental tissues as well as tissues of other mesodermal lineages such as bone, cartilage and fat.

## 2.6 ACKNOWLEDGMENTS

We acknowledge Alison Logar for her assistance in flow cytometry. We thank Dr. William Chung and the supporting staff of the Maxillofacial Surgery department, Kathy Burnhady and Lori Nomides, for providing human third molars. This investigation was supported in part by a grant # DAMD17-02-1-0717 from the Department of Defense and the University of Pittsburgh.

### **3.0 PHOSPHOPHORYN SIGNALING MECHANISM IN HMSCS, INVOLVEMENT OF INTEGRINS AND CROSSTALK AMONG MAPK AND SMAD PATHWAYS**

#### **3.1 SUMMARY**

Stem cell maintenance and differentiation are directed by ECM proteins. Integrins are the key cell surface receptors that mediate cell-ECM interaction. PP, an ECM protein, has been shown to signal osteogenic differentiation in hMSCs through the MAPK and Smad pathways. PP does not activate the Smad pathway by BMP-2/4 receptor and the mechanism governing Smad activation remains elusive. We hypothesized that 1) PP signals by binding to integrins and 2) there is crosstalk between MAPK and Smad in the PP signaling mechanism. To test our first hypothesis, we used antibodies against  $\alpha\beta3$  or  $\alpha2\beta1$  to block the integrins and then treated cells with PP and monitored the downstream signaling events. We showed the involvement of integrins  $\alpha\beta3$  and  $\alpha2\beta1$  in PP signaling. Western blot showed that downstream MAPK was decreased by blocking of the integrins  $\alpha\beta3$  or  $\alpha2\beta1$ . To prove our second hypothesis, small interfering RNA (siRNA) of ERK and p38 were used to assess the effect of PP on MAPK and Smad1. We demonstrated p38 have promoting effects on both ERK and Smad1 activation while ERK has an inhibitory effect on Smad1 activation. We conclude that PP directs hMSC osteogenic differentiation through integrins  $\alpha\beta3$  and  $\alpha2\beta1$  to MAPK signaling pathways and there is signaling crosstalk between ERK and p38 and that MAPK modulates the Smad pathway during PP signaling.

## 3.2 INTRODUCTION

The ECM proteins provide structural support for the cells as well as signal cellular activities. Phosphophoryn belongs to the SIBLING family of proteins found in dentin and bone, has been shown to signal cell differentiation towards the osteogenic lineage.[57] The expression levels of osteogenic genes, such as alkaline phosphatase, runx2/cbfa1, osteocalcin, osterix, and bone sialoprotein, were upregulated in mouse fibroblast (NIH3T3), mouse osteoblast (MC3T3), and human mesenchymal stem cells (hMSCs) when stimulated with PP. We have shown previously that PP signals through integrins, MAPK, and Smad pathways.[57, 58] PP was shown to play an important role in matrix mineralization.[108, 109] PP also has a signaling role in directing cell differentiation into the osteogenic lineage. We previously reported that PP induces upregulation of osteogenic genes Runx2/Cbfa-1 and osteocalcin as well as osteocalcin protein production through the MAPK and Smad1 pathways in hMSCs.

MAPK pathways are involved in a broad range of cellular events from growth, differentiation, and development to inflammation and apoptosis.[110] The extracellular stimulus transduce its signal through MAPK leading to biological responses. MAPK pathways are mediated through a cascade of phosphorylation events by kinases. MAPK has been shown to be activated through integrin binding to the ECM.[111] PP was shown to activate ERK, JNK, and p38 components of the MAPK pathway.[57]

The Smad pathway is important in osteogenic differentiation and it is known to be activated by members of the TGF- $\beta$  family such as BMPs. When Smad1 is activated, it complexes with Smad4 and is translocated into the cell nucleus to regulate targeted gene expression.[112] In our previous study, we have shown that Smad1 is activated by PP, although not through BMP-2/4 receptor.[58] The blocking of BMP-2/4 receptor by noggin did not inhibit

the Smad1 activity stimulated by PP. How PP signals Smad1 and triggers nuclear translocation remains an unanswered question. We hypothesize that the activation of Smad1 could be attributed to signaling crosstalk between MAPK and Smad.

Integrins are the major receptors for cell adhesion to ECM proteins.[113] Integrins are a family of transmembrane proteins composed of  $\alpha$  and  $\beta$  subunits with each  $\alpha\beta$  combination having its specific binding and signaling properties.[111] We observed the gene expression of Runx2 downregulated when integrin  $\alpha\nu\beta3$  was blocked prior to PP treatment of the hMSC.[57] Therefore we deduced that PP signals through  $\alpha\nu\beta3$ . However, the runx2 expression after blocking of  $\alpha\nu\beta3$  did not return to untreated control, suggesting that other receptors such as other types of integrins might be involved. Various integrins are found in hMSCs such as  $\alpha1\beta1$ ,  $\alpha2\beta1$ ,  $\alpha4\beta1$ ,  $\alpha5\beta1$ ,  $\alpha6\beta1$ ,  $\alpha7\beta1$ ,  $\alpha\nu\beta3$ , and  $\alpha\nu\beta5$ . [114, 115] We have selected integrins  $\alpha\nu\beta3$  and  $\alpha2\beta1$  to evaluate their involvement in PP signaling because they have been shown to play a role in osteogenic differentiation and mineralization.[115-117] Integrin  $\alpha\nu\beta3$  is the predominant receptor for vitronectin while  $\alpha2\beta1$  is the receptor for laminin and collagen.[114, 115]

The specific aims of this study were to determine the involvement of integrins in PP signaling pathways and the mechanistic interactions between MAPK and Smad signaling pathways in hMSCs. To determine the involvement of integrins in PP signaling pathways, I looked specifically at the involvement of  $\alpha\nu\beta3$  and  $\alpha2\beta1$  by blocking them with antibodies prior to treatment with PP. I examined the MAPK activated by PP after blocking of the integrins. I examined the crosstalk between MAPK and Smad by siRNA. The activity of ERK was knocked down by siRNA and its effect on Smad and p38 was evaluated. p38 was also knocked down by siRNA and its effect on ERK and Smad1 was examined. For the siRNA study, we have treated

cells with either full-length PP (F-PP) or recombinant PP (rPP), a truncated version of F-PP, to evaluate their signaling effect on hMSCs.

### 3.3 MATERIALS AND METHODS

#### 3.3.1 Antibodies

Primary antibodies used were mouse anti-human  $\alpha v\beta 3$  (Chemicon), mouse anti-human  $\alpha 2\beta 1$  (Millipore), rabbit anti-human ERK (Cell Signaling Technology), rabbit anti-human phospho-ERK (Cell Signaling Technology), rabbit anti-human JNK (Cell Signaling Technology), rabbit anti-human phospho-JNK (Cell Signaling Technology), rabbit anti-human p38 (Cell Signaling Technology), phospho-p38 (Cell Signaling Technology), rabbit anti-human phospho-smad1 (Cell Signaling Technology), rabbit anti-human smad1 (Cell Signaling Technology). Secondary antibody used was goat anti-rabbit IgG (H&L), HRP-linked (Cell Signaling Technology).

#### 3.3.2 Generation of rPP

Recombinant PP (rPP) was generated as previously described.[57] Isolated mouse genomic PP was used as a template to amplify exon 5 by PCR. The primers used were designed with Sall and XbaI at the 5'-ends of the gene-specific sequence for rPP; PstI and XhoI for F-PP. rPP and full-length rPP were generating using the following primers. The primers used for rPP were CTAATGTCGACATGGAGAGTGGCAGCCGTGGAGA-3' (forward) and 5'-GCATTCTAGATTAAAGCACCCGCCATTCAAATCG 3' (reverse). The primers used for full-

length rPP were 5'-CTGGTTCTGCAGGGATCCCCGAATTCCG-3' (forward) and 5'-GCCGCTCGAGCTAATCATCACTGGTTGAGTGGTT3' (reverse).

The thermocycling conditions were three cycles of 94 °C for 70 s (denaturation), 52 °C for 70 s (annealing), and 72 °C for 2 min (extension) followed by 30 cycles of 94 °C for 70 s (denaturation), 62 °C for 70 s (annealing), and 72 °C for 2 min (extension). The amplified PCR fragment was inserted into the pGEX-4T-3 vector and transformed into the bacterial BL21 host cells. Cells were cultured in Luria-Bertani medium with ampicillin for 4 h at 30 °C. Protein expression was induced by 1 mM isopropyl-1-thio- $\beta$ -D-galactopyranoside for 3 h. The bacterial lysate was cleared by centrifugation and applied directly to glutathione-Sepharose 4B. After washing with PBS, the glutathione *S*-transferase-bound protein was eluted with thrombin. Thrombin was removed from eluates with *p*-aminobenzamidine immobilized on a Sepharose 4 Fast Flow matrix. rPP and F-PP was stored at -80 °C until use.

### 3.3.3 Cell Culture

hMSCs (Center for Gene Therapy, Tulane University) were cultured in Minimal Essential Medium Alpha (GIBCO) supplemented with 16.5% Fetal bovine serum (Atlanta Biologicals), 1% penicillin/streptomycin (GIBCO), and 1% L-glutamine (GIBCO) medium at 37 °C, 5% CO<sub>2</sub> with humidity. hMSCs were cultured up to passage four before use for experiments.

### 3.3.4 Blocking of Integrins

hMSCs were plated in 6-well plates and cultured until 80% confluent. Cells were serum-starved overnight. Antibodies  $\alpha v\beta 3$  or  $\alpha 2\beta 1$  (20  $\mu$ g/mL) were added to the cells for 90 min. rPP (250

ng/mL) was then added to the cells for 10, 20, or 30 min. Negative controls include cells that were not treated with either antibodies or PP as well as cells treated with the antibody only. Cells were washed twice with cold PBS then ice cold radio immunoprecipitation assay buffer (RIPA) buffer (250  $\mu$ L/well) was added and incubated on a shaker at 4 °C for 20 min. RIPA buffer was consisted of 150 mM NaCl, 1% Igepal CA-630, 0.5% sodium deoxycholate, 0.1% SDS, 50 mM Tris, pH 8.0, 1 tablet/50 mL protease inhibitor cocktail tablet (Roche). Cells lysates were collected by scraping of the wells. Cell lysates were sonicated and centrifuged at 13,000 rpm for 15 min. Supernatants were collected and stored at -80 °C until further use. Three sets of experiments were performed for each antibody and each time point was done in triplicates.

### **3.3.5 siRNA**

Cells were cultured in 6-well plates for 24 h prior to siRNA transfection. 50 nM of siRNA (p38 and ERK, Santa Cruz) were transfected using Lipofectamine 2000 (Invitrogen) for 12 h. After 72 h from siRNA transfection, the media was supplemented with 250 ng/mL of rPP or F-PP for 10, 20, 30, and 60 min. Concentration of PP and treatment time points were based on previous studies.

### **3.3.6 Western Blot Analysis**

Cell lysates were quantified by BCA protein assay kit (Pierce) and loaded equally (15  $\mu$ g) on homemade 10% SDS gels and resolved by SDS-PAGE. Gels were run at 120 V for 2 h then transferred onto PVDF membranes at 60 V for 2 h. Membranes were blocked with 5% milk and probed with primary antibodies (1:1000 dilution) overnight at 4 °C with gentle rotation.

Membranes were washed with Tris-buffered saline with Tween20 (TBST) and incubated with secondary antibody (1:8000 dilution) for 1 h at room temperature. Membranes were washed and bands were detected by chemiluminescence of HRP using Western Lightning enhanced chemiluminescence substrate (Perkin Elmer) and exposure to X-OMAT film (Kodak). Quantification of band intensities was performed by Kodak 1D 3.6 Image Analysis Software. For statistical analysis, two tailed paired student t-test was performed.

### 3.4 RESULTS

#### 3.4.1 PP Signals through Integrins $\alpha v\beta 3$ and $\alpha 2\beta 1$

To examine whether PP signal through integrins, specific antibodies against  $\alpha v\beta 3$  or  $\alpha 2\beta 1$  integrins were used to block ligand-receptor interactions. The hMSCs were then treated with PP and the downstream MAPK (p-ERK, p-JNK and p-p38) signals were detected by Western blot. Antibodies against total ERK, JNK, p38 were probed on the same membrane as loading control for western blot. p-ERK, p-JNK and p-p38 were activated after PP treatment for 10, 20, and 30 min (Figure 3-1 and 3-2). Western blot results showed PP signals through both  $\alpha v\beta 3$  and  $\alpha 2\beta 1$ . When  $\alpha v\beta 3$  or  $\alpha 2\beta 1$  were blocked prior to PP treatment, the downstream MAPK signals were downregulated. When  $\alpha v\beta 3$  was blocked, p-ERK, p-JNK, and p-p38 were downregulated at 10, 20, and 30 min (Fig 3-1). Similarly, when  $\alpha 2\beta 1$  was blocked prior to PP treatment, p-ERK, p-JNK, and p-p38 were downregulated (Figure 3-2). Band intensity of the western blots was quantified by Kodak 1D 3.6 software (Figures 3-3 - 3-8). Band intensities of p-ERK, p-JNK, and p-p38 were normalized by total ERK, JNK, and p38 then divided by the control group to obtain

percent control values. Although not all groups showed statistical significant differences ( $p < 0.05$ ), the trends are similar among different western blots performed for MAPK activation by PP with or with ought inhibition of integrins  $\alpha v \beta 3$  or  $\alpha 2 \beta 1$ .

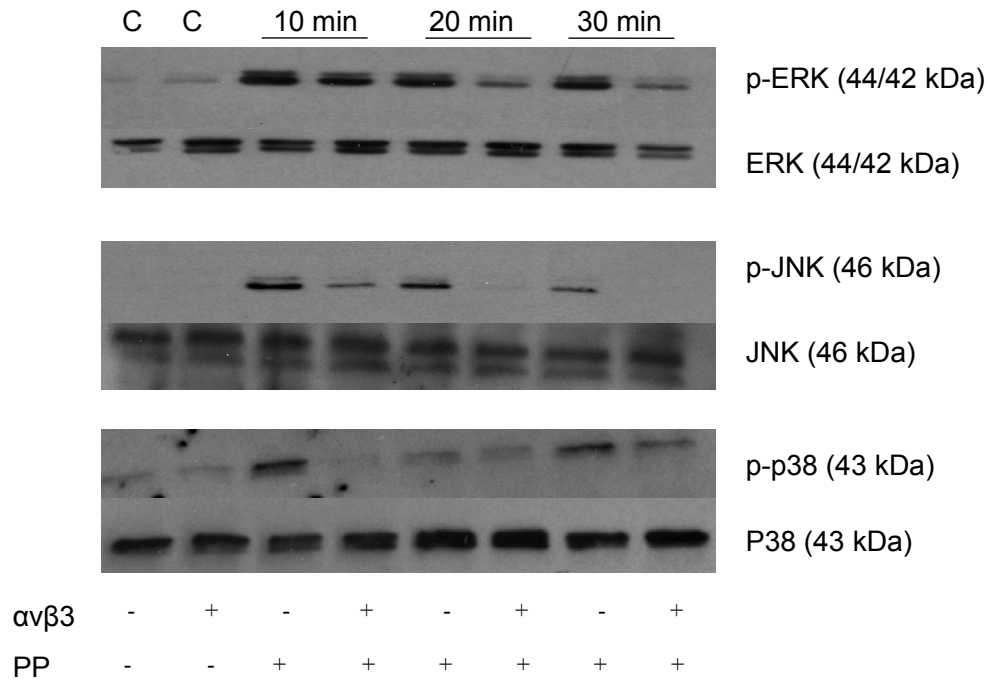


**Figure 3-1.** Blocking of  $\alpha v \beta 3$  in hMSCs prior to treating the PP.

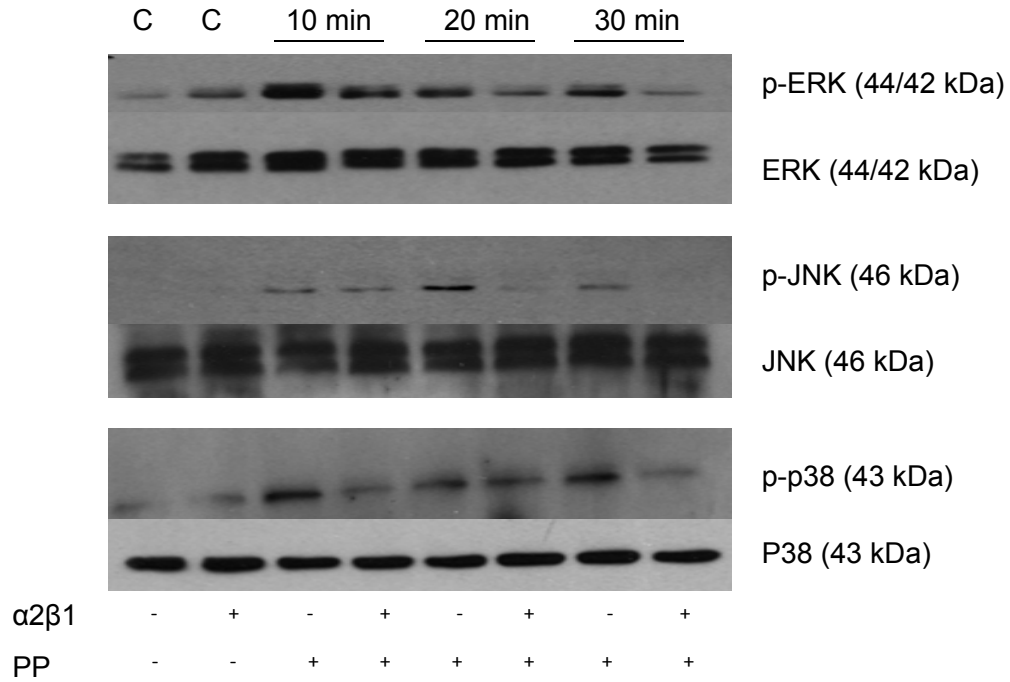


**Figure 3-2.** Blocking of  $\alpha 2\beta 1$  in hMSC prior to treating the PP.

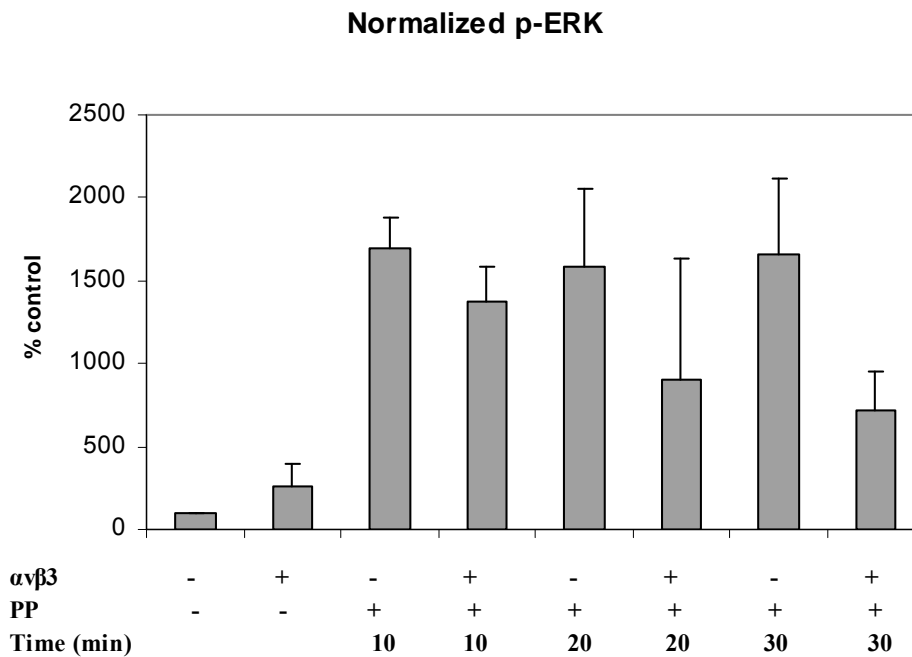


**Figure 3-3.** Blocking of  $\alpha v\beta 3$  in hMSC prior to treating the PP. Normalized p-ERK.

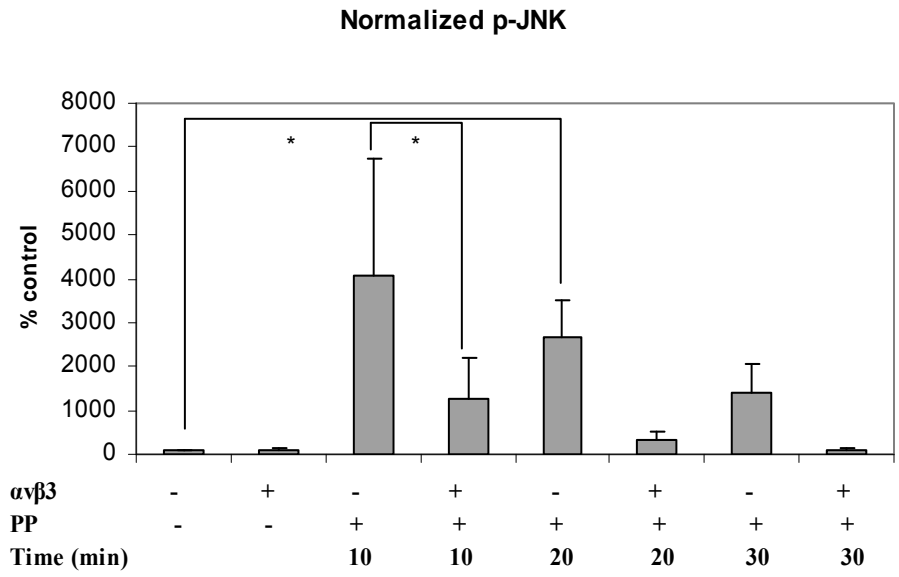


**Figure 3-4.** Blocking of  $\alpha\beta 3$  in hMSC prior to treating the PP (student t-test,  $*p < 0.05$ ). Normalized p-JNK.

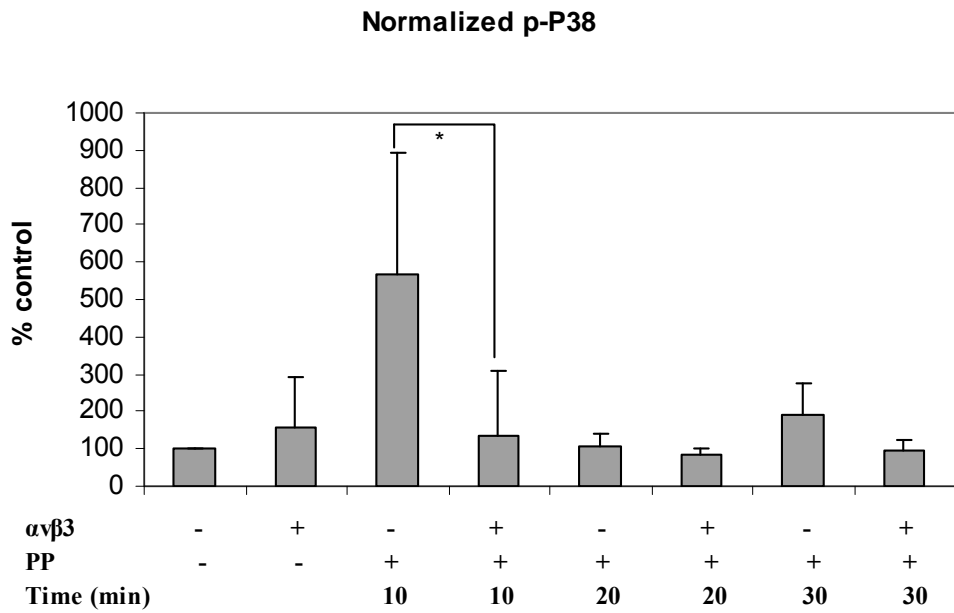


**Figure 3-5.** Blocking of  $\alpha\beta 3$  in hMSC prior to treating the PP (student t-test,  $*p < 0.05$ ). Normalized p-p38.

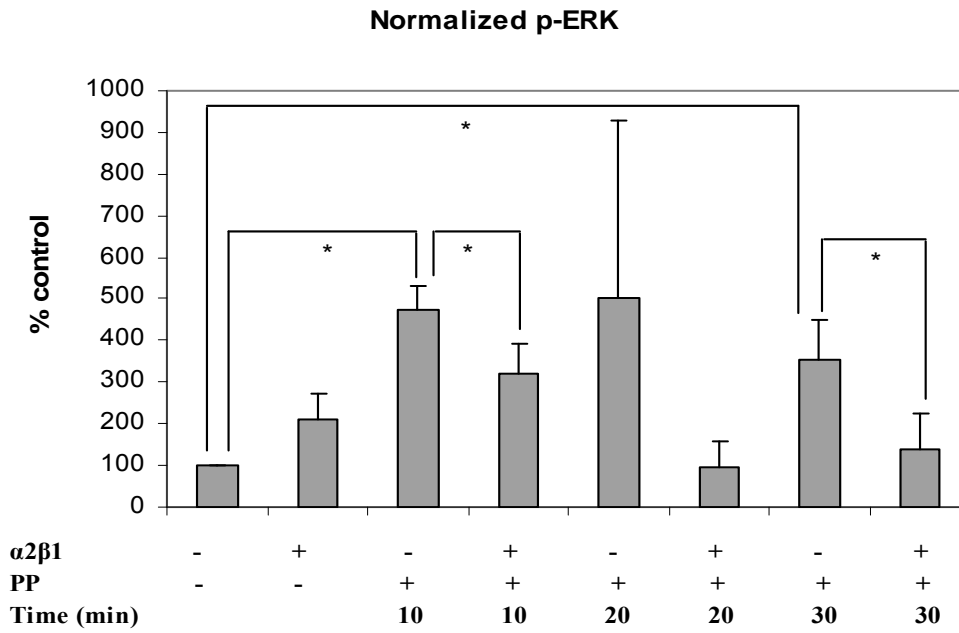


**Figure 3-6.** Blocking of  $\alpha 2\beta 1$  in hMSC prior to treating the PP (student t-test, \*p<0.05). Normalized p-ERK.

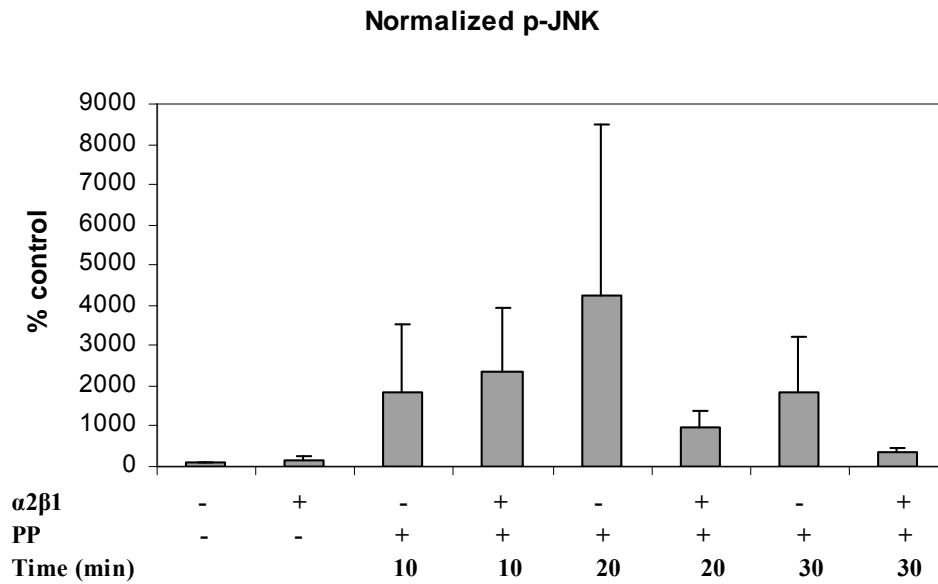


**Figure 3-7.** Blocking of  $\alpha 2\beta 1$  in hMSC prior to treating the PP. Normalized p-JNK.

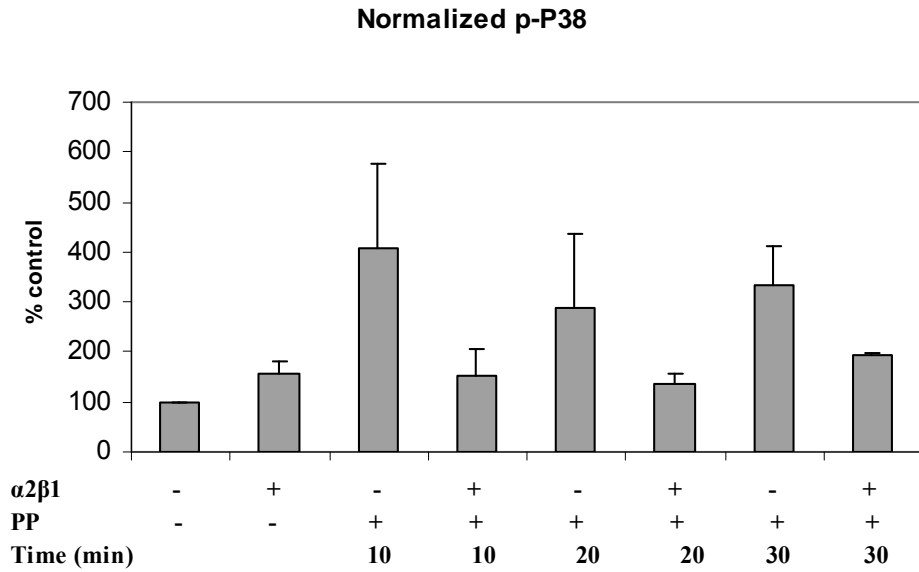


**Figure 3-8.** Blocking of  $\alpha 2\beta 1$  in hMSC prior to treating the PP. Normalized p-p38.

### 3.4.2 MAPK and Smad Crosstalk

PP's signal is channeled via both the MAPK and Smad pathways and the crosstalk among these two pathways defines the downstream effect of PP. We have performed siRNA experiments of the MAPK and assessing the effect on the Smad pathway. We knockdown ERK or p38 components of MAPK using siRNA and examine the activation of Smad1 by PP. We also knocked down ERK and look at the effect on p38 activation by PP.

### 3.4.2.1 ERK Inhibits the Activation of Smad1

hMSCs were treated with ERK siRNA and then treated with rPP or F-PP for 10, 30, or 60 min. rPP is the truncated version of F-PP and we will compare the signaling effect of both forms of PP. Figure 3-9 shows the effect of ERK knockdown on the activation of MAPK and Smad1 by rPP and F-PP. When cells were treated with ERK siRNA, we observed a decrease of phospho-ERK, ERK, Smad1. However, we observed an increase in phospho-Smad1 when ERK is knocked down. Similar results were observed for rPP and F-PP for all time points tested.

Results from siRNA experiments were in agreement with previous results obtained from chemical inhibition experiments. Activation of MAPKs influences the Smad pathway at the level of pSmad1 nuclear translocation. PP signals through the Smad pathway and when Smad1 is activated, it is complexed with Smad4 and translocated to the nucleus. To investigate the effect of ERK on Smad signaling, chemical inhibitors were used to block the activity of ERK then examine their effect on Smad1 translocation to the nucleus. When U0126 inhibited MEK-1 from phosphorylating ERK, activation of ERK was blocked by U0126, phospho-Smad1 is translocated to the nucleus after PP treatment.[118]

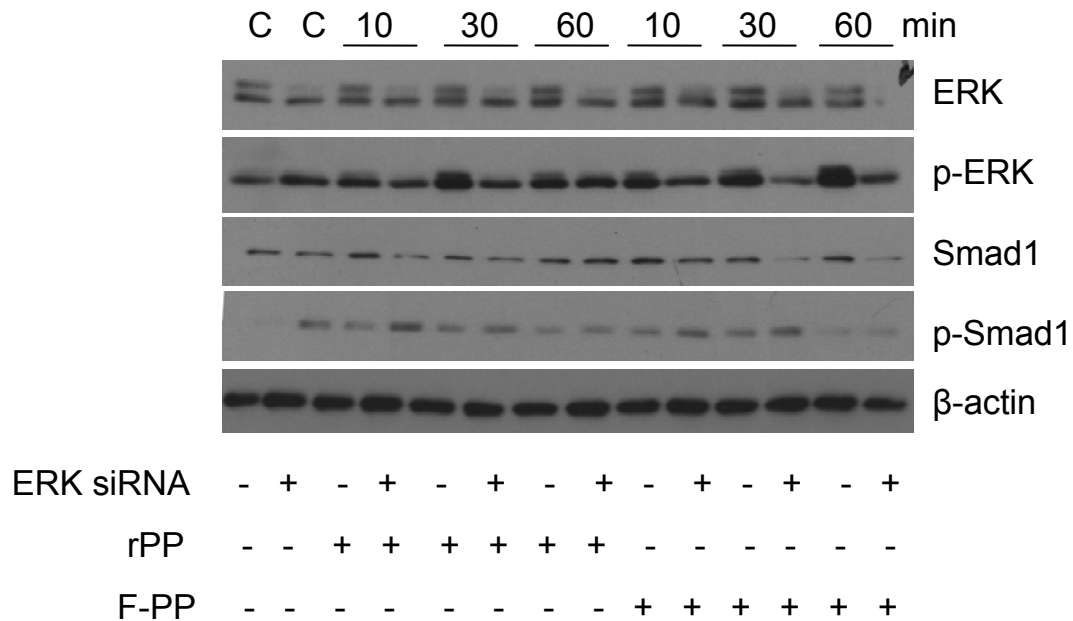


**Figure 3-9.** ERK and Smad1 activity after ERK knockdown by siRNA

### 3.4.2.2 p38 Enhances the Activation of ERK and Smad1

hMSCs were treated with p38 siRNA and then treated with rPP or F-PP for 10, 30, or 60 min. Figure 3.10 shows the effect of p38 knockdown on the activation of MAPK and Smad1 by rPP and F-PP. When cells were treated with p38 siRNA, we observed a decrease in p38, phospho-ERK, Smad1, and pSmad1. However, we observed an increase in phospho-smad1 when ERK is knocked down. Similar results were observed for rPP and F-PP for all time points tested.

siRNA results were in agreement with previous results obtained from chemical inhibition experiments. When SB203580 inhibited MAPKK3/6 from phosphorylating p38, Smad1 nuclear translocation by PP was reduced.[118]

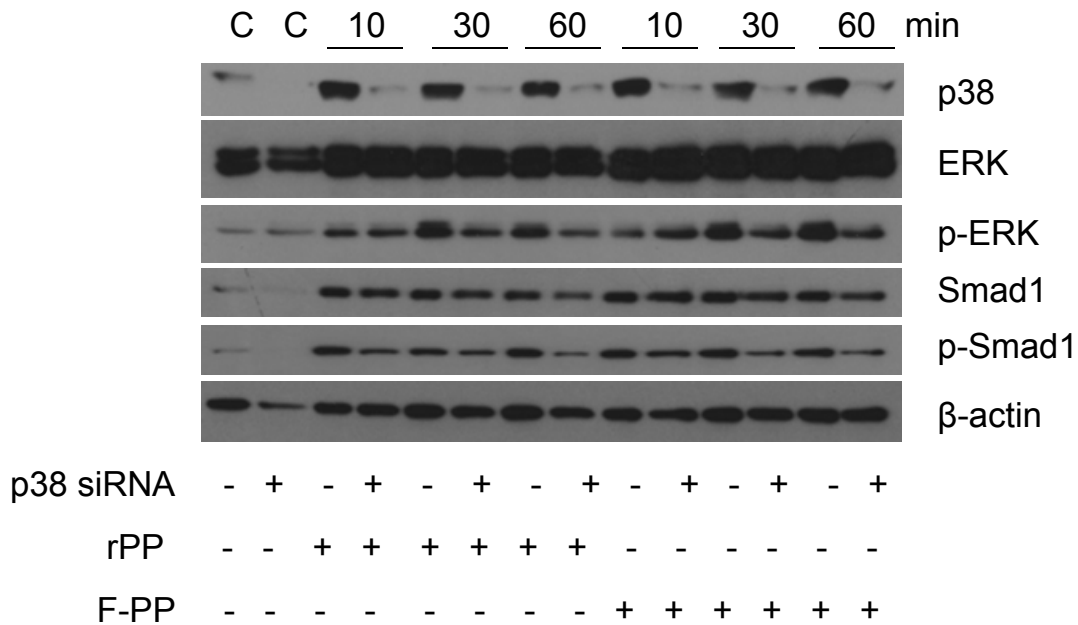


**Figure 3-10.** ERK and Smad1 activity after p-38 knockdown by siRNA

### 3.5 DISCUSSION

ECM-cell interaction plays a crucial role in stem cell maintenance and differentiation. Identifying cell surface receptors for ECM proteins is important in understanding how cells interact with the environment and ECM protein induced differentiation. In this study we report PP signal through integrins  $\alpha\beta3$  and  $\alpha2\beta1$ . Previous results showed by blocking  $\alpha\beta3$ , the gene expression of runx2 and osteocalcin downregulated in hMSCs.[57] Here we showed that the MAPK is inhibited when integrins  $\alpha\beta3$  or  $\alpha2\beta1$  are blocked. This provided explanations for the downregulation of the runx2 and osteocalcin gene expressions.

Crosstalk among signaling pathways can modulate signal transduction from ECM to the nucleus. It was unclear how Smad1 is activated during PP signaling and we have demonstrated

that MAPK modulates the Smad1 pathway. We show that there is signaling crosstalk between ERK and p38 in the MAPK pathways during PP signaling. By siRNA we showed that, 1) ERK inhibits activation and the translocation of Smad1 to the nucleus, 2) p38 enhances the activation Smad1, and 3) p38 enhances the activation of ERK. The siRNA and chemical inhibition data were both in agreement.

Our result indicated that ERK has an inhibitory effect on Smad1 activation and nucleus translocation and it is supported by the literature. Activation of ERK has been shown to have an opposite effect on the activation of Smad1. Smad1 consists of two globular domains, MH1 and MH2 domains, with a linker region between these domains that can be phosphorylated by ERK. The phosphorylation on the linker region opposes the effect of phosphorylation on the C-terminus of Smad1 by BMPs leading to inhibition of nuclear translocation of the Smad complex.[75] In addition, ERK activation by anti-BMP, FGF, IGF-II has been shown to block epidermal differentiation, ventralization of the mesoderm and neural induction by inhibition of Smad nuclear translocation.[74]

The p38 component of the MAPK pathway influences pSmad1 nuclear translocation. Our immunocytochemistry data showed that activation of p38 is required for Smad signaling and nuclear translocation. It has been shown in osteoblasts that Smad1 phosphorylation and translocation to the nucleus is suppressed when p38 is inhibited.[76] We showed that p38 not only affects the activation of Smad1, it also has a positive effect on the activation of ERK. It has been demonstrated that p38 modulates ERK signaling.[119-121]

ECM-cell interaction plays a key role in signaling cell differentiation. The processes involved in stem cell differentiation into the osteogenic lineage and mineralization are complex and remain an area of research interest. Future studies include finding additional receptors for PP

and further understanding the complex signaling events involved in hMSCs differentiation into osteoblasts. PP may signal through receptors other than the integrins and trigger signaling pathways other than the MAPK and Smad pathways. Together these signaling pathways are modulated through crosstalk and lead to transduction to the nucleus to elicit cellular response. Cellular activities are controlled by highly complex and dynamic signaling pathways. Studying how these diverse signaling pathways are integrated by defining the crosstalk among the signaling pathways is essential for understanding cell fate decisions and tissue development.

### **3.6 ACKNOWLEDGEMENT**

I would like to thank Hong Wu and Janice Kim for their assistance in western blot analysis and Jin hua Li for her contribution for the siRNA assays.

## **4.0 PROTEOMIC PROFILING OF PP AND BMP-2 DIRECTED STEM CELL DIFFERENTIATION**

### **4.1 SUMMARY**

ECM proteins can direct stem cell differentiation through a variety of complex signaling pathways. To better understand the signaling pathways involved in stem cell differentiation into the osteogenic and odontogenic lineages, we stimulated mouse embryonic fibroblasts (C3H10T1/2) with PP or BMP-2 respectively. Using a quantitative mass spectrometry approach, we identified and quantified relative protein abundance differences for 1625 and 1973 unique proteins from total cell lysates obtained from the PP and BMP-2 treated groups with ratios (treated versus control) quantified. Proteins that were determined to be significantly up- or downregulated were further scrutinized and proteins of interest were selected for validation. In addition to a global proteome analysis, the phosphoproteome was evaluated in order to identify phosphoproteins involved in PP and BMP-2 directed stem cell differentiation.

### **4.2 INTRODUCTION**

Stem cells have the ability to self-renew and differentiate into at least one of a number of different lineages.[122] Indeed, different populations of stem cells such as embryonic or adult

stem cells have very different differentiation potentials. Understanding the protein complement of these stem cell populations is important in helping to better classify their origin and to enhance our understanding of the proteins that govern cell fate decisions.[123] Multiple complex signaling events are involved during stem cell proliferation and differentiation. Recent advances in the field of proteomics provide the opportunity to identify proteins on either a global or targeted scale to study the mechanisms involved during stem cell differentiation in a systemic method.[124]

ECM proteins signal cell differentiation, typically through activation of signaling cascades by phosphorylation of participating signaling proteins. Phosphorylation of these signaling proteins transduces stimuli from outside of the cell into the nucleus to instruct transcription of specific genes involved in differentiation. An evaluation of the phosphoproteome will allow us to identify signaling pathways involved during stem cell differentiation.

Our goal is to identify and quantify proteins and phosphoproteins involved in stem cell differentiation towards the osteogenic and odontogenic lineages. In our model, we used PP and BMP-2 to stimulate C3H10T1/2 cell differentiation. PP has been shown to express in the dentin extracellular matrix while BMP-2 has been shown to stimulate osteogenic differentiation.[125] PP is a non-collagenous ECM protein found primarily in the dentin. It has been shown to signal through integrin, MAPK, and Smad pathways and upregulate Runx-2/Cbfa-1, alkaline phosphatase, OCN, and Osx genes expression in hMSCs, MC3T3 cells, and NIH3T3 cells.[57] BMP-2 belongs to the TGF- $\beta$  super family and it is known to signal through the Smad pathway.[67] Smad1 is phosphorylated by BMP-2 receptors and then, in complex with Smad4, translocates to the nucleus and participates in gene transcription with other factors such as

runx2.[126] Understanding the signaling proteins and mechanisms involved in bone and dentin is important for future mineralized tissue regeneration applications.

In this study, we utilized stable isotope labeling of amino acids in cell culture (SILAC) to identify and quantify the total proteins and phosphoproteins found during cell differentiation towards osteogenic and odontogenic differentiation by PP and BMP-2 respectively. Our preferred cells to perform this study would be hMSCs, but hMSCs are not suited for SILAC experiments since they require a high number of cell passages which might change their phenotype. We then selected the mouse embryonic fibroblasts (C3H10T1/2) which are multipotent cells that can differentiate into osteoblasts, chondrocytes, adipocytes similarly to hMSCs.[127] The data obtained from the SILAC experiments was then validated with western blot and immunohistochemistry.

### **4.3 MATERIALS AND METHODS**

#### **4.3.1 SILAC and Cell Treatment**

C3H10T1/2 (ATCC) were cultured in SILAC DMEM medium (Pierce) containing 10% dialyzed FBS and either the heavy ( $^{13}\text{C}_6$ ) or light ( $^{12}\text{C}_6$ ) L-lysine and L-arginine for more than six cell doubling time to ensure complete labeling of the proteome with the heavy labeled amino acids. In total, approximately sixty million cells were obtained from the culture, half each from the light media and heavy media cultured cells. Cells were serum starved overnight after which fifteen million cells from the heavy media culture were treated with 250 ng/mL of PP for 15 min, while the other fifteen million cells from the heavy media culture were treated with 150 ng/mL

of BMP-2 for 15 min. The thirty million cells from the light media received only serum-free medium to be used as an untreated control. After the treatment, cells were washed with ice-cold PBS, harvested from the tissue culture plates by scraping (to avoid tryptic digestion of cell surface proteins), and pelleted by centrifugation. Excess PBS was removed and the pellets were stored at -80 °C.

#### **4.3.2 Cell Lysis**

Cell lysis buffer (10 mM Tris pH 7.4, 5 mM EDTA, 6 M urea, 5 mM TCEP, 10 µM NaF, 50 µM Na<sub>3</sub>VO<sub>4</sub>, 1 mM PMSF) were added to the cell pellets (0.8 mL/pellet). Sonication was performed at a setting of 1, three times of 15-20 strokes with cooling on ice in between each set of pulses.

#### **4.3.3 Desalting**

Cell lysates were desalted with Pierce D-salt columns (Pierce). Columns were pre-equilibrated with 20 mL of 100 mM ammonium bicarbonate (AmB). Samples were lyophilized to ~300 µl and loaded on the columns followed by an initial wash of 700 µl of 100 mM AmB and then consecutive washes of 500 µl of 100 mM AmB and each fraction (for a total of six) was collected. Each fraction was assayed to determine protein content using the Coomassie Plus Protein Assay (Pierce; 300 µl assay buffer + 10 µl sample). Fractions containing protein (typically 3-5) were combined and the final protein concentration for each pool/sample was determined by BCA (Pierce).

#### **4.3.4 Fractionation by 1D-PAGE and In-Gel Digestion**

Samples were mixed at a 1:1 ratio of total protein for each heavy:light comparison (PP/control and BMP/control). For one dimensional (1D)-sodium dodecyl sulfate polyacrylamide gel electrophoresis (PAGE) fractionation, thirty  $\mu\text{L}$  of total cell lysates (heavy and light mixed at 1:1 ratio) were resolved on a 4-12% Bis-Tris gradient gel (Invitrogen) in MES running buffer at 170 V and the gel was stained with Coomassie (Simply Blue Safe Stain, Invitrogen). Gels lanes for each sample mixture were separated into ten bands, excised and cut into approximately 1 mm x 1 mm pieces, and placed into individual eppendorf tubes. Gel pieces were destained in 1 mL of 50 mM AmB/50% acetonitrile (ACN) with a fresh solution change after 30 min. Destain solutions were removed and 200  $\mu\text{L}$  of 100% ACN was added to each tube for 5 min, the solution aspirated out and gel pieces were incubated at 37 °C to dehydrate the gel pieces. Samples were then incubated with 100  $\mu\text{L}$  of porcine sequencing-grade modified trypsin (20 ng/ $\mu\text{L}$ , Promega) on ice for 40 min. Excess trypsin solution was removed and 100  $\mu\text{L}$  of 25 mM AmB was added and samples were incubated at 37°C overnight. The digest solution was removed to a new tube and 75  $\mu\text{L}$  of extraction buffer containing 70% ACN/5% FA was added and samples were sonicated for 10 min in a water bath, and the solution was combined with the overnight digest previously replaced to a new tube. The extraction procedure was repeated two more times and the samples were, lyophilized to dryness and stored at -80 °C.

#### **4.3.5 Phosphoenrichment with Titanium Dioxide (TiO<sub>2</sub>)**

Cell lysates from PP/control or BMP-2/control groups (mixed at 1:1 ratio for 1 mg of total protein) were boiled for 5 min and digested with trypsin (1:50 enzyme:protein ratio) overnight at

37 °C. Samples were lyophilized to dryness and resuspended in 1 mL of TiO<sub>2</sub> enrichment loading buffer (80% ACN, 0.1% TFA, 30 g/L dihydroxybenzoic acid (DHB)). Each sample was divided equally into two eppendorf tubes and phosphoenrichment was performed using a slightly modified protocol described in the literature.[128] First, 20 mg of TiO<sub>2</sub> beads were washed in 400 µL 20% ACN, pH 10.5, then with 400 µL of 50% ACN/0.1% TFA, and finally with 420 µL 80% ACN, 0.1% TFA, 30 g/L DHB. The washed beads slurry was split equally into four eppendorf tubes (~5 mg of TiO<sub>2</sub> beads per tube) and incubated with 500 µL of the sample for 1 h with gentle rotation at 4 °C. Sample mixtures (with beads) were transferred to spin columns and were washed with 500 µL of 80% ACN, 0.1% TFA, 30 g/L DHB and then again with 500 µL of 50% ACN/0.1% TFA at 100 x g for 1 min. Phosphopeptides were eluted with three consecutive washes with 100 µL 20% ACN (pH>10.5), and samples were neutralized immediately with 25 µL of 10% TFA (placed in the collection tube). Samples were lyophilized to dryness, resuspended in 0.1% TFA and desalted with C18 ZipTip microcolumns (Millipore) according to the manufacturer's instructions, lyophilized again and stored at -80 °C until analysis.

#### **4.3.6 Mass spectrometry and Data Analysis**

For the global analysis, each band from the in-gel digestion was resuspended in 0.1% TFA and analyzed in duplicate by nanoflow reverse phase liquid chromatography (RPLC)-MS/MS using a Dionex Ultimate 3000 LC system coupled online with a hybrid linear ion trap (LIT)-Orbitrap mass spectrometer. Following injection, samples were loaded onto a C-18 reversed-phase trap column for 3 minutes at a flow rate of 30 µL/min with mobile phase A (2% ACN, 0.1% FA). Peptides were eluted from the C-18 trap column onto an analytical column (75 µm i.d. x 360 µm

o.d. x 45 cm fused silica with a flame-pulled tip and packed in-house with Jupiter 5  $\mu\text{m}$  C-18 reversed phase stationary phase [Phenomenex] using a slurry packer) for increased peptide separation prior to electrospray ionization (1.6 kV) and analysis in the mass spectrometer. Peptides were eluted from the analytical column over the course of 130 minutes increasing mobile phase B (100% ACN, 0.1% FA) from 2% to 42% and then increasing mobile phase B to 95% over the next 15 minutes. The column was washed at 95% mobile phase B for 20 minutes before re-equilibration at 100% mobile phase A prior to the next injection. The mass spectrometer was operated in a data-dependent mode where the first scan event was a broad mass range scan in the Orbitrap from  $m/z$  375-1800 at a resolution of 60,000 followed by tandem MS (MS/MS) of the top seven most abundant ions in the LIT using collision induced dissociation at a normalized collision energy of 35. To avoid redundant identification of abundant ion species, molecular ions selected for MS/MS were dynamically excluded from being selected for tandem MS again for ninety seconds or until their signal-to-noise dropped below a certain threshold (early expiration). For the phosphoproteome analyses,  $\text{TiO}_2$ -enriched samples were resuspended and analyzed similarly but with five replicate injections rather than in duplicate to increase the number of identifications due to lack of the gel fractionation step used in the global analyses.

Raw data from the nanoflow RPLC-MS/MS analyses were searched against the mouse protein database (UniProt, 10-08 version, [www.expasy.org](http://www.expasy.org)) using Sequest (Bioworks Browser, ThermoFisher Scientific). Peptides were searched using the following parameters: tryptic criteria with up to two missed cleavages, 20 ppm mass tolerance for the molecular ion and dynamic modifications of 6.0201 for lysine, 10.0336 for arginine, and 15.9949 for methionine. SILAC ratios were determined from the areas obtained from reconstructed ion chromatograms of the heavy and light peptides for a given peptide pair using the PepQuan software in the Bioworks

Browser Software. For the phosphopeptide analyses, an additional dynamic modification of 79.9663 on serine, threonine and tyrosine was allowed. Data were further filtered by stringent cross correlation versus charge state criteria as follows;  $[M+H]^+$ ,  $\geq 1.9$ ;  $[M+2H]^{2+}$ ,  $\geq 2.2$ ;  $[M+3H]^{3+}$ ,  $\geq 3.5$ ; and  $[M+4H]^{4+}$  and higher,  $\geq 5.0$ ; and a delta correlation of  $\geq 0.08$  for all cases. Tables of unique proteins (identified by peptide sequences that can be found in only one protein entry in the database) and common proteins (identified by peptide sequences that can be found in more than one protein entry in the database) were generated with average and standard deviation of heavy-to-light ratios (H:L), from which only those proteins with a percent standard deviation less than forty ( $SD/Avg*100$ ) were considered for further scrutiny. Gaussian distributions of these highly filtered groups of proteins were generated and statistically significant over- and under-expressed proteins were determined for each. Proteins of interest were manually verified from the raw data prior to validation by IHC and western blotting.

#### **4.3.7 Ingenuity Pathway Analysis**

Ingenuity Pathways Analysis (IPA) 7.1 – 2002 was used to aid data analysis of the SILAC experiment. The IPA software is used for exploring functions of a gene or protein of interest, interpretation of protein interactions, network construction of a set of proteins, and data set comparisons. IPA's search, analysis, and network construction functions are based on the Ingenuity knowledge base, which is compiled from published peer-reviewed literature and facilitates analyzing large sets of data in a systematic manner. Protein accessions and their corresponding average ratios were imported to IPA for core analysis. Analysis settings are as follows: Functions/Pathways/Tox List Analyses Reference Set - Ingenuity knowledge base (genes only), Network Analysis – direct and indirect relationships, includes endogenous

chemicals, and consider all species, tissues & cell lines, and data sources. From the core analysis, top networks with associated network functions of a particular dataset is constructed along with top biofunctions (diseases and disorders, molecular and cellular functions, physiological system development and function), top canonical pathways, top molecules (fold change up-regulated and down-regulated). For the global analyses, the PP/control and BMP/control data sets (unique and common) were imported into IPA for further analysis of the networks and functions of proteins identified.

#### **4.3.8 Western Blot Analyses**

Cells were treated identically as those for SILAC experiment without the supplementation of the labeled isotopes. C3H10T1/2 cells were serum starved overnight and treated with PP or BMP-2 (both at 250 ng/mL) for 15 min. After washing twice with ice-cold PBS, cells were incubated in lysis buffer (150mM NaCl, 1% Igepal CA-630, 0.5% sodium deoxycholate, 0.1% SDS, 50mM Tris, pH 8.0, 1 tablet/50mL protease inhibitor cocktail tablet (Roche)) for 20 min, harvested, sonicated, and pelleted by centrifugation at 13,000 rpm for 15 min. Supernatants were collected and protein concentrations were determined by BCA. Equivalent amounts of each sample (20 µg) were resolved by 1D-PAGE on 10% SDS gels at 120 V for 2 h, then blotted onto PVDF membranes at 60 V for an additional 2 h. Membranes were blocked with 5% milk and probed with primary antibodies overnight at 4 °C with gentle rotation. Membranes were washed with tris-buffered saline with Tween20 (TBST) and incubated with secondary antibody for 1 h at ambient temperature and washed again prior to band detection by chemiluminescence of HRP using Western Lightning enhanced chemiluminescence substrate (Perkin Elmer) and exposure to X-OMAT film (Kodak). Primary antibodies used were rabbit anti-14-3-3 ε (1:1000 dilution, Cell

Signaling Technologies), rabbit anti-eIF2A-phosphoS51 (1:500 dilution, abCam) rabbit anti-eIF2A (1:500 dilution, abCam), rabbit anti-Ras (1:1000 dilution, Cell Signaling Technology), rabbit anti-Coronin 1C (1:500 dilution, Santa Cruz Biotechnology), rabbit anti-androgen receptor (1:200 dilution, Santa Cruz Biotechnology). Secondary antibody used was anti-rabbit HRP (1:8000 dilution, Cell Signaling Technology).

#### **4.3.9 Immunohistochemistry**

Cells were treated identically as those for SILAC experiment without the supplementation of the labeled isotopes. C3H10T1/2 cells were plated in 48-well tissue culture plates, serum starved overnight, and treated with PP or BMP-2 (both at 250 ng/mL) for 15 min. Cells were then washed twice with ice-cold PBS and fixed in 4% paraformaldehyde for 15 min. Cells were washed with wash buffer (0.05% Tween-20 in PBS), permeabilized with 0.1% Triton X-100 in PBS for 5 min, and incubated with blocking buffer (5% donkey serum in PBS) for 1 h at ambient temperature. Cells were incubated in primary antibody overnight at 4 °C and washed three times in wash buffer prior to addition of secondary antibody and incubated for 1 h. Cells were washed twice with PBS and imaged with a Nikon fluorescent microscope. Primary antibodies used were AR (1:50 dilution, Santa Cruz Biochemistry). The secondary antibody used was donkey anti-rabbit Alexa 488 (1:500 dilution, Invitrogen).

#### 4.4 RESULTS

Cells were labeled with heavy or light lysine and arginine by culturing in media for at least 5 passages to ensure complete incorporation of the heavy isotope amino acids into the proteome. A flow chart summarizing the SILAC-based experimental workflow is shown in Figure 4-1. Heavy-labeled cells were treated with PP or BMP (250 ng/mL) for 15 min while light-labeled cells were used as untreated control. Cells were lysed and mixed at a heavy to light ratio of 1:1 based on total protein content. For global proteome analyses, total cell lysates were resolved by 1D-PAGE and sample lanes were separated into ten fractions and bands were excised for in-gel trypsin digestion. For phosphoproteome analyses, cell lysates were digested in-solution with trypsin then enriched for phosphopeptides with an established protocol using TiO<sub>2</sub> beads.

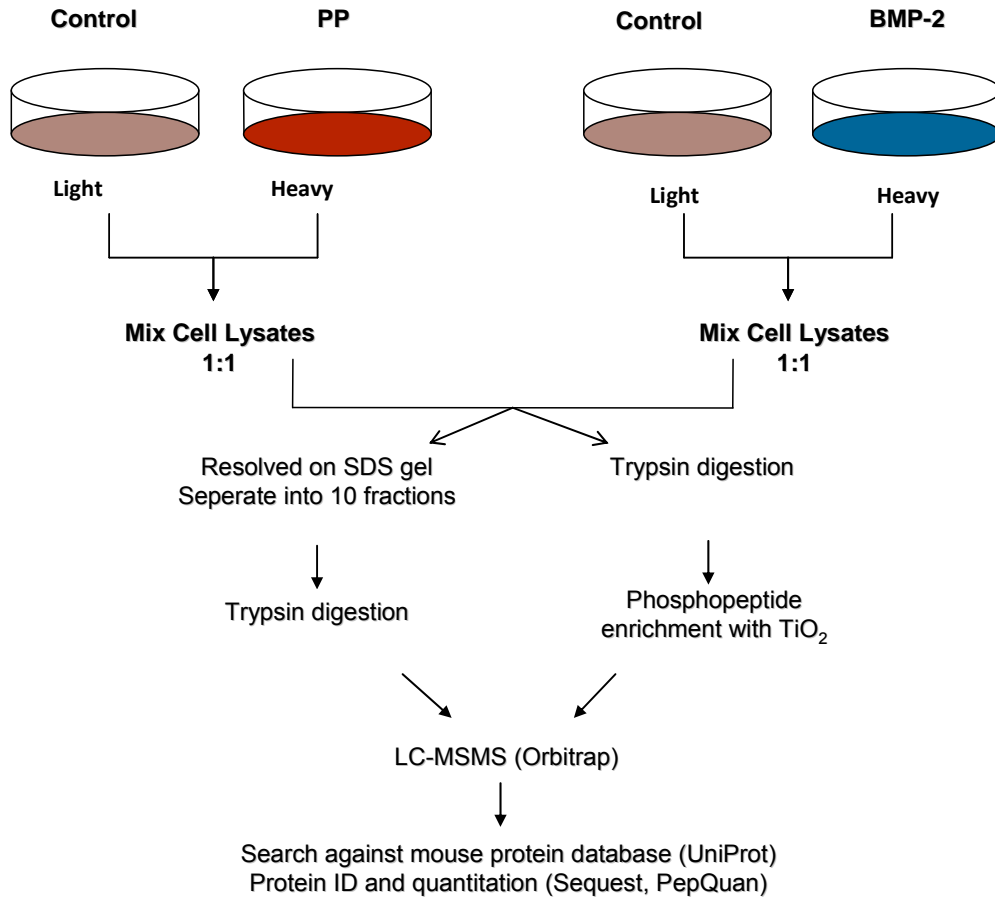


**Figure 4-1.** SILAC-based experimental workflow

#### 4.4.1 Heavy Lysine and Arginine Labeling in C3H10T1/2 Cells

Prior to PP or BMP-2 treatment, cells cultured in heavy or light lysine and arginine medium were lysed, digested with trypsin (1:50 enzyme:protein ratio), and the resultant peptides were analyzed to ensure full incorporation of labeling. We observed that complete incorporation of heavy arginine and lysine amino acids into the proteome occurred after a minimum of five cell doubling times. Figure 4-2 illustrates an example of a pair of isotopomeric peptides from

aminopeptidase showing a mass difference of  $m/z$  5 for the doubly charged peptide (10 amu) containing a heavy labeled arginine and an approximate ratio of 1:1 from the relative abundance of the molecular ions for the light and heavy peptides.

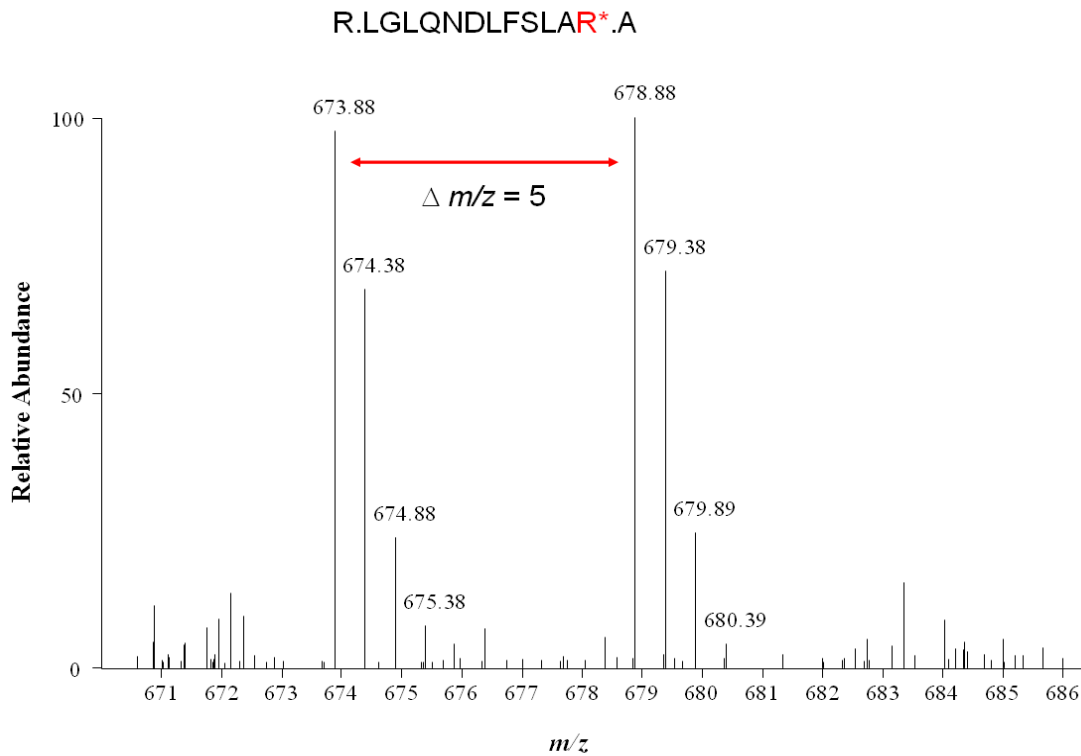


**Figure 4-2.** Peptide isotope pair showing a difference of  $m/z$  5 amu for the heavy arginine-containing peptide with a relative abundance of 1:1 between control and treated.

#### 4.4.2 Protein Fractionation by 1D-PAGE

Mixed cell lysates were resolved by 1D-PAGE, the gel stained by Simply Blue Safe Stain and ten bands were excised for in-gel digestion as shown in Figure 4-3. Following digestion with trypsin, samples were analyzed by nanoflow reversed-phase liquid chromatography-tandem mass

spectrometry. Insets in Figure 4-3 show representative base peak chromatograms from the RPLC-MS/MS analysis of peptides extracted from a few of the individual gel bands showing varying complexities within each band. The use of 1D-PAGE effectively provides an initial dimension of fraction (by gel filtration) prior to mass spectrometric analysis which improves overall protein identification and quantitation.

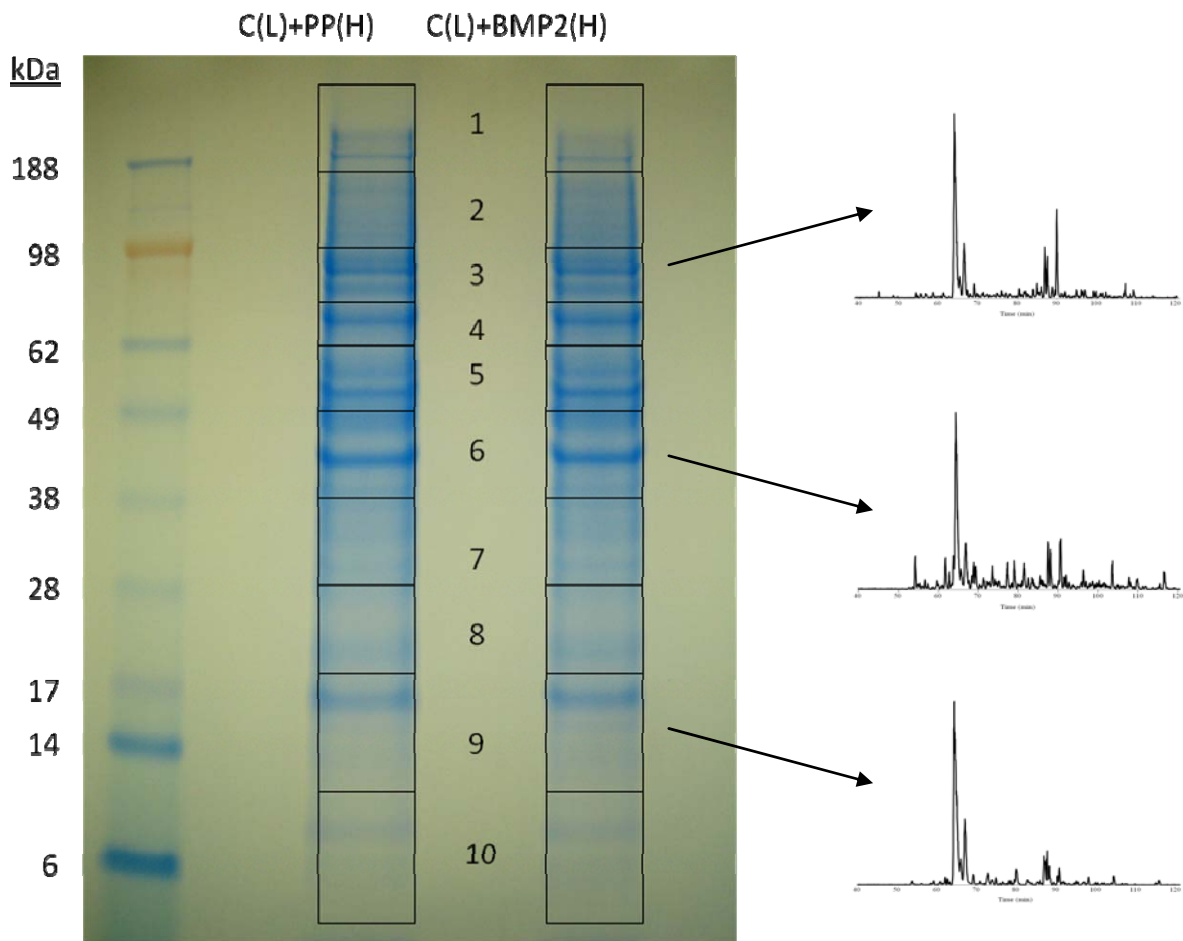


**Figure 4-3.** Protein fractionation by 1D-PAGE

#### 4.4.3 Global Protein Profiling of PP and BMP-2 Treated C3H10T1/2 Cells

Results from the global proteomic analyses of the PP/control and BMP-2/control samples resulted in the identification of 2751 and 3294 proteins respectively with 1924 and 2177 identified by at least two peptides. Of the total number of proteins identified, 1625 (PP/control) and 1973 (BMP-2/control) were identified by unique peptides; 1124 and 1274 of those by two or more peptides respectively. Protein abundance changes were calculated by PepQuan from extracted ion chromatograms generated from heavy and light peptide pairs and reported as H:L values. To generate a list of highly confident proteins with ratios, average and standard deviation determinations of ratios for each protein were first trimmed using cut-offs of H:L of 100:1 and 0.01:1 at the high and low extremes, and then further filtered for average ratios calculated from at least two peptides with different ratio values (a standard deviation greater than zero). Finally, proteins with  $\leq 40\%$  standard deviation (SD), calculated by dividing the standard deviation by the average and then multiplying by 100, were used for further analysis bioinformatic analyses. Normal distributions of the final, filtered data sets (from unique peptides) were generated using binned protein counts vs.  $\log_2$  of the ratio and are shown in Figures 4-4 and 4-5. A Gaussian (normal) distribution was observed for both treatment groups where the majority of the proteins had a ratio (treated over control) around one ( $\text{Log}_2 \text{Ratio} = 0$ ). This analysis allowed us to evaluate a subset of the proteins which were significantly up- or downregulated (in this case  $1\sigma$  from the mean ratio for each sample) to determine those proteins which might merit further validation and analysis.

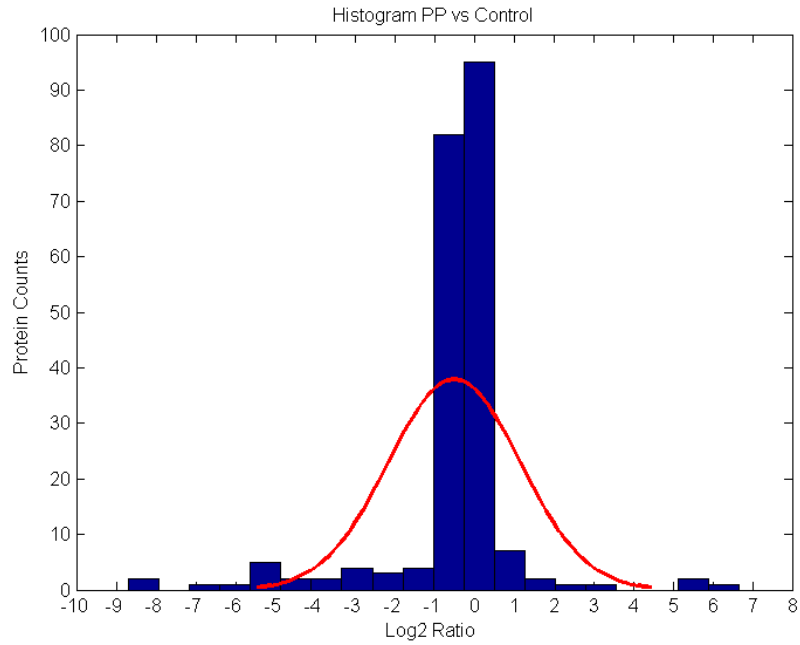


**Figure 4-4.** Normal distribution of binned protein counts vs. Log2 Ratio for PP/control group

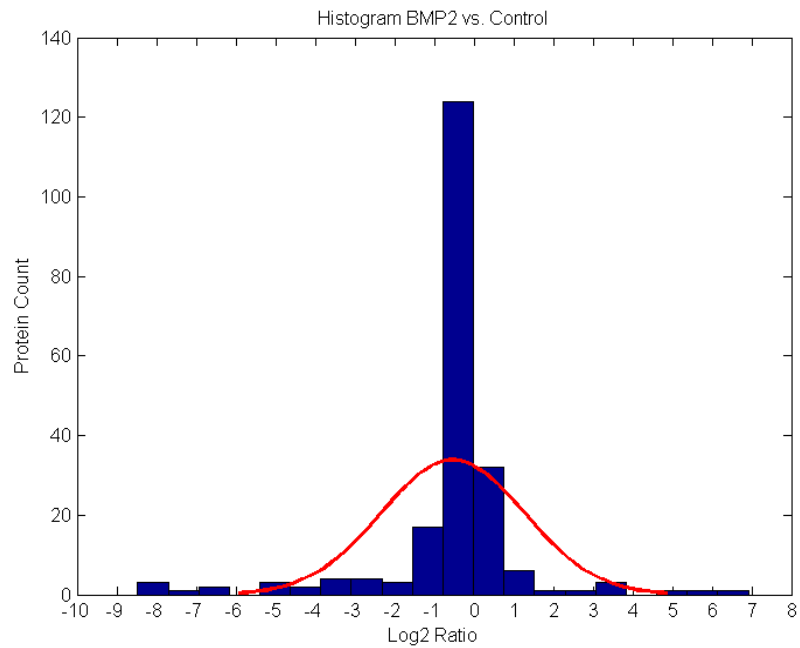


**Figure 4-5.** Normal distribution of binned protein counts vs. Log2 Ratio for BMP-2/control group

In evaluating the data, it was prudent to examine those proteins whose identification was derived from one or more peptides that are not unique to a given sequence within the database and can be found in several protein sequences. For these proteins, while definite assignment of their presence (and therefore the corresponding ratio) to a single, unique protein cannot be made, some insight into the nature of the biology that is taking place may be gleaned from looking at the list of possible proteins such as different isoforms or families of proteins. In these cases, proteins of interest that were selected after the previously described filtering were further inspected manually for the ‘commonality’ of the identification and the quality of the tandem mass spectra for each peptide used to determine the protein identification.

Proteins identified from PP/control and BMP-2/control groups (total lysates, unique and common peptides) were imported to IPA software groups to examine protein functions and relations. The number of proteins identified for a particular cellular function was divided by the total number of proteins identified and multiplied by 100 to calculate the percent coverage. The distribution of cellular functions of proteins identified for PP/control and BMP-2/control groups are shown in Figure 4-6 and 4-7.

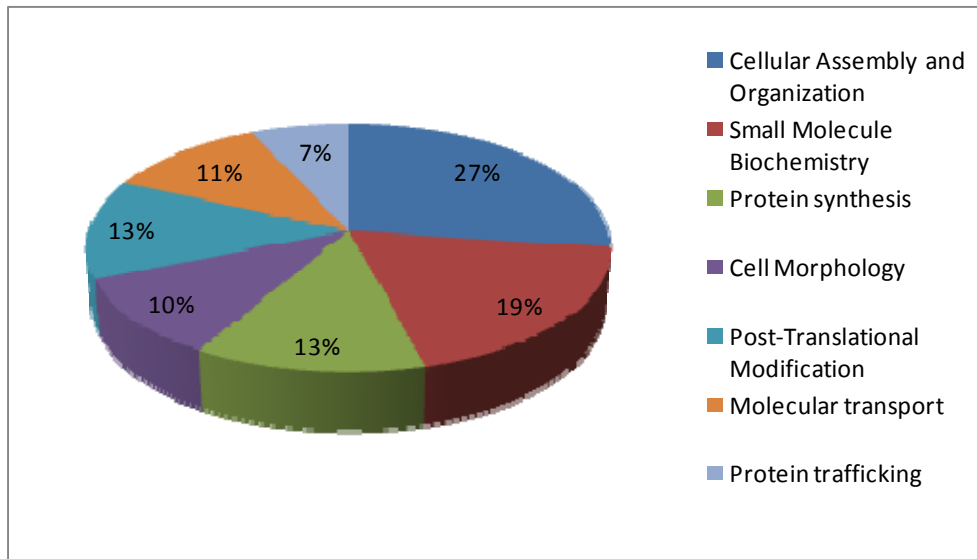


**Figure 4-6.** Distribution of protein functions in PP/control group

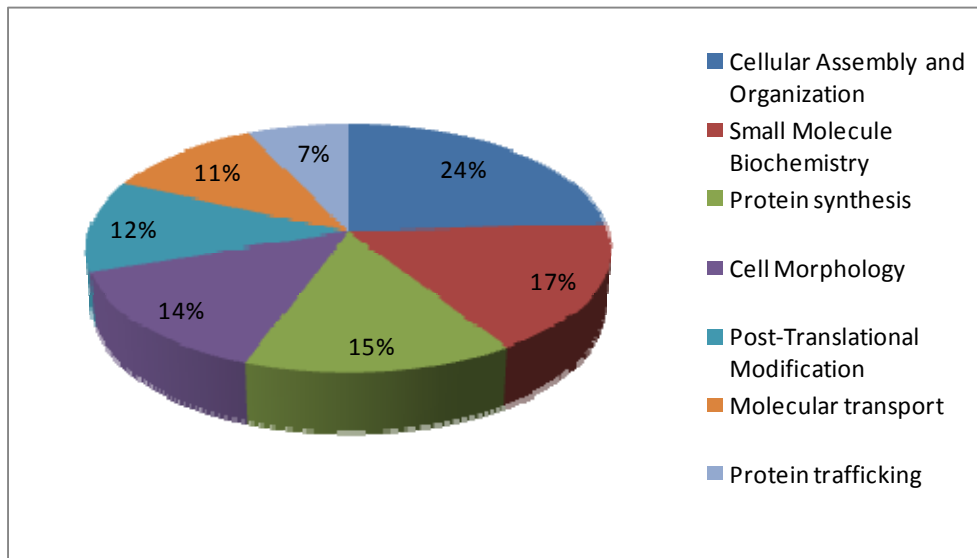


**Figure 4-7.** Distribution of protein functions in BMP-2/control group

#### 4.4.4 Phosphoprotein Profiling of PP and BMP-2 Treated C3H1-T1/2 Cells

To identify the changes in signaling transduction components during stem cell differentiation, we performed phosphopeptide enrichment using  $\text{TiO}_2$  on digested cell lysates from cells treated with PP or BMP-2. From these analyses, 226 and 171 phosphopeptides were identified in the PP/control and BMP-2/control groups, respectively. Of the phosphopeptides identified, 135 and 114 were by unique peptides in the PP/control and BMP-2/control groups, respectively, with 25 proteins observed as upregulated and 26 as downregulated (more than 1 SD away from the mean ratio). However, manual verification of the peptide tandem mass spectra suggested that the complexity of the multiple modifications present in most cases (heavy labels, phosphorylation, etc.) and the lack of complete peptide fragmentation due to predominant loss of the phosphorylation modification during collision induced dissociation (CID), led to the majority of them being questionable identifications, and therefore were not selected for further validation. As an alternative approach for phosphopeptide identification, we re-searched the global proteome data using similar criteria to that used for the  $\text{TiO}_2$ -enrichment data, but encountered the same concerns on the credibility of the peptide identifications.

To gain insights to additional signaling pathways in PP and BMP-2 signaling, top networks of the identified phosphoproteins were constructed by IPA using data from the  $\text{TiO}_2$  enriched samples. The top network for PP/control group (identified from unique peptides) suggests the involvement of MAPK (ERK, JNK, P38) in PP signaling which we have shown previously (Chapter 3). Proteins upregulated by PP are shown in red and downregulated in green with proteins not identified shown in white. Direct relationships are shown in solid lines and

indirect relationships in dotted lines. In addition, other molecules that are involved and related to MAPK such as YWHAH and MAP3K3 were identified and shown in the network.

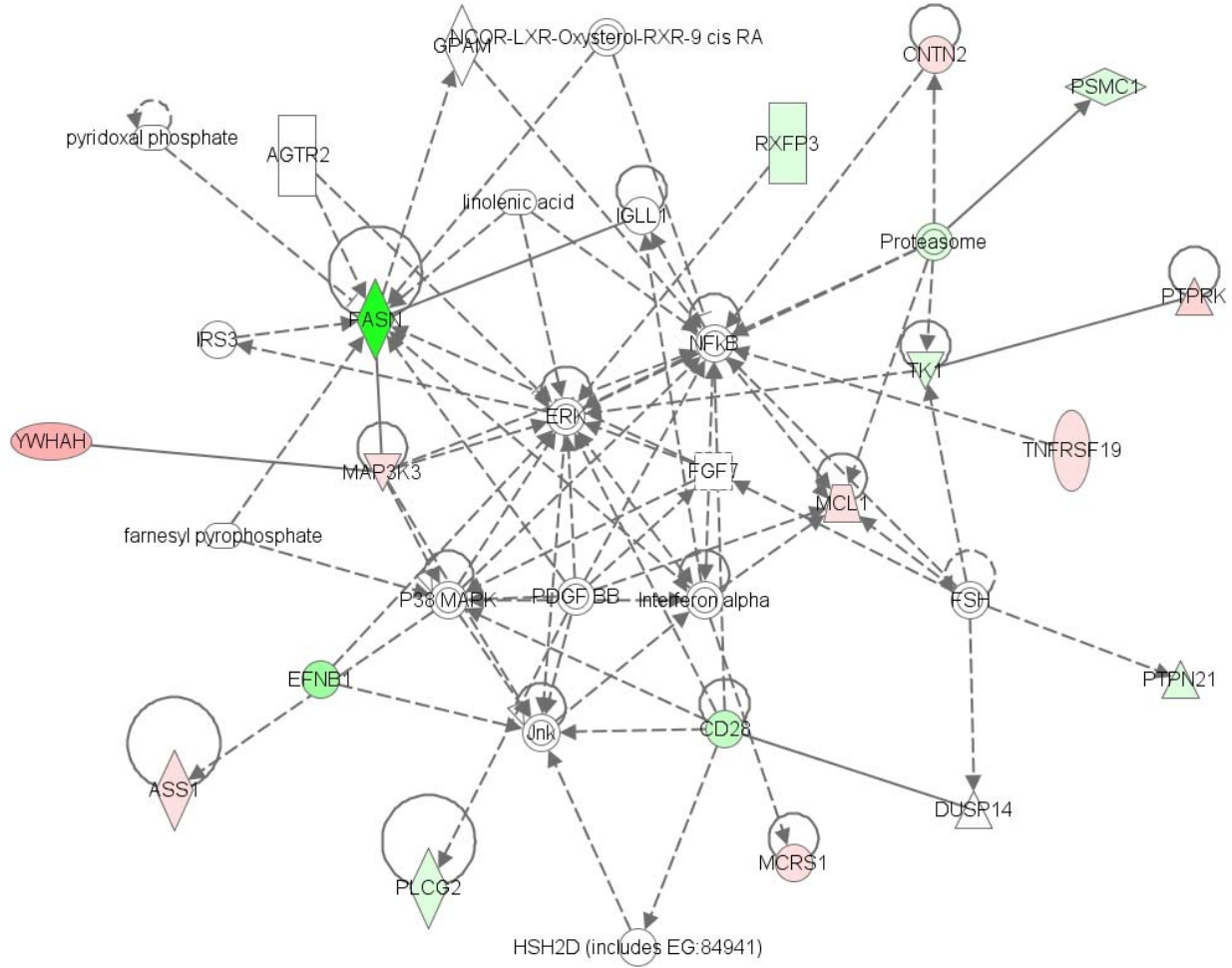


**Figure 4-8.** Top network of PP/control (TiO<sub>2</sub> enriched, unique peptides)

#### 4.4.5 Protein Validation

From the global protein analysis, proteins of interest with significant changes in ratios were selected for validation and were validated manually for robust ion matching (good coverage of the b- and y-type fragment ions) in the tandem mass spectra and also for accurate ratio calculations from the extracted ion chromatograms of the heavy and light peptide pairs. Of the nearly 3,500 proteins identified in the two global data sets, five were finally selected for further validation (Table 4-9) by western blot and/or immunohistochemistry; coronin-1C (PP Unique), androgen receptor and eukaryotic initiation factor 2A (Eif2A) (BMP Unique), 14-3-3  $\epsilon$  (BMP Common), and Ras-related Rab32 (PP/BMP-2 Common). Complete tables of proteins upregulated or downregulated more than one SD away from the mean ratio are shown in Appendix A with Tables 5-1 - 5-4 showing proteins identified by unique peptides and Tables 5-5 – 5-8 showing proteins identified with common peptides.

**Table 4-1.** Proteins selected for validation experiments

<b>UniProt Accession</b>	<b>PP/control Fold Change</b>	<b>BMP-2/control Fold Change</b>	<b>Protein Name (Gene Name)</b>	<b>Peptides Identified</b>
P19091	N/A	0.02	Androgen receptor (AR)	2 (unique)
Q9WUM4	33.52	N/A	Coronin-1C (Coro1C)	2 (unique)
Q8BJW6-1 Q8BJW6-2	4.39	N/A	Isoform 1 of Eukaryotic translation initiation factor 2A (Eif2A)  Isoform 2 of Eif2A	2 (common)
P62259  A2ACM8	N/A	8.51	14-3-3 protein epsilon (Ywhae)  Tyrosine 3- mono- oxygenase /tryptophan-5- mono-oxygenase activation protein, epsilon	2 (common)
Q9CZE3  Q8QZZ8  Q91YQ1	1.95	3.02	Ras-related protein Rab-32  Rab-38  Rab-7L1	2 (common)

For Western blot validation, total cell lysates from cells treated in a similar manner as the SILAC experiment were resolved by 1D-PAGE. Antibodies against proteins of interested were used to evaluate changes in protein abundances (Figure 4-9). Coronin 1C, phospho-Eif2A, and Eif2A increased in both BMP-2 and PP treated groups. Ras increased after PP treatment and no change was observed in the BMP-2 treated group. 14-3-3  $\epsilon$  increased after BMP-2 treatment and no change was observed for the PP treated group. Androgen receptor decreased in both BMP-2 and PP treated groups.  $\beta$ -actin showed equal loading of the protein.

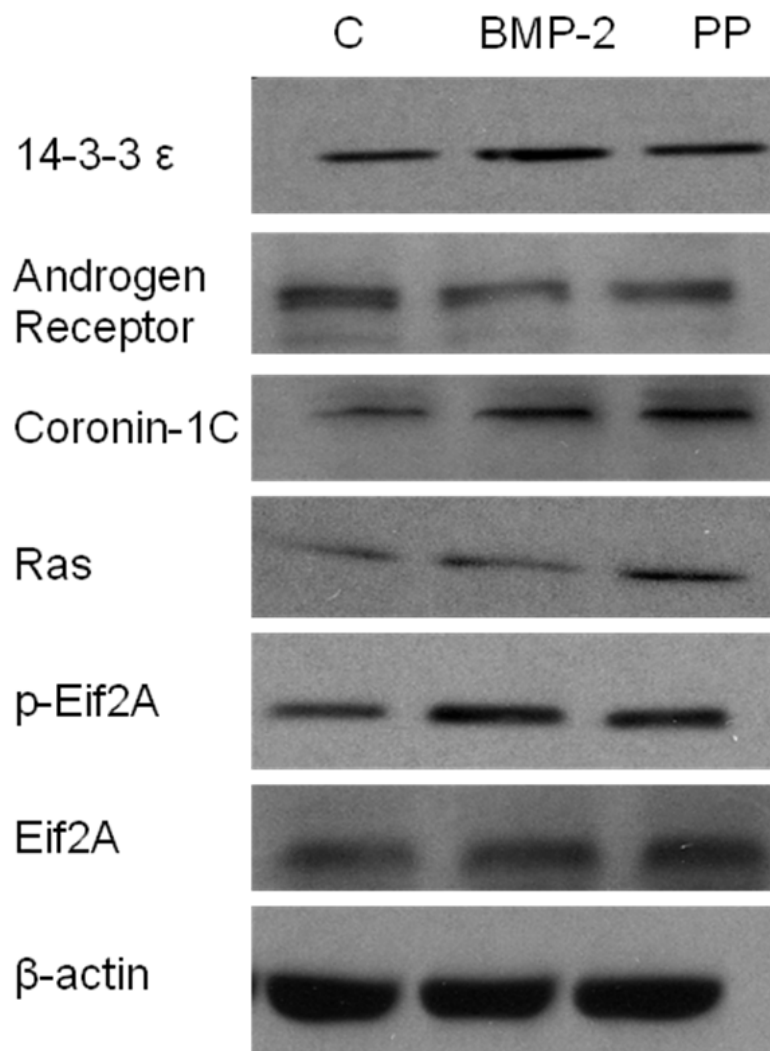


**Figure 4-9.** Western blot validation of proteins identified from mass spectrometry

In addition to western blot, immunocytochemistry was performed on C3H10T1/2 cells treated with PP or BMP-2 (250  $\mu\text{g}/\text{mL}$ ) for 15 min. Androgen receptors were expressed in the cytoplasm as well as the nucleus. No significant change in androgen receptor expression intensity or location for cells treated with PP or BMP-2 when compared to control (Figure 4-10).

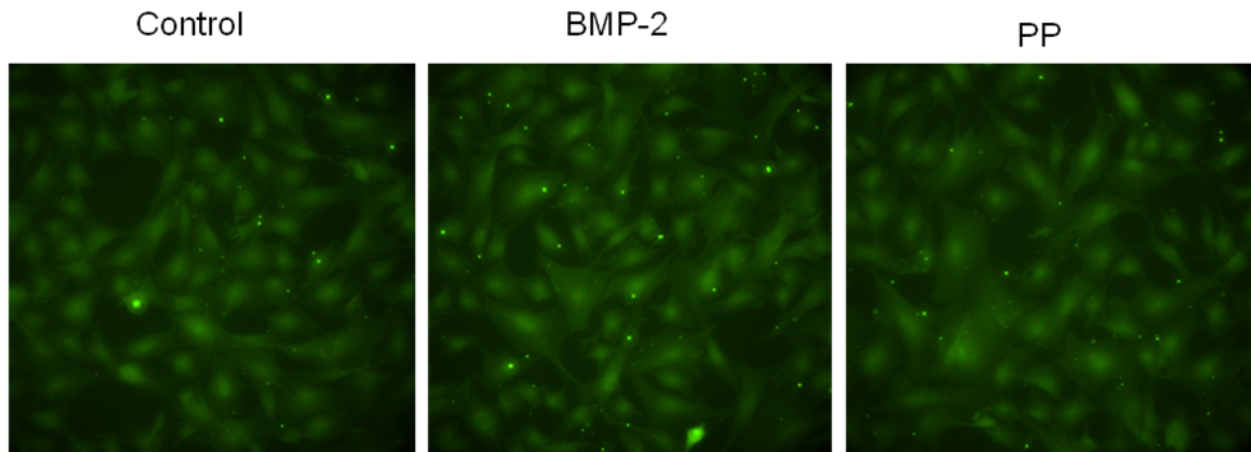


**Figure 4-10.** Androgen receptors staining in cells treated with BMP-2, PP, or untreated control

## 4.5 DISCUSSION

To study the early differentiation mechanism stem cells into the bone or dentin lineages. C3H10T1/2 cells were stimulated with PP to induce odontogenic differentiation or with BMP-2 to stimulate osteogenic differentiation. SILAC was utilized to identify and quantify proteins involved during stem cell differentiation. Proteins found with significant change in ratio were evaluated and five proteins were selected for further validation. We have selected Coronin-1C, 14-3-3  $\epsilon$ , androgen receptor, Ras, and eukaryotic initiation factor 2A (Eif2A) to perform western blot analysis.

Coronin-1C is an actin binding protein that is involved in actin cytoskeletal remodeling, cell motility, and vesicle trafficking.[129] From the SILAC experiment, coronin-1C was identified and had a 33.5 fold increase in the PP treated group. From western blot analysis, we observed an increase in cells treated with either PP or BMP-2. PP has been shown to signal through the integrins (Chapter 3). Integrins are transmembrane proteins that interact with the extracellular matrix and are closely associated with actin cytoskeleton. Clustering of focal adhesion points occurs upon activation of integrins as well as signal transduction.[130] In addition, BMP-2 has been shown to induce actin cytoskeleton reorganization through Cdc42 small GTPase and the alpha-isoform of the phosphoinositide 3-kinase (PI3Kalpha).[131] Coronin 1C could play a role in cytoskeletal remodeling stimulated by PP or BMP-2.

14-3-3  $\epsilon$ , also known as tyrosine 3-monooxygenase/tryptophan 5-monooxygenase activation protein, epsilon polypeptide, (YWHA $\epsilon$ ) belongs to the 14-3-3 family of phosphoserine/phospho-threonine binding proteins that mediate signal transductions including MAPK and AKT signaling pathways.[132] 14-3-3 has also been shown to regulate RSK-mediated cytoskeleton reorganization.[133] I observed an increase in 14-3-3  $\epsilon$  in cells treated with BMP-2 from both mass spectrometry and western blot data. PP has been shown to activate the MAPK.[57] 14.3.3 is involved in initiation of Raf kinase activation that leads to the Ras-Raf-MAPK pathway. Although 14-3-3  $\epsilon$  was not upregulated in cells treated with PP, other members of the 14-3-3 family could be involved in PP signaling.

Ras is a family of guanine-nucleotide binding proteins that could be stimulated by receptor tyrosine kinases and G-protein coupled receptors, which then activate the Raf-MEK-MAPK pathway. Ras-related Rab, identified from the mass spectrometry data, and was increased

in cells treated with PP or BMP-2.[134] The peptides identified were common peptides that could belong to Rab32, Rab38, or Rab7L1. Antibodies against mouse Rab32, Rab38, or Rab7L1 were not commercially available. Therefore, a Ras antibody that binds to K-Ras, N-Ras, and R-Ras was selected for western blot analysis. We observed an increase of Ras in PP treated group. PP has been shown to activate the MAPK and Smad pathways.[58] Smad is activated by PP independent of the BMP-2 receptor. I have shown that Smad1 could be regulated by crosstalk between ERK and P38 (Chapter 3). Ras is upstream of ERK and it has been previously shown to regulate Smad activation.[135] This provides an additional rationale to how PP activates the Smad signaling.

Androgens and androgen receptors are important for bone metabolism.[136] Androgen receptor is a nuclear receptor that is expressed in the cytoplasm and when activated it is translocated into the nucleus and act as a transcriptional factor.[137] Androgen receptor was identified and showed a decrease in BMP-2 treated cells by mass spectrometry and western blot. Studies have shown that androgen receptor is inactivated by phospho-Smad1 that is activated by BMP-2.[138] Immunocytochemistry showed the expression of androgen receptor in the cytoplasm and the nucleus, however the assay was not sensitive enough to differentiate cells treated with PP or BMP-2 with untreated control.

Eukaryotic initiation factor 2 alpha (Eif2A) is phosphorylated by eukaryotic translation initiation factor 2 alpha kinase 3 (Perk). Perk is essential for neonatal skeletal development.[139] Perk knockout mice showed skeletal defects such as deficient mineralization, osteoporosis, and abnormal compact bone development.[140] We showed an increase of Eif2A in the BMP-2 treated cells by mass spectrometry. Western blot analysis showed an increase on phospho-Eif2A

as well as Eif2A for both PP and BMP-2 treated cells. Eif2A could play a role in bone development and mineralization as well as dentin development.

Through a quantitative proteomics approach, we have identified several proteins that could be involved in stem cell differentiation into the dentin and bone lineages. Future experiments include improvement of phosphopeptide enrichment and further validation of the proteins identified such as western blot, immunohistochemistry, siRNA, and drug inhibition assays. Using quantitative proteomic techniques such as SILAC, mechanism of stem cell differentiation into different lineages can be studied in an efficient and systematic manner.

#### **4.6 ACKNOWLEDGEMENTS**

I would like to acknowledge Tom Conrads, Brian Hood, and Mai Sun for their collaboration on the SILAC-based mass spectrometric analyses. I would also like to thank Neil Robertson and Yuan Yuan Duan for their assistance in this project.

## 5.0 CONCLUSIONS AND FUTURE DIRECTIONS

Mineralized tissue engineering requires appropriate cell source, growth factors, and scaffolds. In this study, different cell sources were investigated including dental pulp pericytes, hMSCs, and mouse embryonic fibroblasts (C3H10T1/2). Human dental pulp pericytes were characterized, isolated, and tested for their multilineage differentiation potential (Chapter 2). Interaction between stem cells and ECM-proteins were investigated to better understand the most suitable microenvironment for stem cell differentiation into mineralized tissues. Our goal was to study the signaling roles of ECMs found in bone and dentin and to assess their potential incorporation in a scaffold to create a compatible stem cell microenvironment. The effect of PP on hMSCs cell surface receptors and crosstalk among signaling pathways was assessed (Chapter 3). To further elucidate the mechanism involved in stem cell differentiation into the odontogenic and osteogenic lineages, mass spectrometry (Chapter 4) was utilized to quantify protein abundance differences in mouse embryonic fibroblasts C3H10T1/2 cells that were stimulated with PP or BMP-2. Understanding the cell-ECM interaction and the signaling mechanisms during stem cell differentiation is important in controlling cell fate decision and tissue morphogenesis. Appropriate cell sources and signals to stimulate differentiation are crucial to the bioengineering of mineralized tissues.

## 5.1 DENTAL PULP PERICYTES

### 5.1.1 Differentiation Potential of the Dental Pulp Pericytes

Pericytes from adult human dental pulp were successfully characterized. CD146+CD34-CD45-CD56- could be used to sort pericytes and they can be expanded in culture (Chapter 2). Cultured pericytes showed high clonogenic ability and was able to differentiate in to chondrogenic, osteogenic, and adipogenic differentiation. Cultured pericytes expressed runx2 and osteocalcin. We have not yet assessed the *in-vivo* osteogenic/odontogenic differentiation potential of the dental pulp pericytes.

### 5.1.2 Different Cell Populations in the Dental Tissues

Besides the pericytes, there are other stem cell populations that may exist in the dental pulp. Furthermore, other dental pulp cell populations, such as endothelial cells, could potentially produce growth factors that support the pericytes. It has been shown that Stro-1, an MSC marker, could be used to isolate stem cells from dental tissues such as dental pulp and periodontal ligaments.[3, 141-143] It will be interesting to compare the differential potential of the total population, Stro-1 sorted cells, and pericytes *in-vitro* and *in-vivo*. CD146+CD34-CD45-CD56- has been used to sort pericytes from the dental pulp and it was also used to characterize periodontal ligaments. FACS results of cells from the periodontal ligaments were similar to those from the dental pulp (Appendix B). Besides the dental pulp and periodontal ligament, stem cells have also been suggested to reside in the apical papilla of permanent immature teeth (SCAP). These cells are involved in root maturation of the tooth and could be used in conjunction with

other cell types for bioengineering of the tooth.[144, 145] These cells could then be used to study their differentiation into odontoblasts and ultimately tooth formation. As the isolation and characterization experiments were ongoing, we began to assess the signaling role of PP, a bone/dentin extracellular matrix protein.

## 5.2 PP SIGNALING MECHANISM

### 5.2.1 Receptors for PP

The data presented here shows that PP signals through integrins  $\alpha\beta3$  and  $\alpha2\beta1$  (Chapter 3). The experiments conducted were done by blocking integrins  $\alpha\beta3$  or  $\alpha2\beta1$  individually then looking at the downstream MAPK signaling activation. When integrins  $\alpha\beta3$  or  $\alpha2\beta1$  were blocked prior to PP treatment, the MAPK activity was downregulated but the signal was not completely inhibited. It would be of interest to see the effect of PP signaling when both  $\alpha\beta3$  and  $\alpha2\beta1$  are inhibited. If the MAPK activation from PP were not completely inhibited by blocking both  $\alpha\beta3$  and  $\alpha2\beta1$ , then it will suggest that other receptors might be involved in PP signaling. One method to find additional receptors for PP is by a pull-down assay, similar to immunoprecipitation, followed by mass spectrometry analysis. First, PP would be tagged with biotin, then either cells to be treated with tagged PP or a total cell/membrane lysate would be incubated with the tagged PP and then associated proteins would be isolated using streptavidin to pull down PP-receptor complexes. This mixture would then be resolved by 1D-PAGE for in-gel digestion of bands of interest followed by MS identification. Studies have shown success in identifying novel receptors using the affinity purification and mass spectrometry techniques.[146]

## **5.2.2 Effect of PP on Different Cell Types**

PP signals through the MAPK and Smad1 pathways in hMSCs, MC3T3, and NIH3T3 and upregulates bone/dentin related genes.[57] PP has been shown to upregulate Runx2 and OCN gene expression as well as alkaline phosphatase activity in human periodontal ligament cells (unpublished results). PP signaling in dental pulp pericytes and other stem cell populations are yet to be studied.

## **5.2.3 PP Signaling Mechanisms**

We have shown that PP signals through integrin/MAPK and Smad1 pathways. ERK, JNK, and p38 were activated by PP and there are signaling crosstalk among MAPK and Smad1 (Chapter 3). Activation of ERK inhibits Smad1 activation and nuclear translocation. Activation of p38 has a positive effect on ERK activation as well as Smad1 activation and nuclear translocation. The crosstalk among MAPK and Smad is complex and acts as intrinsic signaling control to regulate gene regulation. ERK activates c-FOS, while JNK activates ATF-2 and c-JUN. The AP-1 transcription complex is composed of activated c-JUN protein which can homo- and/or heterodimerize with c-FOS.[147] For example, c-JUN/c-JUN or c-FOS/c-JUN can complex to form AP-1 transcriptional factor. AP-1 will then bind and activate osteoblast specific genes, enabling osteoblast differentiation.[148, 149] Future studies might include investigating whether c-FOS, c-JUN, AP-1, and ATF-2 are activated by PP.

## 5.3 GLOBAL PROTEOMICS APPROACHES

### 5.3.1 SILAC

We have used a SILAC-based mass spectrometry approach to evaluate changes in protein abundances when C3H10T1/2 cells were stimulated by PP or BMP-2 (Chapter 4). With the same approach, other cell types such as DPSCs and hMSCs could be used to study cell differentiation by various growth factors, keeping in mind that the cells need to be cultured for at least 5-6 cell doubling times in the SILAC medium before treatment to insure successful labeling of the heavy amino acids. In addition, improvements to the TiO<sub>2</sub>-based phosphoenrichment protocol are required (as described below) for a more complete evaluation of the signaling cascades activated in response to the treatment conditions. Therefore, an approach to immortalize these primary cells in the same fashion as the TERT-hMSCs could be incorporated.[150]

### 5.3.2 iTRAQ

Another quantitative proteomics approach, isobaric tag for relative and absolute quantitation (iTRAQ) could be used for the evaluation of multiple time points or dosing studies, of which up to eight different treatment groups can be compared. Unlike SILAC, which is a metabolic labeling process and occurs during cell culture, iTRAQ is a reagent-based chemical reaction which labels peptides at free amine groups, after proteins are isolated from cells. Up to eight experimental groups could be compared in a single iTRAQ experiment.[151, 152] For example, we can compare cells treated with PP or BMP-2 for 10, 20, 30, and 60 min in one set of experiments. While iTRAQ would be useful for comparing cells treated with multiple growth

factors, time points, and dosages, it requires additional steps during sample processing and as most chemical reactions, may suffer from inefficient labeling of the peptide substrates.

### **5.3.3 Phosphoenrichment**

To study the signaling molecules involved in PP and BMP-2 stimulated differentiation, we utilized a TiO<sub>2</sub> enrichment protocol to investigate the phosphopeptides from total cell lysates. However, the results were less than optimal and further modification of the protocol is required. Repeated incubation of the cell lysates with the TiO<sub>2</sub> might improve the binding efficiency. Also, we have used a ‘batch’ or ‘bulk’ method (incubating cell lysates with a TiO<sub>2</sub> bead slurry) in our phosphoenrichment protocol; a column-based method (passing cell lysates through column packed with TiO<sub>2</sub> materials) might provide a more efficient enrichment. Besides using TiO<sub>2</sub> beads, we also briefly evaluated an IMAC-based approach utilizing Ga<sup>3+</sup> (Sigma) in a preliminary study but the results were poor in our hands. An alternative method to enrich the phosphopeptides is to use antibodies that bind to phosphorylated peptides or proteins. It has been shown that 4G10 and PY100 can be used to enrich phospho-Tyrosine peptides.[82] We could use these antibodies to perform an immunoprecipitation, followed by 1D-PAGE and LC-MS to identify and quantify the phosphoproteins in stem cells treated with PP, BMP-2, or other ECM proteins and growth factors.

### **5.3.4 Absolute Quantification**

We have achieved relative quantification of identified proteins by calculating ratios of proteins from PP or BMP-2 treated samples versus untreated controls by SILAC. In order to achieve

absolute quantification of a protein of interest, we could spike the samples with a known amount of peptide (from the protein of interest) and then calculate the amount of protein of interest by comparing its peptide peak intensity to that of the spiked peptide.

#### **5.4 SCAFFOLD FOR MINERALIZED TISSUE ENGINEERING**

Scaffolds can provide support for cells and can be incorporated with growth factors to be implanted in the site of injury of the host. In collaboration with Dr. Steve Little, we tested the mineralization potential of SAOS cells on a biomaterial, poly(ethylene oxide)-modified poly( $\beta$ -amino ester) (PbAE). Cells were seeded on surfaces coated with different percentage mixtures of poly(L-lactic acid) (PLA) and PbAE or KK89 (a form of PbAE). Initial results indicated that cells seeded on 85% PLA + 15% KK89 enhanced mineralization (Appendix C). Different materials could elicit different cellular activities and also varying responses in different cell types. To further study the interaction of cell-scaffolds, cell viability and proliferation, differentiation, mineralization, and functional assays needs to be taken into consideration. Time-lapse video microscopy could be used to study cell migration, proliferation, and differentiation on surfaces coated with different materials. In addition, we could utilize proteomics to investigate proteins involved in cells' responses to different materials. For bone tissue engineering, *in-vivo* studies such as ectopic bone formation and critical size bone defect studies could be conducted. Growth factor and gene delivery systems can also be incorporated into scaffold design to promote regeneration.

## APPENDIX A

### SILAC SUPPLEMENTAL DATA

**Table 5-1.** Proteins with unique peptides upregulated by PP treatment

<b>UniProt Accession</b>	<b>Average Ratio</b>	<b>Protein Name</b>	<b>Peptides</b>
Q9CR51	79.32	V-type proton ATPase subunit G1 (Atp6v1g1)	2
Q9D411-2	62.35	Isoform 2 of Testis-specific serine/threonine-protein kinase 4 (Tsk4)	2
Q8CI04	48.16	Conserved oligomeric Golgi complex subunit 3 (Cog3)	2
Q9WUM4	33.52	Coronin-1C (Coro1c)	2
P05201	11.56	Aspartate aminotransferase, cytoplasmic (Got1)	2
Q8VBT0	6.06	Thioredoxin domain-containing protein 1 (Txndc1)	2
Q9D1A2	4.53	Cytosolic non-specific dipeptidase (Cndp2)	2
Q9R190	2.40	Metastasis-associated protein MTA2 (mta2)	2
Q91X76	2.20	5'-nucleotidase domain containing 2 (Nt5dc2)	5
O70252	1.97	Heme oxygenase 2 (Hmox2)	3
P70280	1.78	Vesicle-associated membrane protein 7	2

**Table 5-2.** Proteins with unique peptides downregulated by PP treatment

<b>UniProt Accession</b>	<b>Average Ratio</b>	<b>Protein Name</b>	<b>Peptides</b>
Q80YQ1	0.14	Thrombospondin 1 (Thbs1)	3
Q8C2Q3-1	0.14	Isoform 1 of RNA-binding protein 14 (Rbm14)	2
Q6Z WV3	0.13	60S ribosomal protein L10 (Rpl10)	3
Q9QZF2	0.13	Glypican-1 (Gpc1)	2
P35486	0.08	Pyruvate dehydrogenase E1 component subunit alpha, somatic form, mitochondrial (Pdha1)	2
Q5M9L1	0.02	60S ribosomal protein L36 (Rpl36)	2
Q6IFT3	0.01	Keratin Kb40 (Krt78)	2
Q9CZX7	0.53	Transmembrane protein 55A (Tmem55a)	2
Q9JJK2	0.50	LanC-like proteins 2 (Lancl2)	2
Q69ZX9	0.50	MKIAA0838 protein (Fragment) (Gls)	27
Q9DBL7	0.38	Bifunctional coenzyme A synthase (Coasy)	2

**Table 5-3.** Proteins with unique peptides upregulated by BMP-2 treatment

<b>UniProt Accession</b>	<b>Average Ratio</b>	<b>Protein Name</b>	<b>Peptides</b>
P62305	63.12	Small nuclear ribonucleoprotein E (Snrpe)	2
Q8CIR4	59.83	Transient receptor potential cation channel subfamily M member 6 (Trpm6)	2
Q5M6W3	51.16	Uncharacterized protein C2orf63 homolog	2
O70146	29.30	Dual specificity testis-specific protein kinase 1 (Tesk1)	2
Q3UW12-2	24.35	Isoform 2 of cyclic nucleotide-gated cation channel alpha-4 (Cnga4)	2
Q9CYL5	12.52	Golgi-associated plant pathogenesis-related protein 1 (Glipr2)	2
Q9Z0N1	3.32	Eukaryotic translation initiation factor 2 subunit 3 (Eif2s3x)	3
Q99LI7	3.11	Cleavage stimulation factor 77 kDa subunit (Cstf3)	2
Q8C7K6	2.63	Prenylcysteine oxidase-like (Pcyox11)	2
P55012	2.32	Solute carrier family 12 member 2 (Slc 12a2)	5
Q01721	2.31	Growth arrest-specific protein 1 (Gas1)	3
Q60967	2.00	Bifunctional 3'-phosphoadenosine 5'-phosphosulfate synthetase 1 (Papss1)	2
Q3UDW8	2.00	Heparan-alpha-glucosaminide N-acetyltransferase (Hgsnat)	2

**Table 5-4.** Proteins with unique peptides downregulated by BMP-2 treatment

<b>UniProt Accession</b>	<b>Average Ratio</b>	<b>Protein Name</b>	<b>Peptides</b>
Q9QZE7	0.08	Translin-associated protein X (Tsnax)	4
Q8C264	0.07	NOD-derived CD11c +ve dendritic cells cDNA (Bak1)	2
P62307	0.07	Small nuclear ribonucleoprotein F (Snrpf)	6
P61967	0.06	AP-1 complex subunit sigma-21A (Ap1s1)	2
O35129	0.05	Prohibitin-2 (Phb2)	2
Q8BFY6	0.04	Peflin (Pef1)	2
Q9Z2Z6	0.03	Mitochondrial carnitine/acylcarnitine carrier protein (Slc25a20)	2
P61226	0.03	Ras-related protein Rap-2b (Rap2b)	3
Q8VED5	0.03	Keratin, type II cytoskeletal 79 (Krt79)	7
P19091	0.02	Androgen receptor (Ar)	2
Q9CPQ1	0.02	Cytochrome c oxidase popyptide (Cox6c)	2
Q8C0C7	0.40	Phenylalanyl-tRNA synthetase alpha chain (Farsa)	3
Q921HB	0.38	3-ketoacyl-CoA thialase A, peroxisomal (Acaa1a)	2
Q9DBZ1-2	0.38	Isoform 2 of Inhibitor of nuclear factor kappa-B kinase-interacting protein (Ikip)	2
Q9D5L2	0.37	Adult male testis cDNA (4940426D05Rik)	2
Q9CQ60	0.28	6-phosphogluconolactonase	2
Q9D5V6	0.25	Synapse-associated protein 1 (Syap1)	2
Q9DBZ1-1	0.22	Isoform 1 of Inhibitor of nuclear factor kappa-B kinase-interactin protein (Ikip)	2

**Table 5-5.** Proteins with common peptides upregulated by PP treatment

<b>UniProt Accession</b>	<b>Average Ratio</b>	<b>Protein Name</b>	<b>Peptides</b>
Q9WVB2	41.67	Transducin-like enhancer protein 2 (Tle2)	2
P63013-1	38.73	Isoform PMX1-B of Paired mesoderm homeobox protein 1(Prrx1)	2
Q9CWU6-1	35.29	Isoform 1 of Ubiquinol-cytochrome c reductase complex chaperone CBP3 homolog (Uqcc)	2
Q64010-1	28.73	Isoform Crk-II of Proto-oncogene C-crk (Crk)	2
P63085	15.04	Mitogen-activated protein kinase 1 (Mapk1)	2
Q9CZW2-1	13.92	Isoform 1 of Centromere protein N (Cenpn)	2
P50247	9.58	Adenosylhomocysteinase (Ahcy)	2
B1ATZ0	4.55	HGF-regulated tyrosine kinase substrate (Hgs)	3
Q8BJW6-1	4.39	Isoform 1 of Eukaryotic translation initiation factor 2A (Eif2a)	2
Q8C0I1	4.27	Alkyldihydroxyacetonephosphate synthase, peroxisomal (Agps)	4
Q69ZB2	2.29	MKIAA1758 protein (Fragment) (Ctnbp2)	2
Q3TIV5-1	2.130	Isoform 1 of Zinc finger CCCH domain-containing protein 15 (Zc3h15)	2
Q9CZE3	1.950	Ras-related protein Rab-32 (Rab32)	2

**Table 5-6.** Proteins with common peptides downregulated by PP treatment

<b>UniProt Accession</b>	<b>Average Ratio</b>	<b>Protein Name</b>	<b>Peptides</b>
Q61703	0.01	Inter-alpha-trypsin inhibitor heavy chain H2 (Itih2)	2
Q9CZH7	0.03	Matrix-remodeling-associated protein 7 (Mxra7)	2
Q3TTY5	0.03	Keratin, type II cytoskeletal 2 epidermal (Krt2)	2
P39061-3	0.27	Isoform 1 of Collagen alpha-1(XVIII) chain (Col18a1)	2
Q8BFS6-1	0.34	Isoform 1 of Uncharacterized metallophosphoesterase CSTEP1 (Cstp1)	3
Q64331	0.35	Myosin-VI (Myo6)	3
Q99LX0	0.48	Protein DJ-1 (Park7)	4
O09159	0.51	Lysosomal alpha-mannosidase (Man2b1)	2
Q60961-1	0.55	Isoform Long of Lysosomal-associated transmembrane protein 4A (Laptm4a)	4
P70302	0.56	Stromal interaction molecule 1 (Stim1)	6

**Table 5-7.** Proteins with common peptides upregulated by BMP-2 treatment

<b>UniProt Accession</b>	<b>Average Ratio</b>	<b>Protein Name</b>	<b>Peptides</b>
A2AQ25-1	69.32	Isoform 1 of Sickle tail protein (Skt)	2
Q9D1L0	31.86	Coiled-coil-helix-coiled-coil-helix domain-containing protein 2, mitochondrial (Chchd2)	2
Q9QYP6-1	29.89	Isoform 1 of 5-azacytidine-induced protein 2 (Azi2)	4
O35855	16.24	Branched-chain-amino-acid aminotransferase, mitochondrial (Bcat2)	2
Q5XG71	14.94	Small subunit processome component 20 homolog (Utp20)	3
B1ATZ0	14.88	HGF-regulated tyrosine kinase substrate (Hgs)	2
Q9Z351-12	13.10	Isoform 12 of Potassium voltage-gated channel subfamily KQT member 2 (Kcnq2)	2
P62259	8.51	14-3-3 protein epsilon (Ywhae)	5
Q9CX30-1	5.74	Isoform 1 of Protein YIF1B (Yif1b)	2
Q9CZE3	3.02	Ras-related protein Rab-32 (Rab32)	2
B2RWW6	2.33	GCN1 general control of amino-acid synthesis 1-like 1 (Yeast) (Gcn11)	2
A2ARJ0	1.92	Signal transducing adaptor molecule (SH3 domain and ITAM motif) 1 (Fragment) (Stam)	4

**Table 5-8.** Proteins with common peptides downregulated by BMP-2 treatment

<b>UniProt Accession</b>	<b>Average Ratio</b>	<b>Protein Name</b>	<b>Peptides</b>
O09106	0.01	Histone deacetylase 1 (Hdac1)	3
P01029	0.02	Complement C4-B (C4b)	3
O35969-1	0.02	Isoform 1 of Guanidinoacetate N-methyltransferase (Gamt)	2
Q9JKF7	0.16	39S ribosomal protein L39, mitochondrial (Mrpl39)	2
Q64331	0.16	Myosin-VI OS=Mus musculus GN=Myo6	4
P08730-1	0.20	Isoform 1 of Keratin, type I cytoskeletal 13 (Krt13)	2
Q9DCG9	0.21	TRM112-like protein	2
Q61584-1	0.23	Isoform E of Fragile X mental retardation syndrome-related protein 1 (Fxr1)	2
Q3U8W9	0.25	Bone marrow macrophage cDNA, RIKEN full-length enriched library, clone:I830045N07 product:heterogeneous nuclear ribonucleoprotein R, full insert sequence (Hnrnpr)	4
O09131	0.33	Glutathione transferase omega-1 OS=Mus musculus GN=Gsto1	4
Q3U882	0.37	Bone marrow macrophage cDNA, RIKEN full-length enriched library, clone:I830063I15 product:Similar to SEC24 related gene family, member B (S. cerevisiae) homolog (Fragment) (Sec24b)	2
Q91ZR2	0.39	Sorting nexin-18 (Snx18)	2
Q9QXG4	0.41	Acetyl-coenzyme A synthetase, cytoplasmic (Acss2)	2

## **APPENDIX B**

### **FACS ANALYSIS OF PERIODONTAL LIGAMENT CELLS**

Total populations of periodontal ligament cells were isolated from four human adult third molars (21 year old male). Periodontal ligament were digested in collagenase for 1.5 h at 37 °C and pass through cell strainers to obtain single cells suspension. Cells were stained with antibodies CD146, CD34, CD56, and CD56. IgGs were used as negative controls. FACS analysis of periodontal ligament cells are shown in Figure 5-1. CD56+ and CD45+ cells are gated out and CD146+CD34- cells can be isolated as shown in P6. P6 = 0.6%.

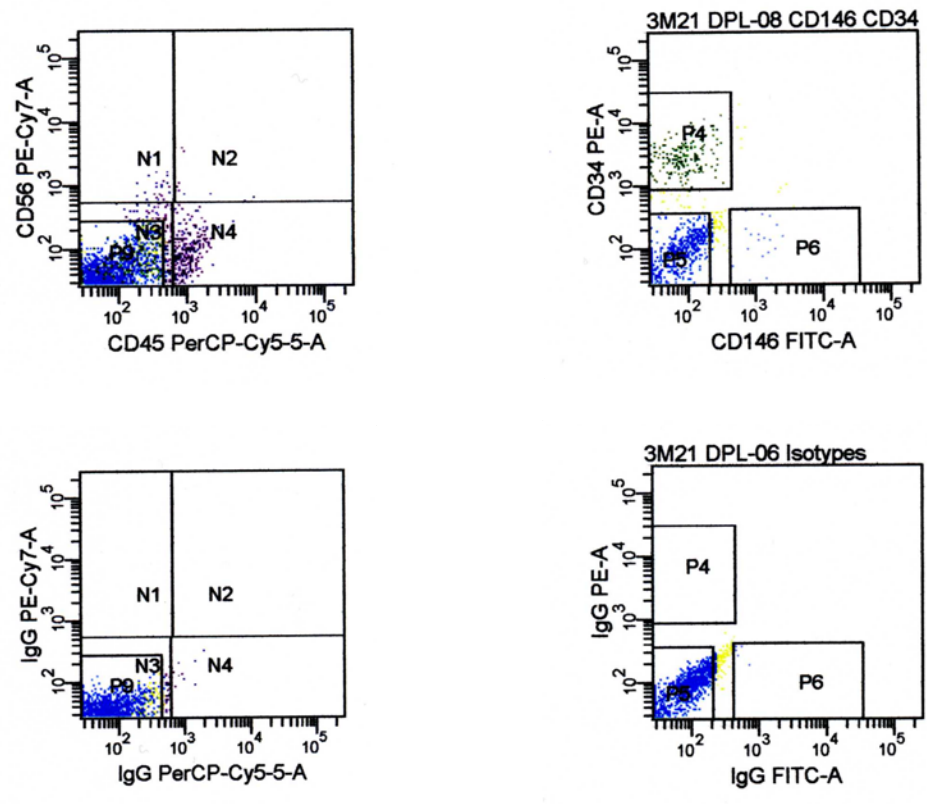


Figure 5-1. FACS analysis of periodontal ligament cells.

## APPENDIX C

### MINERALIZATION OF SAOS CELLS SEEDED ON PBAE (KK89)

SAOS-2 cells were seeded (25,000 cells/cm<sup>2</sup>) on glass slides coated with different percent of KK89 with PLA and placed in 6 well plates. Culture cells in medium Alpha MEM + 10% FBS + 1% Penicillin/Streptomycin + 2 mM L-glutamine without supplements. After cells are attached and appeared normal in cell growth morphology, supplements 50 µg/mL L-ascorbic acid, 5mM β-glycerophosphate, and 100nM dexamethasone were added on day three. Media were changed every 3-4 days and cells were stained for alkaline phosphatase (pink) and von Kossa (black) on Day 14.

**Table 5-9.** Experiment groups with cells grew on different coated surfaces

<b>Groups</b>	<b>Coated surfaces</b>
1	Tissue culture polystyrene
2	100% PLA (Mw 40-45K, H)
3	90% PLA + 10% KK89
4	85% PLA + 15% KK89
5	80% PLA + 20% KK89

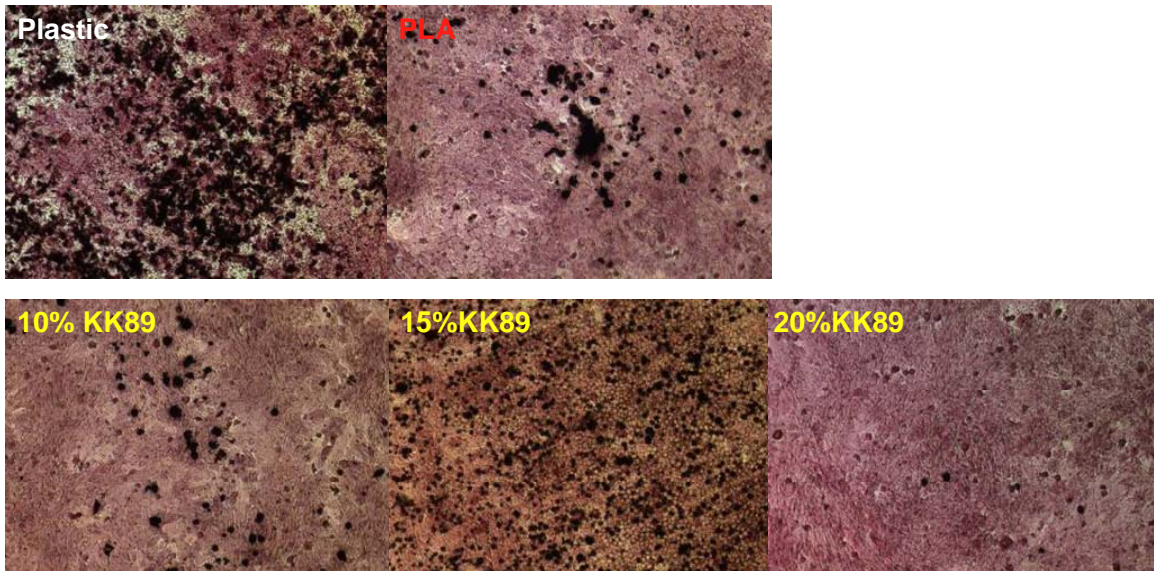


**Figure 5-2.** Alkaline phosphatase and von Kossa staining of SAOS-2 cells seeded on tissue culture plastic, PLA, and different % of KK89 at week two.

## BIBLIOGRAPHY

1. Pittenger, M.F., et al., *Multilineage potential of adult human mesenchymal stem cells*. Science, 1999. **284**(5411): p. 143-7.
2. Akintoye, S.O., et al., *Skeletal site-specific characterization of orofacial and iliac crest human bone marrow stromal cells in same individuals*. Bone, 2006. **38**(6): p. 758-68.
3. Shi, S. and S. Gronthos, *Perivascular niche of postnatal mesenchymal stem cells in human bone marrow and dental pulp*. J Bone Miner Res, 2003. **18**(4): p. 696-704.
4. Avery, J.K., *Oral Development and Histology*. Third ed. Chapter II Development of the Teeth and Supporting Structures, ed. P.F. Steele. 2002, New York: Thieme. 74.
5. Hirschi, K.K. and P.A. D'Amore, *Pericytes in the microvasculature*. Cardiovasc Res, 1996. **32**(4): p. 687-98.
6. Sims, D.E., *Diversity within pericytes*. Clin Exp Pharmacol Physiol, 2000. **27**(10): p. 842-6.
7. Shepro, D. and N.M. Morel, *Pericyte physiology*. Faseb J, 1993. **7**(11): p. 1031-8.
8. Bergers, G. and S. Song, *The role of pericytes in blood-vessel formation and maintenance*. Neuro-oncol, 2005. **7**(4): p. 452-64.
9. Suematsu, M. and S. Aiso, *Professor Toshio Ito: a clairvoyant in pericyte biology*. Keio J Med, 2001. **50**(2): p. 66-71.
10. Doherty, M.J. and A.E. Canfield, *Gene expression during vascular pericyte differentiation*. Crit Rev Eukaryot Gene Expr, 1999. **9**(1): p. 1-17.
11. Armulik, A., A. Abramsson, and C. Betsholtz, *Endothelial/pericyte interactions*. Circ Res, 2005. **97**(6): p. 512-23.
12. Brighton, C.T., et al., *The pericyte as a possible osteoblast progenitor cell*. Clin Orthop Relat Res, 1992(275): p. 287-99.
13. Collett, G.D. and A.E. Canfield, *Angiogenesis and pericytes in the initiation of ectopic calcification*. Circ Res, 2005. **96**(9): p. 930-8.

14. Farrington-Rock, C., et al., *Chondrogenic and adipogenic potential of microvascular pericytes*. *Circulation*, 2004. **110**(15): p. 2226-32.
15. Canfield, A.E., et al., *Role of pericytes in vascular calcification: a review*. *Z Kardiol*, 2000. **89 Suppl 2**: p. 20-7.
16. Brachvogel, B., et al., *Perivascular cells expressing annexin A5 define a novel mesenchymal stem cell-like population with the capacity to differentiate into multiple mesenchymal lineages*. *Development*, 2005. **132**(11): p. 2657-68.
17. Bianco, P. and G. Cossu, *Uno, nessuno e centomila: searching for the identity of mesodermal progenitors*. *Exp Cell Res*, 1999. **251**(2): p. 257-63.
18. Howson, K.M., et al., *The postnatal rat aorta contains pericyte progenitor cells that form spheroidal colonies in suspension culture*. *Am J Physiol Cell Physiol*, 2005. **289**(6): p. C1396-407.
19. Proudfoot, D., et al., *Calcification of human vascular cells in vitro is correlated with high levels of matrix Gla protein and low levels of osteopontin expression*. *Arterioscler Thromb Vasc Biol*, 1998. **18**(3): p. 379-88.
20. Canfield, A.E., et al., *Matrix Gla protein is differentially expressed during the deposition of a calcified matrix by vascular pericytes*. *FEBS Lett*, 2000. **487**(2): p. 267-71.
21. Schor, A.M., et al., *Pericytes derived from the retinal microvasculature undergo calcification in vitro*. *J Cell Sci*, 1990. **97 ( Pt 3)**: p. 449-61.
22. Reilly, T.M., et al., *Similarities in the phenotypic expression of pericytes and bone cells*. *Clin Orthop Relat Res*, 1998(346): p. 95-103.
23. Doherty, M.J., et al., *Vascular pericytes express osteogenic potential in vitro and in vivo*. *J Bone Miner Res*, 1998. **13**(5): p. 828-38.
24. Nayak, R.C., et al., *A monoclonal antibody (3G5)-defined ganglioside antigen is expressed on the cell surface of microvascular pericytes*. *J Exp Med*, 1988. **167**(3): p. 1003-15.
25. Crisan, M., et al., *A perivascular origin for mesenchymal stem cells in multiple human organs*. *Cell Stem Cell*, 2008. **3**(3): p. 301-13.
26. Gronthos, S., et al., *Stem cell properties of human dental pulp stem cells*. *J Dent Res*, 2002. **81**(8): p. 531-5.
27. Lopez-Cazaux, S., et al., *Culture medium modulates the behaviour of human dental pulp-derived cells: technical note*. *Eur Cell Mater*, 2006. **11**: p. 35-42; discussion 42.
28. Shi, S., P.G. Robey, and S. Gronthos, *Comparison of human dental pulp and bone marrow stromal stem cells by cDNA microarray analysis*. *Bone*, 2001. **29**(6): p. 532-9.

29. Shi, S., et al., *The efficacy of mesenchymal stem cells to regenerate and repair dental structures*. *Orthod Craniofac Res*, 2005. **8**(3): p. 191-9.
30. Batouli, S., et al., *Comparison of stem-cell-mediated osteogenesis and dentinogenesis*. *J Dent Res*, 2003. **82**(12): p. 976-81.
31. Miura, M., et al., *SHED: stem cells from human exfoliated deciduous teeth*. *Proc Natl Acad Sci U S A*, 2003. **100**(10): p. 5807-12.
32. Gronthos, S., et al., *Postnatal human dental pulp stem cells (DPSCs) in vitro and in vivo*. *Proc Natl Acad Sci U S A*, 2000. **97**(25): p. 13625-30.
33. Alliot-Licht, B., D. Hurtrel, and M. Gregoire, *Characterization of alpha-smooth muscle actin positive cells in mineralized human dental pulp cultures*. *Arch Oral Biol*, 2001. **46**(3): p. 221-8.
34. Tecles, O., et al., *Activation of human dental pulp progenitor/stem cells in response to odontoblast injury*. *Arch Oral Biol*, 2005. **50**(2): p. 103-8.
35. Laino, G., et al., *In Vitro Bone Production Using Stem Cells Derived From Human Dental Pulp*. *J Craniofac Surg*, 2006. **17**(3): p. 511-515.
36. Fisher, L.W., et al., *Flexible structures of SIBLING proteins, bone sialoprotein, and osteopontin*. *Biochem Biophys Res Commun*, 2001. **280**(2): p. 460-5.
37. Qin, C., O. Baba, and W.T. Butler, *Post-translational modifications of sibling proteins and their roles in osteogenesis and dentinogenesis*. *Crit Rev Oral Biol Med*, 2004. **15**(3): p. 126-36.
38. C., S., et al., *From mouse to zebrafish: dentin matrix proteins genomic characterization*, in *Chemistry and Biology of Mineralized Tissue*, G. M, A.L. Boskey, and G.A. Rodan, Editors. 2000, American Academy of Orthopaedic Surgeons: Chicago. p. 181-184.
39. Miura, M., et al., *A crucial role of caspase-3 in osteogenic differentiation of bone marrow stromal stem cells*. *J Clin Invest*, 2004. **114**(12): p. 1704-13.
40. George, A., et al., *The carboxyl-terminal domain of phosphophoryn contains unique extended triplet amino acid repeat sequences forming ordered carboxyl-phosphate interaction ridges that may be essential in the biomineralization process*. *Journal of Biological Chemistry*, 1996. **271**(51): p. 32869-32873.
41. Ritchie, H.H., D.G. Ritchie, and L.H. Wang, *Six decades of dentinogenesis research. Historical and prospective views on phosphophoryn and dentin sialoprotein*. *Eur J Oral Sci*, 1998. **106 Suppl 1**: p. 211-20.
42. Sabsay, B., et al., *Domain structure and sequence distribution in dentin phosphophoryn*. *Biochemical Journal*, 1991. **276**(Pt 3): p. 699-707.

43. Narayanan, K., et al., *Differentiation of embryonic mesenchymal cells to odontoblast-like cells by overexpression of dentin matrix protein 1*. Proc Natl Acad Sci U S A, 2001. **98**(8): p. 4516-21.
44. MacDougall, M., et al., *Dentin phosphoprotein and dentin sialoprotein are cleavage products expressed from a single transcript coded by a gene on human chromosome 4. Dentin phosphoprotein DNA sequence determination*. J Biol Chem, 1997. **272**(2): p. 835-42.
45. Veis, A. and A. Perry, *The phosphoprotein of the dentin matrix*. Biochemistry, 1967. **6**(8): p. 2409-16.
46. Linde, A., M. Bhowan, and W.T. Butler, *Noncollagenous proteins of dentin. A re-examination of proteins from rat incisor dentin utilizing techniques to avoid artifacts*. Journal of Biological Chemistry, 1980. **255**(12): p. 5931-5942.
47. Richardson, W.S., E.C. Munksgaard, and W.T. Butler, *Rat incisor phosphoprotein. The nature of the phosphate and quantitation of the phosphoserine*. J Biol Chem, 1978. **253**(22): p. 8042-6.
48. Sfeir, C., Butler, S., Lin, E., George, A., and Vies, A., *From mouse to zebrafish: dentin matrix proteins genomic characterization*, in *Chemistry and Biology of Mineralized Tissue*. 2000, American Academy of Orthopaedic Surgeons: Chicago. p. 181-184.
49. Gorter de Vries, I. and E. Wisse, *Ultrastructural localization of dentine phosphoprotein in rat tooth germs by immunogold staining*. Histochemistry, 1989. **91**(1): p. 69-75.
50. MacDougall, M., M. Zeichner-David, and H.C. Slavkin, *Production and characterization of antibodies against murine dentine phosphoprotein*. Biochem J, 1985. **232**(2): p. 493-500.
51. Weinstock, M. and C.P. Leblond, *Radioautographic visualization of the deposition of a phosphoprotein at the mineralization front in the dentin of the rat incisor*. J Cell Biol, 1973. **56**(3): p. 838-45.
52. Veis, A., et al., *Properties of the (DSS)<sub>n</sub> triplet repeat domain of rat dentin phosphophoryn*. Eur J Oral Sci, 1998. **106 Suppl 1**: p. 234-8.
53. Boskey, A.L., et al., *Concentration-dependent effects of dentin phosphophoryn in the regulation of in vitro hydroxyapatite formation and growth*. Bone & Mineral, 1990. **11**(1): p. 55-65.
54. Papin, J.A., et al., *Reconstruction of cellular signalling networks and analysis of their properties*. Nat Rev Mol Cell Biol, 2005. **6**(2): p. 99-111.
55. Zanetti, M., et al., *Ca<sup>2+</sup>-binding studies of the phosphoprotein from rat-incisor dentine*. Eur J Biochem, 1981. **113**(3): p. 541-5.

56. Lee, S.L., A. Veis, and T. Glonek, *Dentin phosphoprotein: an extracellular calcium-binding protein*. *Biochemistry*, 1977. **16**(13): p. 2971-2979.
57. Jadowiec, J., et al., *Phosphophoryn regulates the gene expression and differentiation of NIH3T3, MC3T3-E1, and human mesenchymal stem cells via the integrin/MAPK signaling pathway*. *J Biol Chem*, 2004. **279**(51): p. 53323-30.
58. Jadowiec, J.A., et al., *Extracellular matrix-mediated signaling by dentin phosphophoryn involves activation of the Smad pathway independent of bone morphogenetic protein*. *J Biol Chem*, 2006. **281**(9): p. 5341-7.
59. Saito, T., et al., *Effect of phosphophoryn on rhBMP-2-induced bone formation*. *Arch Oral Biol*, 2004. **49**(3): p. 239-43.
60. Lai, C.F. and S.L. Cheng, *Alphavbeta integrins play an essential role in BMP-2 induction of osteoblast differentiation*. *J Bone Miner Res*, 2005. **20**(2): p. 330-40.
61. Ryoo, H.M., M.H. Lee, and Y.J. Kim, *Critical molecular switches involved in BMP-2-induced osteogenic differentiation of mesenchymal cells*. *Gene*, 2006. **366**(1): p. 51-7.
62. Barboza, E., A. Caula, and F. Machado, *Potential of recombinant human bone morphogenetic protein-2 in bone regeneration*. *Implant Dent*, 1999. **8**(4): p. 360-7.
63. Iohara, K., et al., *Dentin regeneration by dental pulp stem cell therapy with recombinant human bone morphogenetic protein 2*. *J Dent Res*, 2004. **83**(8): p. 590-5.
64. Dragoo, J.L., et al., *Bone induction by BMP-2 transduced stem cells derived from human fat*. *J Orthop Res*, 2003. **21**(4): p. 622-9.
65. Frank, O., et al., *Real-time quantitative RT-PCR analysis of human bone marrow stromal cells during osteogenic differentiation in vitro*. *J Cell Biochem*, 2002. **85**(4): p. 737-46.
66. Wozney, J.M., *Overview of bone morphogenetic proteins*. *Spine*, 2002. **27**(16 Suppl 1): p. S2-8.
67. Chen, D., M. Zhao, and G.R. Mundy, *Bone morphogenetic proteins*. *Growth Factors*, 2004. **22**(4): p. 233-41.
68. Lopez-Lacombe, J.L., et al., *Use of rhBMP-2 activated chitosan films to improve osseointegration*. *Biomacromolecules*, 2006. **7**(3): p. 792-8.
69. Geiger, M., R.H. Li, and W. Friess, *Collagen sponges for bone regeneration with rhBMP-2*. *Adv Drug Deliv Rev*, 2003. **55**(12): p. 1613-29.
70. Li, C., et al., *Electrospun silk-BMP-2 scaffolds for bone tissue engineering*. *Biomaterials*, 2006. **27**(16): p. 3115-24.

71. Ghosh-Choudhury, N., et al., *Requirement of BMP-2-induced phosphatidylinositol 3-kinase and Akt serine/threonine kinase in osteoblast differentiation and Smad-dependent BMP-2 gene transcription*. J Biol Chem, 2002. **277**(36): p. 33361-8.
72. Seoane, J., et al., *Integration of Smad and forkhead pathways in the control of neuroepithelial and glioblastoma cell proliferation*. Cell, 2004. **117**(2): p. 211-23.
73. Aubin, J., A. Davy, and P. Soriano, *In vivo convergence of BMP and MAPK signaling pathways: impact of differential Smad1 phosphorylation on development and homeostasis*. Genes Dev, 2004. **18**(12): p. 1482-94.
74. Pera, E.M., et al., *Integration of IGF, FGF, and anti-BMP signals via Smad1 phosphorylation in neural induction*. Genes Dev, 2003. **17**(24): p. 3023-8.
75. Kretzschmar, M., J. Doody, and J. Massague, *Opposing BMP and EGF signalling pathways converge on the TGF-beta family mediator Smad1*. Nature, 1997. **389**(6651): p. 618-22.
76. Noth, U., et al., *Activation of p38 and Smads mediates BMP-2 effects on human trabecular bone-derived osteoblasts*. Exp Cell Res, 2003. **291**(1): p. 201-11.
77. Park, H.W., J.S. Shin, and C.W. Kim, *Proteome of mesenchymal stem cells*. Proteomics, 2007. **7**(16): p. 2881-94.
78. Zhang, A.X., et al., *Proteomic identification of differently expressed proteins responsible for osteoblast differentiation from human mesenchymal stem cells*. Mol Cell Biochem, 2007. **304**(1-2): p. 167-79.
79. Gafken, P.R. and P.D. Lampe, *Methodologies for characterizing phosphoproteins by mass spectrometry*. Cell Commun Adhes, 2006. **13**(5-6): p. 249-62.
80. Preisinger, C., et al., *Proteomics and phosphoproteomics for the mapping of cellular signalling networks*. Proteomics, 2008. **8**(21): p. 4402-15.
81. Yocum, A.K., et al., *Coupled global and targeted proteomics of human embryonic stem cells during induced differentiation*. Mol Cell Proteomics, 2008. **7**(4): p. 750-67.
82. Kratchmarova, I., et al., *Mechanism of divergent growth factor effects in mesenchymal stem cell differentiation*. Science, 2005. **308**(5727): p. 1472-7.
83. Foster, L.J., et al., *Differential expression profiling of membrane proteins by quantitative proteomics in a human mesenchymal stem cell line undergoing osteoblast differentiation*. Stem Cells, 2005. **23**(9): p. 1367-77.
84. Reinders, J. and A. Sickmann, *State-of-the-art in phosphoproteomics*. Proteomics, 2005. **5**(16): p. 4052-61.

85. Kersten, B., et al., *Plant phosphoproteomics: a long road ahead*. Proteomics, 2006. **6**(20): p. 5517-28.
86. Schlessinger, J., *Cellular signaling by receptor tyrosine kinases*. Harvey Lect, 1993. **89**: p. 105-23.
87. Paradela, A. and J.P. Albar, *Advances in the analysis of protein phosphorylation*. J Proteome Res, 2008. **7**(5): p. 1809-18.
88. Liang, X., et al., *Quantitative comparison of IMAC and TiO<sub>2</sub> surfaces used in the study of regulated, dynamic protein phosphorylation*. J Am Soc Mass Spectrom, 2007. **18**(11): p. 1932-44.
89. Kange, R., et al., *Comparison of different IMAC techniques used for enrichment of phosphorylated peptides*. J Biomol Tech, 2005. **16**(2): p. 91-103.
90. Mann, K., et al., *Phosphoproteins of the chicken eggshell calcified layer*. Proteomics, 2007. **7**(1): p. 106-15.
91. Thingholm, T.E., et al., *Highly selective enrichment of phosphorylated peptides using titanium dioxide*. Nat Protoc, 2006. **1**(4): p. 1929-35.
92. Fitzgerald, M., D.J. Chiego, Jr., and D.R. Heys, *Autoradiographic analysis of odontoblast replacement following pulp exposure in primate teeth*. Arch Oral Biol, 1990. **35**(9): p. 707-15.
93. Hughes, S. and T. Chan-Ling, *Characterization of smooth muscle cell and pericyte differentiation in the rat retina in vivo*. Invest Ophthalmol Vis Sci, 2004. **45**(8): p. 2795-806.
94. Crisan, M., et al., *A Perivascular Origin for Mesenchymal Stem Cells in Multiple Human Organs*. Cell Stem Cell, 2008. **3**(3): p. 301-313.
95. Peault, B., et al., *Stem and progenitor cells in skeletal muscle development, maintenance, and therapy*. Mol Ther, 2007. **15**(5): p. 867-77.
96. Dellavalle, A., et al., *Pericytes of human skeletal muscle are myogenic precursors distinct from satellite cells*. Nat Cell Biol, 2007. **9**(3): p. 255-67.
97. Covas, D.T., et al., *Multipotent mesenchymal stromal cells obtained from diverse human tissues share functional properties and gene-expression profile with CD146(+) perivascular cells and fibroblasts*. Exp Hematol, 2008.
98. Crisan, M., et al., *A Reservoir of Brown Adipocyte Progenitors in Human Skeletal Muscle*. Stem Cells, 2008.
99. Provis, J.M., *Development of the primate retinal vasculature*. Prog Retin Eye Res, 2001. **20**(6): p. 799-821.

100. Carlile, M.J., et al., *The presence of pericytes and transitional cells in the vasculature of the human dental pulp: an ultrastructural study*. Histochem J, 2000. **32**(4): p. 239-45.
101. Alliot-Licht, B., et al., *Dexamethasone stimulates differentiation of odontoblast-like cells in human dental pulp cultures*. Cell Tissue Res, 2005. **321**(3): p. 391-400.
102. Falanga, V., et al., *Autologous Bone Marrow-Derived Cultured Mesenchymal Stem Cells Delivered in a Fibrin Spray Accelerate Healing in Murine and Human Cutaneous Wounds*. Tissue Eng, 2007.
103. Jo, Y.Y., et al., *Isolation and characterization of postnatal stem cells from human dental tissues*. Tissue Eng, 2007. **13**(4): p. 767-73.
104. Mageed, A.S., et al., *Isolation of large numbers of mesenchymal stem cells from the washings of bone marrow collection bags: characterization of fresh mesenchymal stem cells*. Transplantation, 2007. **83**(8): p. 1019-26.
105. Liu, J., D.J. Burkin, and S.J. Kaufman, *Increasing alpha 7 beta 1-integrin promotes muscle cell proliferation, adhesion, and resistance to apoptosis without changing gene expression*. Am J Physiol Cell Physiol, 2008. **294**(2): p. C627-40.
106. Sonoyama, W., et al., *Skeletal stem cells in regenerative medicine*. Curr Top Dev Biol, 2005. **67**: p. 305-23.
107. Yang, X., et al., *Hard Tissue Formation of STRO-1-Selected Rat Dental Pulp Stem Cells In Vivo*. Tissue Eng Part A, 2008.
108. Veis, A., *Phosphoproteins from teeth and bone*. Ciba Found Symp, 1988. **136**: p. 161-77.
109. Veis, A., *Mineral-matrix interactions in bone and dentin*. J Bone Miner Res, 1993. **8 Suppl 2**: p. S493-7.
110. Brown, M.D. and D.B. Sacks, *Compartmentalised MAPK pathways*. Handb Exp Pharmacol, 2008(186): p. 205-35.
111. Giancotti, F.G. and E. Ruoslahti, *Integrin signaling*. Science, 1999. **285**(5430): p. 1028-32.
112. Shi, Y. and J. Massague, *Mechanisms of TGF-beta signaling from cell membrane to the nucleus*. Cell, 2003. **113**(6): p. 685-700.
113. Hynes, R.O., *Integrins: bidirectional, allosteric signaling machines*. Cell, 2002. **110**(6): p. 673-87.
114. Goessler, U.R., et al., *Integrin expression in stem cells from bone marrow and adipose tissue during chondrogenic differentiation*. Int J Mol Med, 2008. **21**(3): p. 271-9.

115. Salasznyk, R.M., et al., *ERK signaling pathways regulate the osteogenic differentiation of human mesenchymal stem cells on collagen I and vitronectin*. Cell Commun Adhes, 2004. **11**(5-6): p. 137-53.
116. Jikko, A., et al., *Collagen integrin receptors regulate early osteoblast differentiation induced by BMP-2*. J Bone Miner Res, 1999. **14**(7): p. 1075-83.
117. Schneider, G.B., R. Zaharias, and C. Stanford, *Osteoblast integrin adhesion and signaling regulate mineralization*. J Dent Res, 2001. **80**(6): p. 1540-4.
118. Jadlowiec, J.A., *Investigation of phosphotyrosine signaling mechanisms as a model for ECM-directed morphogenesis of mineralized tissues*. PhD Thesis, 2005. **Chapter 5**.
119. Estrada, Y., J. Dong, and L. Ossowski, *Positive cross-talk between ERK and p38 in melanoma stimulates migration and in vivo proliferation*. Pigment Cell Melanoma Res, 2008.
120. Rauch, C. and P.T. Loughna, *Stretch-induced activation of ERK in myocytes is p38 and calcineurin-dependent*. Cell Biochem Funct, 2008. **26**(8): p. 866-9.
121. Xiao, Y.Q., et al., *Cross-talk between ERK and p38 MAPK mediates selective suppression of pro-inflammatory cytokines by transforming growth factor-beta*. J Biol Chem, 2002. **277**(17): p. 14884-93.
122. Blau, H.M., T.R. Brazelton, and J.M. Weimann, *The evolving concept of a stem cell: entity or function?* Cell, 2001. **105**(7): p. 829-41.
123. Unwin, R.D., et al., *The potential for proteomic definition of stem cell populations*. Exp Hematol, 2003. **31**(12): p. 1147-59.
124. Baharvand, H., et al., *Concise review: trends in stem cell proteomics*. Stem Cells, 2007. **25**(8): p. 1888-903.
125. Butler, W.T., H.H. Ritchie, and A.L. Bronckers, *Extracellular matrix proteins of dentine*. Ciba Found Symp, 1997. **205**: p. 107-15; discussion 115-7.
126. Ebara, S. and K. Nakayama, *Mechanism for the action of bone morphogenetic proteins and regulation of their activity*. Spine, 2002. **27**(16 Suppl 1): p. S10-5.
127. Zhao, L., et al., *Comparison of multipotent differentiation potentials of murine primary bone marrow stromal cells and mesenchymal stem cell line C3H10T1/2*. Calcif Tissue Int, 2009. **84**(1): p. 56-64.
128. Zanivan, S., et al., *Solid Tumor Proteome and Phosphoproteome Analysis by High Resolution Mass Spectrometry*. J Proteome Res, 2008.
129. Roadcap, D.W., C.S. Clemen, and J.E. Bear, *The role of mammalian coronins in development and disease*. Subcell Biochem, 2008. **48**: p. 124-35.

130. Geiger, B., J.P. Spatz, and A.D. Bershadsky, *Environmental sensing through focal adhesions*. Nat Rev Mol Cell Biol, 2009. **10**(1): p. 21-33.
131. Gamell, C., et al., *BMP2 induction of actin cytoskeleton reorganization and cell migration requires PI3-kinase and Cdc42 activity*. J Cell Sci, 2008. **121**(Pt 23): p. 3960-70.
132. Morrison, D.K., *The 14-3-3 proteins: integrators of diverse signaling cues that impact cell fate and cancer development*. Trends Cell Biol, 2009. **19**(1): p. 16-23.
133. Correll, R.N., et al., *The RGK family of GTP-binding proteins: regulators of voltage-dependent calcium channels and cytoskeleton remodeling*. Cell Signal, 2008. **20**(2): p. 292-300.
134. Boguski, M.S. and F. McCormick, *Proteins regulating Ras and its relatives*. Nature, 1993. **366**(6456): p. 643-54.
135. Lee, H.J., et al., *Activation of bone morphogenetic protein signaling by a Gemini vitamin D3 analogue is mediated by Ras/protein kinase C alpha*. Cancer Res, 2007. **67**(24): p. 11840-7.
136. Vanderschueren, D., et al., *Androgens and bone*. Curr Opin Endocrinol Diabetes Obes, 2008. **15**(3): p. 250-4.
137. Centenera, M.M., et al., *The contribution of different androgen receptor domains to receptor dimerization and signaling*. Mol Endocrinol, 2008. **22**(11): p. 2373-82.
138. Qiu, T., et al., *Control of prostate cell growth: BMP antagonizes androgen mitogenic activity with incorporation of MAPK signals in Smad1*. EMBO J, 2007. **26**(2): p. 346-57.
139. Wei, J., et al., *PERK is essential for neonatal skeletal development to regulate osteoblast proliferation and differentiation*. J Cell Physiol, 2008. **217**(3): p. 693-707.
140. Zhang, P., et al., *The PERK eukaryotic initiation factor 2 alpha kinase is required for the development of the skeletal system, postnatal growth, and the function and viability of the pancreas*. Mol Cell Biol, 2002. **22**(11): p. 3864-74.
141. Gay, I.C., S. Chen, and M. MacDougall, *Isolation and characterization of multipotent human periodontal ligament stem cells*. Orthod Craniofac Res, 2007. **10**(3): p. 149-60.
142. Seo, B.M., et al., *Investigation of multipotent postnatal stem cells from human periodontal ligament*. Lancet, 2004. **364**(9429): p. 149-55.
143. Yang, X., et al., *Multilineage potential of STRO-1+ rat dental pulp cells in vitro*. J Tissue Eng Regen Med, 2007. **1**(2): p. 128-35.
144. Huang, G.T., et al., *The hidden treasure in apical papilla: the potential role in pulp/dentin regeneration and bioroot engineering*. J Endod, 2008. **34**(6): p. 645-51.

145. Sonoyama, W., et al., *Characterization of the apical papilla and its residing stem cells from human immature permanent teeth: a pilot study*. J Endod, 2008. **34**(2): p. 166-71.
146. Tompkins, K., A. George, and A. Veis, *Characterization of a mouse amelogenin [A-4]/M59 cell surface receptor*. Bone, 2006. **38**(2): p. 172-80.
147. Karin, M., Z. Liu, and E. Zandi, *AP-1 function and regulation*. Curr Opin Cell Biol, 1997. **9**(2): p. 240-6.
148. Hipskind, R.A. and G. Bilbe, *MAP kinase signaling cascades and gene expression in osteoblasts*. Front Biosci, 1998. **3**: p. d804-16.
149. Ziros, P.G., et al., *The bone-specific transcriptional regulator Cbfa1 is a target of mechanical signals in osteoblastic cells*. J Biol Chem, 2002. **277**(26): p. 23934-41.
150. Abdallah, B.M., et al., *Maintenance of differentiation potential of human bone marrow mesenchymal stem cells immortalized by human telomerase reverse transcriptase gene despite [corrected] extensive proliferation*. Biochem Biophys Res Commun, 2005. **326**(3): p. 527-38.
151. Ow, S.Y., et al., *Quantitative shotgun proteomics of enriched heterocysts from Nostoc sp. PCC 7120 using 8-plex isobaric peptide tags*. J Proteome Res, 2008. **7**(4): p. 1615-28.
152. Phanstiel, D., et al., *Peptide quantification using 8-plex isobaric tags and electron transfer dissociation tandem mass spectrometry*. Anal Chem, 2009. **81**(4): p. 1693-8.